Vav2 Inhibits T Cell Calcium Signaling by Activating Cdc42

A thesis

submitted by

Michael A. Fray

In partial fulfillment of the requirements for the degree of
Doctor of Philosophy

in

Immunology

TUFTS UNIVERSITY

Sackler School of Graduate Biomedical Sciences

May 2016

Advisor
Stephen Bunnell

Committee Members
Joan Mecsas
David Thorley-Lawson
Henry Wortis
Outside Examiner
Tanya Mayadas

1 Abstract

1.1 Vav proteins at critical points in health

Vav proteins are tyrosine kinase-dependent guanine nucleotide exchange factors (GEFs) essential for a functional immune system. This family of proteins consists of three mammalian isoforms, Vav1, Vav2, and Vav3. Studies in mice have shown that knocking out all three of these isoforms leads to an almost complete loss in the number and function of T and B cells (Fujikawa et al., 2003), serious defects in innate immune cells, and impacts on the cardiovascular and nervous systems (Bustelo, 2012). The different Vav isoforms have unique signaling properties: in T cells, Vav1 promotes and Vav2 opposes TCR-induced calcium entry despite their structural similarity. I show here that, while Vav1 facilitates calcium entry via non-catalytic mechanisms, the suppressive activity of Vav2 is largely dependent on its catalytic activity and can be transferred into Vav1 by exchanging the catalytic cores of these proteins.

Although Vav1 and Vav2 have been reported to target identical Rho family GTPases, my data indicate that this cannot be the case. Among the GTPase targets of Vav proteins, I find that only active Cdc42 potently inhibits TCR-induced calcium entry. Using a novel *in vivo* 'GEF trapping' assay to screen GEF-GTPase interactions, I demonstrate that Cdc42 interacts with the catalytic surface of Vav2, but not Vav1. I further identify a single amino acid that prevents the recognition of Cdc42 by Vav1. Lastly, I show that the pharmacological suppression of Cdc42 activation prevents the inhibition of TCR-induced calcium entry by Vav2. Since Vav2 and Cdc42 both contribute to the initiation of immunoreceptor-dependent calcium signals in B cells, these

observations suggest a profound point of divergence in the signaling pathways of T cells and other immune cells.

2 Acknowledgements

I'd like to thank Gilles Benichou for bringing me into his lab while I was still collecting the prerequisites to apply to graduate school, Alessandro Alessandrini for mentoring me at that critical time, and Karla Stenger and Susan Shea for having the patience to teach me basic and advanced lab skills. I am indebted to Thereza Imanishi-Kari for allowing me to start an early rotation in her lab during my transition to Tufts, and for her help throughout the rest of my time at school. I was lucky to have David Thorley-Lawson, Henry Wortis, and Joan Mecsas as my committee members, and they have ensured that my committee meetings were careful examinations of my science rather than perfunctory check-ins. My career at Tufts was also greatly enriched through my interactions with Mercio Perria-Perrin, both in class and in his academic and career guidance outside of class.

I can't imagine making it through grad school without the help of my lab mates. Joining the lab in the company of Nicholas Sylvain, Juliana Lewis, and Rosemary Brewka, made my daily life in the lab an enjoyable and rewarding experience. My special thanks go to Michael Ophir for always being willing to engage in scientific and non-scientific discussions at all hours of the day, even after he had graduated. Joanne Russo will always have my gratitude for helping me in hundreds of ways in my time at Tufts, and for just being a really good friend.

Any scientific successes in my future, and any that I had at Tufts, will be due in large part to the mentoring that I received from Stephen Bunnell. The breadth and depth of scientific knowledge that Steve has is astounding. Equally impressive are his patient willingness to share this knowledge with his students and his ability to convey abstract

ideas in ways both accessible and memorable. Thanks also to Maria-Christina Seminario for always taking the time to share her wealth of knowledge with me.

My family has been incredibly supportive during my long and indirect path to a PhD. My parents, Mary and Robert Fray, have given me a foundation of support composed of the assumption that I could achieve this type of academic goal; but they have given an equal amount of support during the times that I followed different paths with different goals. My sister, Suzanne Fray, has managed to consistently encourage my choices while doing far more than her share of the work needed to keep our family functional.

And finally, I doubt I would have been able to take the first step away from my comfortable career to start all over and follow my passion without the help of my amazing wife. Julian has provided me with the encouragement to keep moving ahead, along with the absolutely essential help in all aspects of my work, from proofreading to long-term planning. Most of all, Julian has made me want to undertake a path towards a career that can be at least partially as rewarding as my home life. And finally, thanks to my daughter Indie for filling every day with a joy that I had never expected to have, and to give me a reason to persevere though difficult and frustrating times.

Table of Contents

1 Abstract ii
1.1 Vav proteins at critical points in health ii

2 Acknowledgements iv
3 Index of Figures ix
4 Abbreviations and Acronyms used in this Thesis xi
5 Introduction 1
5.1 The Vav family of proteins 1
5.1.1 Vav proteins as GEFs 1
5.1.2 Vav domain structure 2
5.1.3 Tissue distribution of Vav isoforms 7
5.2 Vav proteins in T cell signaling 10
5.2.1 Vav1 and SLP-76 microclusters 10
5.2.2 Catalytic and scaffolding functions of Vav1 in T cell signaling 11
5.3 Calcium signaling in T cells 15
5.3.1 Calcium signaling is essential for T cell activation 15
5.3.2 Calcium signals halt T cells 15
5.3.3 Intracellular calcium activates the NF-AT transcription factor 17
5.3.4 Calcium influxes trigger vesicle mobilization 20
5.3.5 TCR triggering of calcium influx and SLP-76 microcluster formation 20
5.3.6 The role of Vav proteins in TCR calcium signaling 23
5.3.7 The catalytic activity of Vav1 is not necessary for calcium signaling 24
5.4 Vav proteins in disease 24
5.4.1 Vav proteins in cancer 24
5.4.2 Vav proteins as therapeutic targets in cancer and immunosuppression 27
5.5 Rho GTPases 28
5.5.1 The GTPase activation cycle 28
5.5.2 Functions of Rho GTPases 29
5.6 Rho GTPases in T cell signaling 33
5.6.1 Roles of Rac1 and Rac2 in T cell development and function 33
5.6.2 Roles of Cdc42 in T cell activation 34
5.6.3 Effects of Rho GTPases on immune cell calcium signaling 35
5.7 Rho GTPases in disease 37
5.7.1 The GEF-GTPase interaction as a target for therapy 38
5.8 Models of Vav function 39
5.8.1 Reports of Vav GEF specificity 39
5.8.2 Assays used to determine GEF catalytic specificity 39
5.8.3 Jurkat cells as a model of T cell signaling. 41
5.8.4 Calcium signaling in Jurkat T cells 42
5.8.5 Methods for determining expression-dependent effects on calcium signaling 45
5.9 Summary and Goals 47

6 Materials and Methods 48

6.1 Reagents 48
6.1.1 Antibodies 48
6.1.2 Inhibitors 48
6.1.3 Fluorescent reporters 49
6.1.4 Cell culture 49
6.1.5 Cell staining 49
6.1.6 Cell selection 50
6.1.7 Cell lysate preparation and Western blotting 50
6.2 Calcium assay 50
6.2.1 Flow cytometry-based assessment of intracellular calcium 50
6.2.2 Inhibitor effects on calcium influx 52
6.3 Molecular biology 52
6.3.1 Construct creation 52
6.4 Western blotting 58
6.5 Transfections and Transductions 58
6.5.1 Transient Transfections 58
6.5.2 Lentiviral transduction 59
6.6 Imaging 59
6.6.1 Plating cells for imaging 59
6.6.2 Confocal imaging 60
6.7 Analysis and Quantification 60
6.7.1 Image collection 60
6.7.2 Image quantification 61
6.7.3 Calcium assay analysis and quantification 62

7 Results 63
7.1 Vav family members in Jurkat calcium signaling 63
7.1.1 Vav1 and Vav3 support TCR induced calcium entry 63
7.2 The CH domains of Vav1 and Vav2 support calcium signaling 68
7.3 The catalytic core of Vav2 inhibits calcium signaling downstream of TCR ligation. 71
7.3.1 Effects of terminating the GTPase exchange ability of Vav2 73
7.3.2 Inhibition of calcium signaling by ΔCH Vav1 is not catalytic 76
7.4 Calcium profiles of Rho family GTPases 78
7.4.1 Determining the Calcium phenotype of Rho Family GTPases 78
7.4.2 Cdc42 strongly inhibits Ca++ influx in J.Vav 79
7.4.3 Calcium inhibition is common to Cdc42 isoforms and CA mutants 82
7.5 Determining the GTPase specificity of Vav isoforms 85
7.5.1 Designing an *in vivo* assay for GEF specificity 85
7.5.2 Imaging GEF – GTPase interactions 85
7.5.3 'GEF-Trap' Assay shows Rac1 co-localization with catalytically active Vav1 and Vav2 88
7.5.4 Identifying and quantifying co-localization 92
7.6 Cdc42 is trapped in the catalytic core of Vav2, but not Vav1 94
7.6.1 Vav2 interacts with a wider range of GTPases than Vav1 94
7.6.2 The Vav2 GEF domains recruit Cdc42 to the SLP-76 MC 99
7.7 Narrowing down the portion of Vav1 that excludes Cdc42 101
7.7.1 GTPase specificity is determined by the DH domain of Vav1 101
7.7.2 The GTPase proximal amino acids of Vav1 are not sufficient to convey GTPase specificity 104

7.7.3 The first and last helical portion of the Vav1 DH domain do not provide GTPase specificity 106
7.8 Vav1 specificity is determined by tryptophan 56 on Rac1 111
7.8.1 Tryptophan 56 from Rac1 confers interaction with Vav1 to Cdc42 111
7.8.2 Rac1 tryptophan 56 does not suggest an obvious mechanism of Vav1 specificity 117
7.9 Assessing the requirements for Rac1 and Cdc42 on calcium influx downstream of TCR ligation 120
7.9.1 Vav2 requires Cdc42 to inhibit TCR initiated calcium influx 120
7.10 The portions of Vav1 sufficient to positively impact calcium signaling in Jurkat T cells 127
7.10.1 The GEF region of Vav1 is not sufficient to support strong calcium signaling in T cells 127

8 Discussion 133
8.1 Summary of major findings 133
8.1.1 Overview of the differential contributions of Vav1 and Vav2 to calcium signaling in Jurkat T cells 133
8.1.2 T cell calcium inhibition by Vav2 is independent of its CH domain 136
8.1.3 The catalytic activities of Vav1 and Vav2 play different roles in Jurkat T cell signaling 136
8.1.4 Vav1 has multiple regions that are necessary to fully support calcium signaling. 137
8.1.5 Active Cdc42 dramatically suppresses TCR signaling 138
8.1.6 Vav2 interacts with a number of Rho GTPases, while Vav1 only interacts with Rac1 140
8.2 Implications 141
8.2.1 Other Rho family GEFs in T cells 141
8.2.2 Differential use of Vav2 in immune cell subsets 142
8.2.3 Vav2 upregulation in regulatory T cells 143
8.3 A new assay to assess GEF-GTPase interactions 145
8.3.1 GEF-GTPase interactions can be visualized in live cells 145
8.3.2 Expression levels in the GEF trapping assay 146
8.3.3 Expanding the reach of the GEF trapping assay 147

9 References 150

3 Index of Figures

Figure 1: The structure of Vav proteins 5
Figure 2: Conformational regulation of Vav GEF activity 6
Figure 3: Relative expression levels of Vav1 and Vav2 in hematopoietic cell types 9
Figure 4: Imaging SLP-76 Microclusters 13
Figure 5: Activation of NF-AT by cytosolic calcium in T cells 19
Figure 6: Initiation of calcium influx by TCR ligation 22
Figure 7: Location and frequency of Vav1 mutations in ATL 26
Figure 8: GTPase activation cycle 31
Figure 9: Rho GTPase subfamilies 32
Figure 10: J.Vav1 Jurkat cells serve as models for primary T cells 44
Figure 11: Level-dependent effects of constructs on calcium signaling 46
Figure 12: Sequence alignment of the CH domain deletions and chimeras used 54
Figure 13: Alignments of Vav CH domain mutants 55
Figure 14: Alignment of Vav1 and Vav2 constructs that contain mutations in the catalytic core 56
Figure 15: Sequences of major GTPases used 57
Figure 16: Vav1 and Vav3 support calcium signaling in Jurkat while Vav2 inhibits calcium influx. 65
Figure 17: Vav family expression in Jurkat cells 66
Figure 18: Relative amounts of Vav2 expression 67
Figure 19: Vav1 and Vav2 CH domains support calcium signaling 70
Figure 20: The catalytic core of Vav2 conveys calcium inhibition into a Vav1 chimera 72
Figure 21: Vav1 and Vav2 amino acid conservation around the critical LK residues 74
Figure 22: Vav2 catalytically inhibits Jurkat T cell calcium signaling 75
Figure 23: ΔCH Vav1 does not require catalytic activity for calcium inhibition 77
Figure 24: Rho family GTPases: Subfamilies and T cell expression 80
Figure 25: Calcium profiles of select active Rho family GTPases 81
Figure 26: Cdc42 isoform differences and expression pattern 83
Figure 27: Both Cdc42 isoforms and CA mutations inhibit calcium signaling 84
Figure 28: Overview of the 'GEF-trapping' imaging assay 87
Figure 29: Verifying the 'GEF-Trapping' assay with Vav1, Vav2, and Rac1 90
Figure 30: Limiting co-localization assessment to the periphery of the cell 93
Figure 31: Only Vav2 shows localization with Rac2 96
Figure 32: RhoA shows no colocalization with Vav1 and little with Vav2 97
Figure 33: RhoG shows no colocalization with Vav1 and little with Vav2 98
Figure 34: The Vav2 GEF domains recruit Cdc42 to the SLP-76 MC, but the Vav1 GEF does not 100
Figure 35: The DH domain of Vav1 conveys GTPase specificity to Vav2 103
Figure 36: Vav2 with the GEF surface of Vav1 maintains Cdc42 interaction 105
Figure 37: The first helix of the Vav1 DH does not convey Rac1 specificity 108
Figure 38: Transfer of the DH core of Vav1 does not support GTPase binding 109
Figure 39: The Vav1 DH long helix does not transfer Rac1 specificity 110
Figure 40: Representation of the Rac1 / Cdc42 divisions used for section swaps 113
Figure 41: GTPase chimeras with the N-terminus of Rac1 co-localize with Vav1 114

Figure 42: Amino acids 46-77 of Rac1 cause Cdc42 to co-localize with Vav1 115
Figure 43: Cdc42 with a F56 to W mutation gains co-localization with Vav1 116
Figure 44: The W56 residue of Rac1 has no obvious interactions with Vav1 119
Figure 45: Rac inhibition reduces TCR activation initiated calcium influx, Cdc42 inhibition has no effect..... 124
Figure 46: Inhibition of Cdc42 increases the calcium influx of cells expressing Vav2 126
Figure 47: The Minimal Amount of Vav1 that Can Convey Calcium Signaling Enhancement to Vav2 130
Figure 48: Sequence conservation of the Vav1 polybasic region..... 132
Figure 49: Proposed model of Vav1/2 involvement in T cell calcium signaling 134

4 Abbreviations and Acronyms used in this Thesis

APC	Antigen-presenting cell
αPIX	also ARHGEF6, a GEF for Rho family GTPases
ATL	Adult T cell leukemia/lymphoma
βPIX	also ARHGEF7, a GEF for Rho family GTPases
C1 domain	Domains that are often involved in binding DAG
CA	Constitutively Active
CH domain	Calponin homology domain
CRAC	Calcium release-activated calcium channel – PM calcium channel in T cells, made of Orai1 proteins
DAG	Diacylglycerol
DH domain	Dbl homology domain – a common catalytic domain among Dbl family GEFs
DN	Dominant Negative
DOCK (2/8/180)	Dedicator of cytokinesis – GEFs for Rho family GTPases
ER	Endoplasmic reticulum
GADS	GRB2-related adapter protein 2 – constitutively bound to SLP-76 and recruits to phosphorylated LAT
GAP	GTPase-Activating Protein – catalyzes the hydrolysis of GTP to GDP in GTPases
GDI	Guanosine nucleotide dissociation inhibitor – locks GTPases in an inactive, cytosolic state
GEF	Guanine nucleotide exchange factor
GTPase	Small proteins that can bind and hydrolyze guanosine triphosphate (GTP)
IP3	Inositol 1,4,5-trisphosphate – released from PIP2 by PLC proteins. Bind and open IP3R1 in the ER membrane
IP3R1	Inositol 1,4,5-Trisphosphate Receptor, Type 1 – a calcium channel in the ER membrane that opens in response to IP3
Itk	Interleukin-2-inducible T-cell kinase – phosphorylates and activates Plcγ1
LAT	Linker for Activation of T cells – membrane-bound adapter protein that serves as a scaffold for SLP-76 microclusters
LCK	A member of the SRC family of tyrosine kinases. T cell specific and critical for early TCR signaling

MC	Microcluster – a complex of adapter and effector intracellular proteins
mCer3	mCerulean3 – a monomeric blue protein
NF-AT	Nuclear Factor of Activated T cells – critical transcription factors that are activated downstream of calcium influxes
Orai	Proteins that make up the CRAC calcium channel in T cells that responds to TCR stimulation.
PB region	Polybasic region – a stretch of lysines and arginines in Vav1
PH domain	Pleckstrin homology domain – often binds PIP2 or PIP3
Plcβ	Phospholipase C, Beta – hydrolyzes PI(4,5)P2 into DAG and IP3
Plcγ1/2	Phospholipase C, Gamma 1/2 – hydrolyzes PI(4,5)P2 into DAG and IP3
PM	Plasma membrane
PIP5K	Phosphatidylinositol-4-Phosphate 5-Kinase, Type I, Alpha – Phosphorylates PI(4)P to form PI(4,5)P2
PIP2	Phosphatidylinositol 4,5-bisphosphate – cleaved by Plc proteins to make DAG and IP3
PIP3	Phosphatidylinositol 3,4,5-trisphosphate – a membrane bound phospholipid, serves as a ligand for PH domains of pro-growth proteins
Ras family	A family of small GTPases that stimulate cell growth and are implicated in many forms of tumors
STIM1	Stromal interaction molecule 1 – an ER transmembrane protein that interacts with Orai1 to facilitate calcium influx
SCID	Severe combined immunodeficiency
SRC family	A family of non-receptor tyrosine kinases that includes LCK
SYK family	Spleen Tyrosine Kinase family – non-receptor tyrosine kinases that include ZAP-70
Trio	A GEF for Rho family GTPases
TIAM1	T-Cell Lymphoma Invasion And Metastasis 1 – a GEF for Rho family GTPases
WASP	Wiskott-Aldrich Syndrome Protein – cytoskeletal protein associated with actin filaments. An effector of Cdc42
LK-AA	Leu-334-Ala, Lys-335-Ala

SH2	Src Homology 2 – a protein domain that typically binds phospho-tyrosines
SH3	Src Homology 3 – a protein domain that typically binds proline-rich regions
SLP-76	SH2 domain–containing Leukocyte Protein of 76 kD
TCR	T Cell Receptor
TRT	Tag-RFP Turbo – a red fluorescent protein
Vav	A group of GEFs for Rho family GTPases
WAVE	WASp Family Verprolin-homologous Protein – a Rac cytoskeletal effector that contributes to membrane ruffling
ZAP70	Zeta-chain-associated protein kinase 70kDa – a member of the SYK family. Critical for T cell activation

Notes to readers:

-My research has involved the creation and testing of numerous mutant and chimeric proteins, especially between Vav1 and Vav2. I have a provided a visual guide to help keep them organized. This guide is included in one of the first pages of the Discussion section, on page 135; but it may be helpful to refer to it earlier.

-Vav1 was the first of three isoforms to be discovered, and was initially referred to simply as ‘Vav’ in the literature until Vav2 and Vav3 were discovered and reported. For the sake of brevity, I will repurpose ‘Vav’ along with ‘Vav proteins’ in this thesis to refer to common characteristics of these proteins, and use their individual names to discuss unique characteristics.

4 Introduction

4.1 The Vav family of proteins

4.1.1 Vav proteins as GEFs

Vav1 was originally discovered in carcinoma tissue (Katzav et al., 1989). As it was the sixth transforming protein identified in that lab, it was named for the sixth character in the Hebrew alphabet, *vav*. Shortly after the discovery of Vav1, the protein was characterized as a phosphorylation-dependent guanine nucleotide exchange factor (GEF) that activates Rho-family GTPases (Crespo et al., 1997). This family of small GTPases has ~25 members, including Rac1, Rac2, RhoG, RhoA, and Cdc42. These GTPases play important roles in a variety of functions, including cytoskeletal remodeling, vesicle trafficking, transcription factor activation, DNA synthesis, and apoptosis (Pernis, 2009).

Vav proteins are activated by a wide variety of external stimuli. The downstream signaling from numerous receptors relies on Vav proteins, including signals from T cell and B cell receptors (TCR and BCR), growth factor receptors, integrins (Martinez Gakidis et al., 2004), complement receptors (Hall et al., 2006), Fc receptors (Utomo et al., 2006), costimulatory receptors such as CD28 in T cells and CD19 in B cells, and numerous others (Turner and Billadeau, 2002). Once activated, Vav proteins are responsible for amplifying these signals by, among other things, catalytically activating GTPases

4.1.2 Vav domain structure

The Vav family of proteins is represented by a single protein, *vav*, in *Drosophila* and other invertebrates, and in mammals by the three family members: Vav1, Vav2, and Vav3 (Malartre et al., 2010; Turner and Billadeau, 2002). These mammalian Vav isoforms share a common domain structure (Figure 1). The N-terminus of the protein is a calponin homology (CH) domain followed by an unstructured, flexible region characterized by multiple acidic residues (the acidic linker). The putative role of CH domains is to bind actin when expressed as a tandem pair on the same protein. However, Vav proteins only contain a single CH domain, and appear to have utilized this CH domain for auto-regulation (discussed below). The catalytic surface of Vav exists only on the DH domain. However, the full catalytic activity of Vav requires contacts between the DH domain and the adjacent PH and C1 domains (Chrencik et al., 2008; Rapley et al., 2008). Therefore, we call this DH-PH-C1 portion of the protein the 'catalytic core' of the protein. The PH and C1 domains appear to primarily play roles in supporting catalytic activity. Although PH domains can bind phosphoinositides, the Vav PH domain lacks membrane binding signatures (Lenoir et al., 2015). Similarly, C1 domains often bind diacylglycerol for membrane recruitment; but Vav has an 'atypical' C1 domain with no obvious function other than supporting the catalytic activity of the DH domain (Geczy et al., 2012).

The C-terminal portion of Vav consist of two SH3 domains bookending a single SH2 domain. The n-terminal SH3 (nSH3) is a non-canonical SH3 domain that interacts with a proline-rich sequence of Vav itself (Ogura et al., 2002). The C-terminal SH3 domain (cSH3) and the SH2 domains bind proline-rich and

phosphorylated tyrosine ligands, respectively, and have been reported to bind dozens of proteins (Bustelo, 2012). Among this list of potential binding partners are growth factor receptors (i.e. epidermal growth factor receptor, or EGF-R), immuno-receptor activated tyrosine kinases (ZAP-70 and spleen tyrosine kinase, or SYK), cytoskeletal proteins (zyxin), and even RNA binding proteins. Although it seems unlikely that so many proteins are actually vying for direct binding to this region of Vav in the normal functioning of T cells, the size and diversity of the list of purported binding partners for Vav proteins emphasizes the number of cellular processes these proteins can potentially influence.

Vav proteins are conformationally auto-inhibited in the cytosol of resting cells. The crystal structure of the N-terminus of Vav1, from the CH domain through the C1 domain, shows that the acidic linker winds around the CH domain, and this structure is tucked into the catalytic pocket, obstructing GTPase contact (Figure 2)(Yu et al., 2010). The acidic region contains three tyrosines that coordinate with hydrophobic pockets on the CH domain (Tyr^{143} and Tyr^{160}) and on the DH domain (Tyr^{174}). Cell stimulation, such as TCR ligation, leads to the phosphorylation of these tyrosines by Src family kinases (Crespo et al., 1997; Han et al., 1997b). Phosphorylation disrupts the tight integration of the CH domain and acidic linker with the DH. This disruption leads to the exposure of the catalytic pocket of the DH domain and the activation of Vav (Aghazadeh et al., 2000; Han, 1998; López-Lago et al., 2000; Yu et al., 2010; Zugaza et al., 2002). Mutations of Vav that remove portions of the CH domain, the entire CH domain, or the CH domain and acidic linker up through Tyr^{174} result in constitutively active proteins. A similar activation is achieved by mutating these

tyrosines, particularly Tyr^{174}, to either phenylalanines or aspartic acids (a phospho-tyrosine mimic) (Yu et al., 2010; Zugaza et al., 2002).

The mechanism of the autoinhibition of Vav proteins by N-terminus has been appreciated for well over a decade. However, a new study has uncovered another form of Vav regulation. Data from the Bustelo lab show that the C-terminal SH3 domain is also important to maintain Vav proteins in an inactivate state. This SH3 domain is thought to fold back into the catalytic core of the protein in resting cells (Figure 2) and this configuration contributes to an inhibition of Vav proteins. Phosphorylation of Tyr^{836} on the C-terminus of the domain releases the cSH3 from binding to the core of Vav, helping to activated the protein (Barreira et al., 2014). Mutations that disrupt the interactions of the cSH3 with the DH-PH-C1 domains create Vav proteins with basal catalytic activity. This newly discovered extra level of inhibition underscores the need for tight regulation of the activity of Vav proteins in cells.

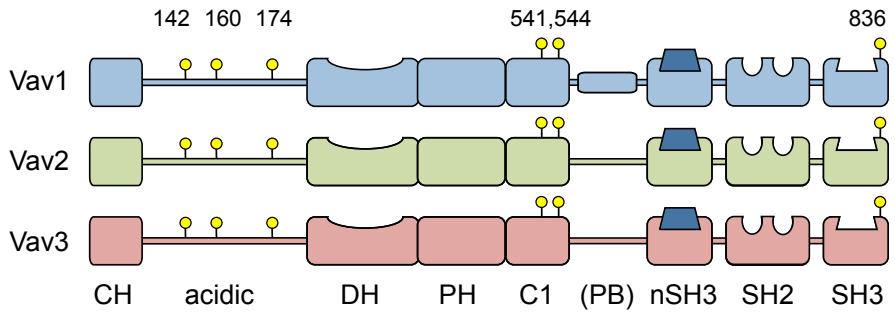

Figure 1: The structure of Vav proteins

Graphical, linear representation of the domain structure of the three mammalian Vav proteins. The N-terminal CH domain coordinates with the acidic linker region to inhibit resting Vav (see below). The three critical activating tyrosines are labeled in the acidic region with Vav1 numberings. The DH domain contains the catalytic surface that activates Rho family GTPases. The PH and C1 domains support the catalytic activity of the DH domain. Two tyrosines in the C1 domain that are involved in regulation are shown with Vav1 residue numberings. Following the C1 domain is a linker region in Vav2 and Vav3, but this region in Vav1 has a special motif we call the 'polybasic' (PB) region (discussed later in the thesis). The C-terminus of Vav proteins contain an atypical SH3 that binds a proline region in itself (denoted by the blue trapezoid). This is followed by an SH2 domain that binds phospho-tyrosines of other proteins, notably SLP-76 in T cells. The C-terminal SH3 domain (cSH3) is regulatory in the resting cell, and contains another activating tyrosine indicated here with Vav1 numbering. On activated Vav proteins, the cSH3 is capable of binding proline motifs in numerous proteins.

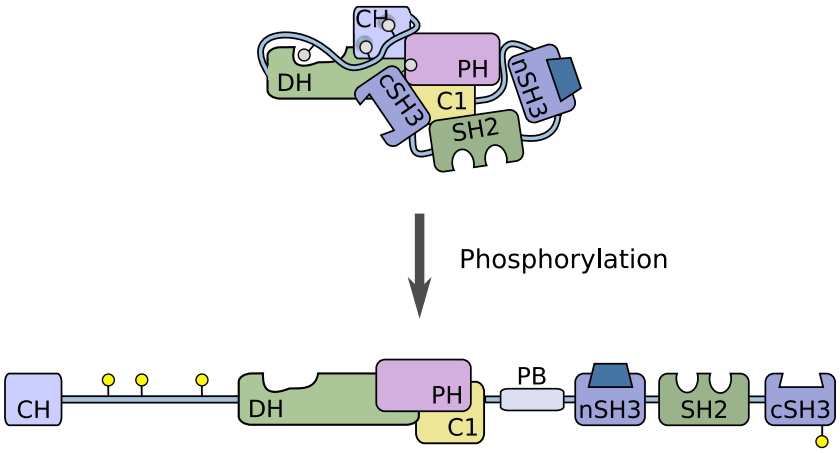

Figure 2: Conformational regulation of Vav GEF activity

A model of the levels of regulation of Vav proteins. **Upper:** in the cytoplasm of resting cells, Vav proteins are normally held in a conformationally inactive configuration. Un-phosphorylated tyrosines in the acidic linker region coordinate with pockets in the CH domain and DH domain to pull these domains together and occlude the catalytic pocket of the DH domain. The cSH3 domain also coordinates with surfaces on the DH, PH, and C1 domains to further inactivate the catalytic potential of Vav. When a stimulus to the cell causes the activation of tyrosine kinases, tyrosines in Vav are phosphorylated, opening up the C-terminus of the protein and allowing its recruitment to signaling complexes. Once there, the tyrosines in the acidic region are phosphorylated, displacing the CH domain and acidic region from the catalytic pocket of the DH domain. Fully phosphorylated Vav proteins serve roles as both GEFs and scaffolding proteins.

4.1.3 Tissue distribution of Vav isoforms

The three mammalian Vav isoforms have different patterns of tissue distribution. Vav1 is almost exclusively expressed in hematopoietic tissue. Vav2 expression is also mainly in hematopoietic tissue, but it can be found in a number of tissues outside of this compartment, such as pancreatic beta cells (Veluthakal et al., 2015). Vav3 has the broadest expression pattern in the body. These patterns suggest that the individual Vav isoforms have unique properties that benefit specific cell types. Within hematopoietic cells, Vav isoforms have different expression patterns in distinct immune cell subsets. Moreover, elegant knockout studies in mice have shown that B cells rely on different Vav isoforms than T cells for development and activation. T cell development and function are severely impaired in Vav1 knockout (KO) mice, but relatively unaffected in Vav2 or Vav2/Vav3 double KO mice. In contrast, Vav2 plays a critical role in the development and activation of B cells. Vav3 has minimal unique contributions to T cells and B cells, but can partially compensate for the loss of either of the others (Fujikawa et al., 2003; Tedford et al., 2001; Zakaria et al., 2004).

One explanation for the results of these knockout studies is that a cell's reliance on a particular Vav isoform simply mirrors the relative expression level of that isoform. T cells rely primarily on Vav1 for development and activation, and these cells express far more Vav1 than Vav2 or Vav3 (Figure 3 and Figure 17). Accordingly, B cells express higher levels of Vav2 and lower levels of Vav1 than T cells, and they show a much greater impact from the loss of Vav2. However, other studies have revealed unique signaling properties of Vav1 and Vav2. Overexpression of Vav2 leads to the inhibition of key transcription factors in T cells, but augments the

activity of the same transcription factors in B cells (Doody et al., 2000; Tartare-Deckert et al., 2001). The mechanisms behind these differences are not yet understood, and have been a major focus of my research. Of course, my investigations on these differences have relied on the substantial understanding that we do have on the mechanisms of Vav activity.

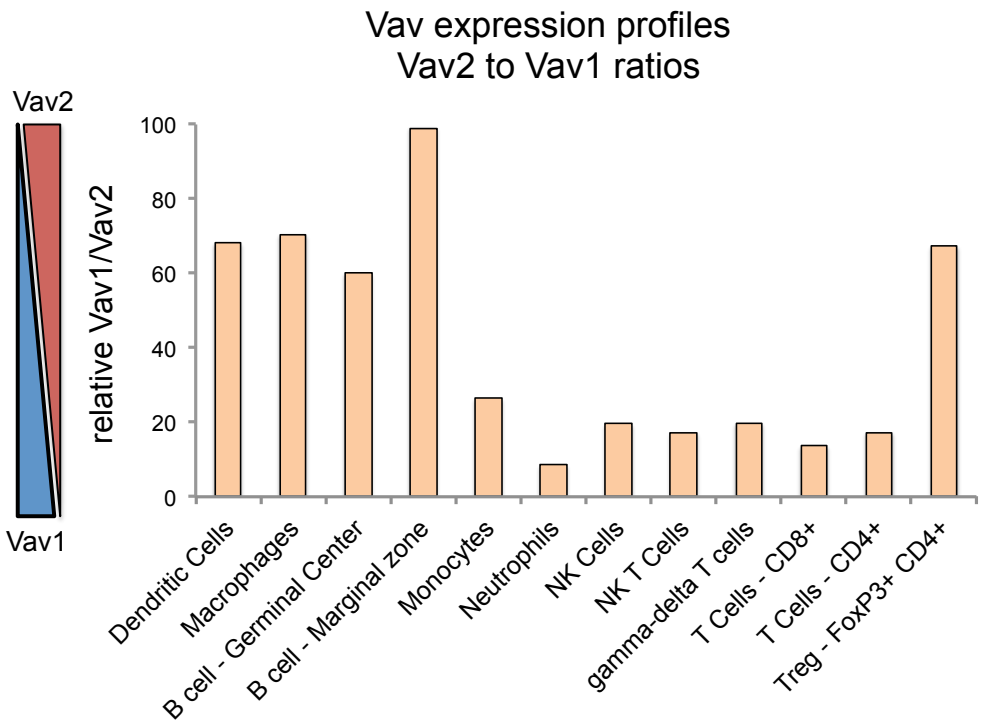

Figure 3: Relative expression levels of Vav1 and Vav2 in hematopoietic cell types

Comparison of the relative amounts of Vav2 and Vav1 in a selection of immune cell subsets. mRNA expression data on murine hematopoietic cells was collected from Immgen.com (Heng and Painter, 2008). Higher bars represent greater amounts of Vav2 relative to Vav1. Of note, this graph is meant to convey the cells that express more or less Vav2, the cells with higher Vav2 expression still typically express substantial amounts of Vav1.

4.2 Vav proteins in T cell signaling

4.2.1 Vav1 and SLP-76 microclusters

The presence of an SH2 domain makes the Vav family of proteins unique among Dbl family GEFs, which are GEFs that contain a DH domain (Bustelo, 2012). The ligation of many cell surface receptors result in the activation of tyrosine kinases, and the SH2 domain of Vav positions it to respond to these signals. In T cells, the activation of the TCR, either by interaction with cognate pMHC or by activating antibodies, leads to the phosphorylation of tyrosines the CD3 chains by the SRC family kinase Lck. These tyrosines are found in amino acid patterns called immunotyrosine activation motifs (ITAMs). Phosphorylated ITAMs recruit the SYK family tyrosine kinases ZAP-70, which is activated in turn by Lck. Active ZAP-70 phosphorylates the adapter protein Linker of Activated T cells (LAT), and then the SH2 domain containing Leukocyte Protein of 76 kD (SLP-76) that recruits to phosphorylated LAT.

SLP-76 and LAT form the foundation for the recruitment of multiple other effector and adapter proteins, and we refer to this complex as the SLP-76 microcluster (Bunnell et al., 2002; Bunnell et al., 2006). These microclusters can be imaged by expressing fluorescently tagged SLP-76 constructs, along with other microcluster components with fluorescent tags (Figure 4). Live cell imaging of SLP-76 microclusters show a consistent phenotype. Microclusters form within seconds of the cell contacting a surface coated with anti-CD3 antibodies. As the cell is spread out on the stimulatory surface, SLP-76 microclusters continue to form in the periphery and flow in to the center of the contact. The formation and persistence of these clusters can

be recorded, and different mutations in SLP-76 or other microcluster components have been found to cause perturbations in the nucleation or longevity of the clusters.

The formation of SLP-76 microclusters is critical for T cell activation. Mutations of SLP-76 that lead to defects in the nucleation, movement, and persistence of SLP-76 MC also lead to defects in T cell thymic development and activation-induced proliferation (Bunnell et al., 2006; Myung et al., 2001). These mutations likewise cause defects in T cell calcium signaling, CD69 upregulation, and the activation of critical transcription factors (Singer et al., 2004).

Vav1 is recruited to SLP-76 microclusters after TCR ligation in both Jurkat T cells (Sylvain et al., 2011) and in murine T cells (Ksionda et al., 2012). This localization is facilitated by the SH2 domain of Vav1 binding phospho-tyrosines 113 and/or 128 on SLP-76. Moreover, our lab has shown that Vav1 is an integral component of SLP-76 microclusters. Jurkat T cells with endogenous levels of Vav1 form stable, persistent SLP-76 microclusters. Jurkat T cells with a targeted knockdown of Vav1 (J.Vav1) form fewer clusters, and the clusters that do form quickly lose coherence (Sylvain et al., 2011). The defects in SLP-76 microclusters caused by a Vav1 KO are not due to the loss of the GEF activity of Vav1, as an a addback of either catalytically inactive or wild-type Vav1 completely restores the formation and persistence of SLP-76 microclusters. Thus, Vav1 contributes to the scaffolding of the SLP-76 MC independently of its catalytic functions.

4.2.2 Catalytic and scaffolding functions of Vav1 in T cell signaling

The T cells defects in development and activation shown by Vav1 KO mice closely parallel the T cell defects in mice with SLP-76 mutations that disrupt the

formation and persistence of microclusters (Fujikawa et al., 2003; Myung et al., 2001; Tedford et al., 2001). As the loss of Vav1 also disrupts SLP-76 microclusters, the T cell abnormalities in Vav1 KO mice could be explained by the loss of SLP-76 microcluster coherence, rather than the loss of specific signaling contributions by Vav1.

A more recent mouse model was created in an attempt to separate the catalytic and scaffolding contributions of Vav1 to T cell signaling. The authors of this study added a catalytically dead Vav1 (using an 'LK-AA' mutation discussed later) to a Vav1 knockout mouse (Saveliev et al., 2009). They found that the catalytic activity of Vav1 contributes to T cell thymic development, and to the proliferation, cytokine expression, and upregulation of activation markers of peripheral T cells. However, the catalytic activity of Vav1 was not necessary for stimulated T cells to flux calcium, activate key transcription factors, and polarize the microtubule organizing center to the point of T cell and APC contact (Saveliev et al., 2009). These data, combined with the findings of our lab (Sylvain et al., 2011), establish that Vav1 has both structural and catalytic roles, and that both are necessary for the normal functioning of T cells. My thesis studies were designed to further tease apart the catalytic and scaffolding contributions of Vav1 to T cell activation. However, as the dysregulated expression and activation of Vav proteins is implicated in pathologies (see below for a discussion), an understanding of how Vav functions in immune cells can both benefit from and add to the knowledge of the roles Vav proteins play in human disease.

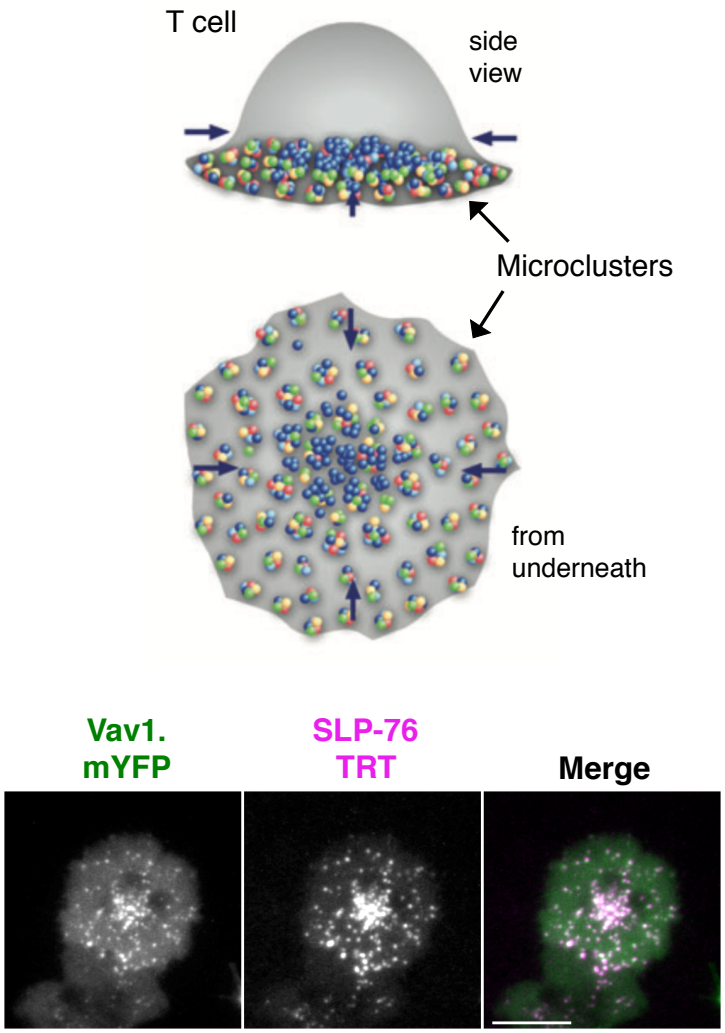

Figure 4: Imaging SLP-76 Microclusters

Upper: Drawing of a T cell that has landed and spread out on a stimulatory surface. The top images is a 'side view' of the cell, and the lower image is the same cell, but viewed from the perspective of the imaging surface, as with a microscope. The colored dots represent different fluorescently labeled proteins in the same microcluster. When cells are only stimulated with anti-CD3, as is the case in this thesis, the SLP-76 microclusters will form in the periphery and centralize over time to accumulate in the center of contact. Image is adapted from Yokosuka and Saito (2009). **Lower:** Representative confocal image of SLP-76 microclusters. Vav1

deficient Jurkat T cells (J.Vav1) expressing TRT (red) tagged SLP-76 and mYFP tagged Vav1 were plated on a glass surface coated with anti-CD3. Cells were fixed after seven minutes and imaged. The three panels are from the same, representative cell. The first column shows the YFP channel, the second the TRT/RFP channel, and the third column is a merge of the YFP channel in green and the TRT channel in magenta. Puncta/microclusters of SLP-76 and Vav1 co-localize to appear white. Scale bar represents 10 micrometers.

4.3 Calcium signaling in T cells

4.3.1 Calcium signaling is essential for T cell activation

Calcium is used as a second messenger in almost every cell type. In T cells, a dramatic increase in intracellular calcium has long been used as an early readout for productive TCR signaling. This increase in cytosolic calcium is critical for T cell activation. Accordingly, people who have genetic defects in calcium channels experience severe combined immunodeficiency (SCID) (Oh-hora and Rao, 2008). On the other end of the spectrum, patients needing immunosuppression can be treated with drugs that disrupt the calcium signaling pathway. These therapies, including rapamycin (also called sirolimus), or tacrolimus (also called FK-506), are often effective enough to suppress the T cell mediated rejection of allogeneic organ transplants.

4.3.2 Calcium signals halt T cells

Increases in intracellular calcium trigger a number of responses in T cells. One of the early effects of a calcium influx is to halt the migration of T cells. The initiation of a T cell driven adaptive immune response requires the T cells to recognize specific antigens in the context of major histocompatibility proteins (MHC) on the surface of antigen presenting cells (APCs). The pool of T cells is quite large, approximately $4x10^{10}$ CD8+ T cells in an adult human. Of these cells, an estimated $4x10^{3}$ to $4x10^{5}$ have a T cell receptor (TCR) that is specific for a particular antigen (Alanio et al., 2010). Therefore, the vast majority of the naïve T cells that come into contact with an APC will not recognize presented peptides. Each T cell that contacts an APC needs to make relatively quick decision on whether to halt or move on. Thus, a productive

ligation of a TCR by its cognate peptide-MHC (pMHC) must initiate a rapid cytosolic signal to halt the cell.

Changes in cytosolic calcium concentrations are ideal for this type of rapid signaling. Calcium is maintained at nanomolar levels (~100-200 nM) in the cytosol, while it exists at micromolar concentrations (~1-2 mM) in extracellular fluids. This dramatic gradient allows for a rapid movement of calcium ions into the cell when calcium channels in the PM are opened. TCR activation leads to a strong increase in cytosolic calcium within seconds. Calcium ions also rapidly diffuse throughout the cytosol, ensuring that signals from the TCR are not restricted to the local point of ligation.

Increases in cytosolic calcium have immediate effects on T cell morphology and behavior. At low levels of calcium, lymphocytes adopt a mobile, crawling phenotype, useful for scanning for activating stimuli. High intracellular calcium levels cause T cells to halt migration and become rounded. Although calcium is not the only ion that plays important roles in T cell signaling, calcium influxes are both necessary and sufficient to halt the migration of T cells at APCs (Negulescu et al., 1996). Of course, the *in vivo* interactions of T cells and APCs are more complicated than a simple model of a T cell making a binary decision on whether to halt at an activating APC or not. Experiments using intravital microscopy have shown that, in lymph nodes, T cells typically make serial contacts with multiple activating APCs before creating a long-lasting interaction with a single one (Marangoni et al., 2013). However, each T cell interaction with an activating APC is characterized by a calcium-driven pause in migration.

4.3.3 Intracellular calcium activates the NF-AT transcription factor

One of the most important long-term consequences of TCR induced calcium signaling is the activation of the transcription factor Nuclear Factor of Activated T cells (NF-AT). This transcription factor plays an essential role in the transcription of a variety of cytokines, including IFN-γ, IL-2, IL-4, TNF, and IL-10. NF-AT is also necessary for the upregulation of cell surface markers such as CD40L and CD95L (Fas ligand) (Macian, 2005). Along with its role in T cell activation, NF-AT activation is critical for the initiation of T cell anergy or the development of regulatory T cells (Tregs), depending on the absence or presence of costimulatory signals (Müller and Rao, 2010). NF-AT activation is often used as a downstream readout of robust calcium signaling in studies of T cell activation, as the link between the two is so well established.

In order to activate NF-AT, high levels of cytosolic calcium first activate the protein calmodulin (see Figure 5). A molecule of calmodulin has four calcium binding sites, which become occupied in the presence of high calcium concentrations and lead to a conformational change. In the calcium bound state, calmodulin then binds to and activates calcineurin, a serine/threonine phosphatase. Activated calcineurin dephosphorylates NF-AT proteins, exposing a nuclear localization signal (NLS), leading to the nuclear localization of NF-AT where it can initiate transcription. Real-time imaging of primary cells show that the majority of NF-AT translocates from the cytosol to the nucleus within the first 2-15 minutes of T cell stimulation by an APC (Singleton et al., 2009). The dynamics of calcium influx and NF-AT localization may depend on the type of T cell, and may vary between Th-1, Th-2, and Th-17 cells

(Weber et al., 2008). Nevertheless, the activation of NF-AT transcription is necessary for T cell activation. The powerful immunosuppressants cyclosporine and tacrolimus, mentioned earlier, function by inhibiting calcineurin, thus keeping NF-AT out of the nucleus.

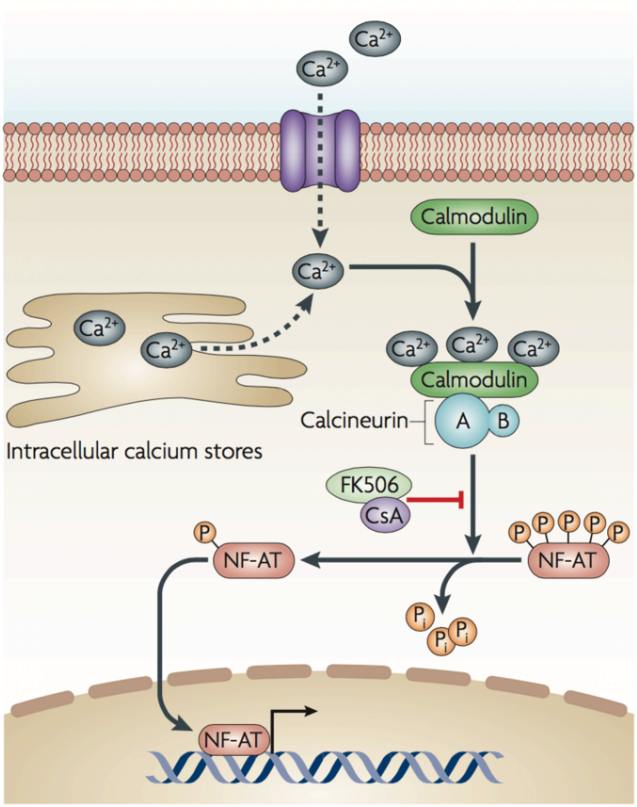

Figure 5: Activation of NF-AT by cytosolic calcium in T cells

A depiction of the sequence of events that lead to the activation of NF-AT transcription factors. Opening of calcium channels in the PM and/or ER lead to increases in the concentration of cytosolic calcium. Calcium molecules then bind to the adapter protein calmodulin, causing a conformation change in the protein. This form of calmodulin binds and activates the phosphatase calcineurin. Multiple phosphorylated residues on NF-AT transcription factors are then de-phosphorylated by calcineurin. This exposes a nuclear localization signal (NLS) on NF-AT, and NF-AT enters the nucleus to initiate transcription. Also pictured are the immunosuppressants cyclosporine (CsA) and FK506, that serve to block immune cell activation by inhibiting the phosphatase activity of calcineurin. The figure is adapted from (Steinbach et al., 2007).

4.3.4 Calcium influxes trigger vesicle mobilization

In addition to halting T cells and activating NF-AT, calcium influxes influence the movement of intracellular vesicles and the delivery of the contents of these vesicles to the exterior of the cell. Analogous to the delivery of neurotransmitters to the neuronal synapses after calcium spikes in these cells, vesicles containing cytokines or perforin and granzymes can be delivered to the immunological synapse from a T cell or NK cell when these cells experience an increase in cytosolic calcium. Calcium influxes into mast cells also drive their degranulation (Oh-hora and Rao, 2008).

4.3.5 TCR triggering of calcium influx and SLP-76 microcluster formation

A great deal has been discovered about the signaling pathway that leads from TCR ligation to the full influx of calcium into the cytosol. This section gives an overview of the state of our understanding, with Figure 6 as a graphical representation of this pathway. The sequence of events that leads from TCR ligation to the formation of SLP-76 microclusters has been covered above. In T cells, the initiation of calcium signaling relies on the phosphorylation of phospholipase C gamma 1 (PLCγ1) by the IL-2 inducible tyrosine kinase ITK, both of which interact with SLP-76 and SLP-76 microcluster components (Braiman et al., 2006; Bunnell et al., 2000; Cruz-Orcutt et al., 2014; Sherman et al., 2011). Active PLCγ1 cleaves phosphatidylinositol-3,4-bisphosphate (PIP_2) to produce membrane-bound diacylglycerol (DAG), and soluble inositol-1,4,5-trisphosphate (IP3). The liberated IP3 binds to an IP3 receptor (IP3R) in the ER membrane and leads to the opening of this calcium-permeable channel. Calcium in the ER lumen is maintained at micromolar concentrations (~100-800 μM), compared to the nanomolar concentrations in the cytosol. Therefore, opening of the

IP3R leads to a rapid but moderate increase in cytosolic calcium. The depletion of the calcium stores in the ER leads to the oligimerization of transmembrane Stromal interaction molecule 1 (STIM1). Once clustered, STIM1 interacts with the cytoplasmic portion of the PM-spanning ORAI proteins that constitute the calcium-release activated calcium channel (CRAC). This calcium channel then opens to the 1-2mM concentration of calcium in the extracellular fluid, and the cell experiences the full calcium influx associated with TCR ligation.

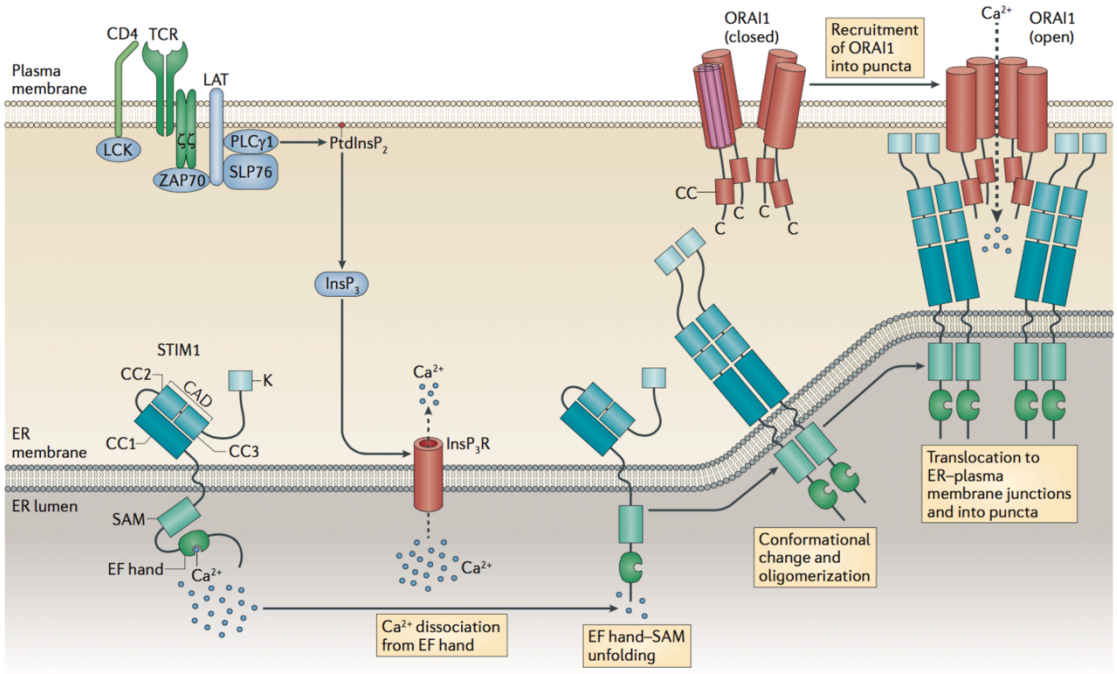

Figure 6: Initiation of calcium influx by TCR ligation

An overview of the events that lead from TCR activation to a full increase in cytosolic calcium. TCR activation with costimulation (CD4 here) leads to the activation of kinases and the formation of signaling structures, notably the SLP-76 microcluster. Here, the SLP-76 microcluster is represented with only LAT, SLP-76, and PLCγ1, but many other proteins, including Vav1, are involved. PLCγ1 is activated by phosphorylation, and proceeds to cleave PIP2 ($PtdInsP_2$) into diacylglycerol (DAG, not pictured) and soluble IP3 ($InsP_3$). Binding of IP3 to the IP3 receptor ($InsP_3R$) in the ER membrane, leading to the opening of this calcium channel and a moderate increase in cytosolic calcium through release of the calcium stores in the ER. Release of calcium from the ER lumen changes the conformation of the luminal portion of STIM1 proteins, which then oligimerize. The ER membrane moves proximal to the PM, and oligimerized STIM1 can interact with ORAI1 proteins in the PM. Multiple ORAI1 proteins form a calcium permissive channel in the PM, allowing for a large influx of calcium ions into the cell. Diagram is from Feske and Prakriya (2013).

4.3.6 The role of Vav proteins in TCR calcium signaling

The canonical T cell calcium signaling, described above, has no obvious role for Vav1. Nevertheless, Vav1 has long been known to be crucial for a strong calcium influx following TCR activation (Fischer et al., 1995; Krawczyk et al., 2000). Moreover, a triple knockout of the three Vav isoforms abolishes the calcium response in murine T cells (Fujikawa et al., 2003). The mechanism by which Vav1 influences T cell calcium signaling has not been resolved, but the CH domain is known to be necessary. Vav1 constructs lacking an intact CH domain inhibit calcium influx and NF-AT activation (Billadeau et al., 2000; Sylvain et al., 2011; Wu et al., 1995; Zhou et al., 2007). Because of these findings, the Vav1 CH domain has been the focus of most of the research into the role of Vav1 in T cell calcium signaling.

Two recent studies by the Cao lab have attempted to identify the binding partner of the Vav1 CH domain responsible for supporting calcium signaling. The first paper argues that the Vav1 CH binds calmodulin, and that the loss of this interaction leads to the calcium suppression by the ΔCH Vav1 mutant (Zhou et al., 2007). The second paper shows calmodulin binds the first twenty amino acids of the Vav1 CH domain. Also, chimeras of Vav1 with this portion of the CH domain replaced with the equivalent amino acids from Vav2 or Vav3 can no longer increase calcium influx downstream of TCR ligation (Li et al., 2012). However, it is not clear if these chimeric CH domains are folding correctly and are otherwise functional. Moreover, the authors show that moving the N-terminal 20 amino acids of Vav1 into Vav2 or Vav3 enable these isoforms to bind to calmodulin, but then fail to assess if these constructs can now

enhance calcium signaling in T cells. Therefore, the role of calmodulin binding to the Vav1 CH domain in calcium signaling downstream of the TCR remains unresolved.

4.3.7 The catalytic activity of Vav1 is not necessary for calcium signaling

Although the mechanisms by which Vav1 supports a strong calcium influx downstream of TCR ligation are still unknown, multiple studies have found that the catalytic activity of Vav1 is not necessary for this effect. Early studies in Jurkat T cells showed that adding back a GEF inactive mutant of Vav1 rescued the calcium signaling defects of Vav1 deficient cells (Kuhne et al., 2000). This report was followed up with independent confirmations of this finding using addbacks into murine cells (Miletic et al., 2009), and with a different inactivating mutant in knock-in mice (Saveliev et al., 2009). Our lab has used the mutant reported in Saveliev *et al.* to demonstrate that the catalytically dead Vav1 mutant both supports calcium signaling and SLP-76 microcluster persistence (Sylvain et al., 2011).

4.4 Vav proteins in disease

4.4.1 Vav proteins in cancer

The discovery of the *VAV* gene occurred in a screen for transforming genes expressed in human esophageal carcinomas (Katzav et al., 1989). The transforming potential of Vav1 (as it was later named) was determined to be a result of the lack of an intact N-terminal CH domain. However, the authors of the study found that this transforming mutation was the result of a recombination event of the *VAV* gene with the plasmid that was co-transfected to act as a selection marker in the assay. Therefore, the 'oncogenic' form of Vav1 was not present in the tumor samples. So while Vav1

gained fame as a proto-oncogene, the oncogenic form, as defined by a partial or total loss of the inhibitory N-terminus, has not been observed in the clinic (Katzav, 2007). Although this specific mutation may not be physiologically relevant, the ectopic expression or dysregulation of Vav proteins can contribute to tumorigenesis and the development of invasive cancer cells.

The roles of Vav proteins in tumors are the subject of ongoing study. Recent reports have linked ectopic Vav isoform expression or aberrant activation to breast cancer (Aguilar et al., 2014; Citterio et al., 2012; Du et al., 2014; Grassilli et al., 2014; Sebban et al., 2013), gastric cancer (Tan et al., 2014), metastatic melanoma (Liu et al., 2014), and other cancers. Recently, an exhaustive analysis of the mutations involved in 83 cases of Adult T cell leukemia/lymphoma (ATL) found that Vav1 was the seventh of the top 50 most frequently mutated genes in these cells (Kataoka et al., 2015) (Figure 7). More informatively, the mutations in Vav1 are mostly coding mutations that cluster around areas involved in the conformational inhibition of Vav1. One group of mutations occurs around the critical tyrosines at 160 and 174 (Figure 7). These mutations likely disrupt the auto-inhibition of Vav1 and increase basal GEF activity. Other mutations of Vav1 reported in this study involve residues likely necessary for the GEF inhibition imposed by the C-terminal SH3 domain (Figure 7). These findings are strong evidence that disruptions of normal Vav1 auto-inhibition can lead to the development of leukemia/lymphoma.

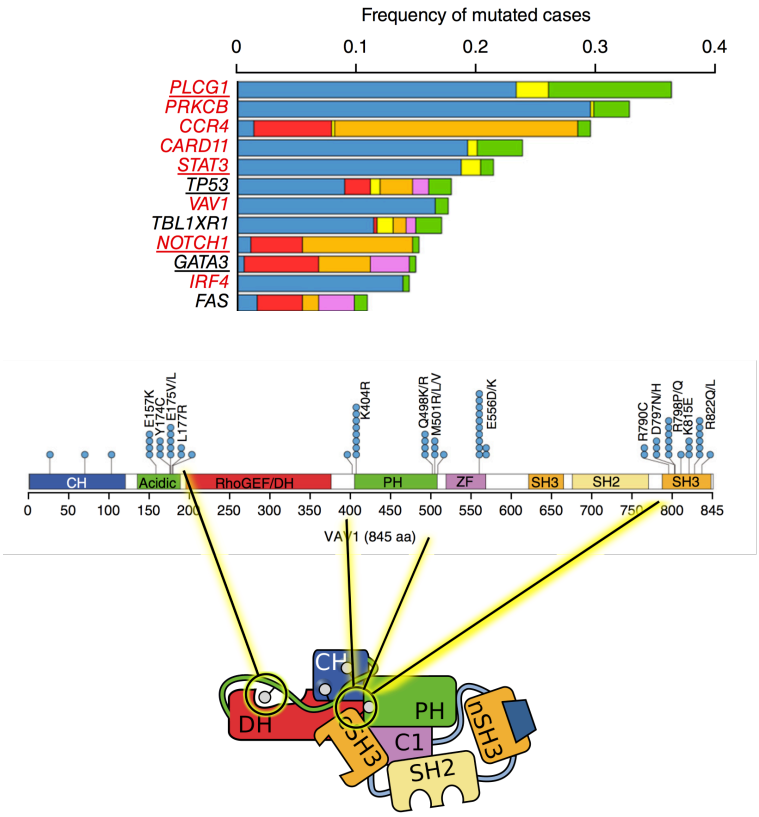

Figure 7: Location and frequency of Vav1 mutations in ATL

Placing the recent findings of mutations in Adult T cell leukemia/lymphoma (ATL) in the context of our understanding of Vav1 regulation. Figures adapted from (Kataoka et al., 2015). **Upper:** Partial representation of the most frequently mutated proteins found in the cancerous tissue of 83 patients with ATL. Vav1 is the seventh most frequently represented. **Lower:** The published analysis of the most frequently mutated residues within Vav1 in these patients, showing the connections with the regulatory regions in Vav1 as I have depicted them here. The collection of mutations in the acidic region is likely to affect the coordination of tyrosine 174 in Vav1 with the DH domain, leading to constitutive exposure of the catalytic surface. The other groups of mutations bear a striking similarity to residues recently implicated in the conformational regulation caused by the cSH3 domain folding back into the catalytic center of the proteins (Barreira et al., 2014). Disruptions of these interactions likely lead to basal activation of Vav1.

4.4.2 Vav proteins as therapeutic targets in cancer and immunosuppression

The evidence linking dysregulated Vav activity to cancer has led to interest in developing new therapies targeting the activation of Rac proteins by Vav1. However, possibly the most interesting therapy targeting Vav1 is one that has been in use since the 1950s: Azathioprine (Elion, 1989). This drug was developed as a treatment for leukemia, and had an immediate and dramatic impact on the survival of children suffering from acute forms of leukemia. The use of Azathioprine quickly spread to other diseases, and it has been widely used to block rejection of organ transplants and to ameliorate autoimmune diseases. Azathioprine was thought to disrupt nucleic acid synthesis, leading to the apoptosis of rapidly dividing cells such as T and B cells, and hence suppress the immune response (Maltzman and Koretzky, 2003). However, recent studies have suggested that the main mechanism of Azathioprine is to disrupt the activation of Rac proteins.

Some of the metabolites of Azathioprine are GTP analogs (6-ThioGTP). These GTP analogs can be loaded into Rac and hydrolyzed to GDP analogs, but cannot then be released, which locks Rac1 into an inactive conformation. Without the ability to activate Rac1, T cells lose effective costimulatory signals from CD28, and undergo apoptosis (Tiede et al., 2003). As Vav1 plays a major role in both CD28 signaling and Rac1 activation, the effect of Azathioprine has been attributed almost entirely to blocking the activation of Rac by Vav1 (Marinkovic et al., 2014; Poppe et al., 2006). While this mechanism has not been conclusively demonstrated, research is actively continuing. For example, Azathioprine is being investigated as means to block Rac and Vav1 dependent metastasis in pancreatic cancer (Razidlo et al., 2015).

To improve our use of therapies targeted at Vav proteins, it will be necessary to understand the differences in signaling properties of each isoform. For instance, Vav2 and Vav3 have both overlapping and non-redundant functions in the initiation of breast cancer metastasis (Citterio et al., 2012). The authors of that study speculate that the differences between the Vav isoforms may lie in GTPase specificities, but we have lacked the tools to decisively test this hypothesis. I proposed that the imaging assay presented in this thesis could be used to determine Vav/GTPase interactions in cancerous cells and improve our ability to therapeutically target these interactions.

4.5 Rho GTPases

4.5.1 The GTPase activation cycle

A single GEF can activate many small GTPases to amplify a signaling cascade. Most small GTPases undergo a cycle of regulation from an inactive, GDP bound state to an active, GTP bound conformation. Vav proteins act on Rho family GTPases, and these small proteins are post-translationally prenylated on the C-terminus with a lipophilic carbon-chain that inserts into membranes. However, in resting cells, the majority of inactive Rho GTPases are held in the cytosol by guanine nucleotide dissociation inhibitors (GDI). These GDIs lock GTPases in a GDP-bound state and contain a binding pocket that sequesters the hydrophobic prenylation. Upon cell stimulation, the GTPase is delivered to a membrane and liberated from the GDI. Activation of a GTPase occurs when the bound GDP is displaced by a GEF, then replaced by one of the free GTP molecules that exist in excess in the cytosol. Active, GTP-bound GTPases have a much lower affinity for the catalytic pocket of the GEF,

and therefore dissociate and go on to bind and activate downstream effectors. The cycle is completed when the GTPase is inactivated by hydrolysis of GTP to GDP by the GTPase, typically catalyzed by the action of a GTPase activating protein (GAP). Inactive GTPases can then be removed from the membrane by GDIs and return to the cytosol.

4.5.2 Functions of Rho GTPases

Rho GTPases are a subset of ~25 GTPases belonging to the RAS superfamily of ~150 members (Rossman et al., 2005). All members of the RAS superfamily are small (~21 kDa) second messenger proteins. These proteins play central roles in a wide variety of cellular events: cytoskeletal rearrangement including cell movement, cell cycle progression, vesicle trafficking and delivery to the PM, activation of MAP kinases, and others (Vigil et al., 2010). Of these roles, Rho family GTPases are primarily known to affect actin cytoskeletal dynamics, but can impact all of the other processes.

Within the Rho family, there are a number of subfamilies based on sequence similarity (Figure 9). Hematopoietic cells mainly include members of the Rac subfamily (Rac1, Rac2, Rac3, and RhoG), the Cdc42 subfamily (Cdc42, RhoJ, and RhoQ), RhoH, and the RhoA family (RhoA, RhoB, and RhoC). In broad strokes, these subfamilies affect different cytoskeletal dynamics. Rac1/2/3 are known to induce the formation of lamellipodia and membrane ruffles when activated. Accordingly, T cells overexpressing the Rac GEF Vav1 have larger lamellipodia compared to controls (Acuto and Cantrell, 2000). Cdc42 is involved in the formation of filopodia, small finger-like protrusions of the membrane. And RhoA is essential for the creation of

actin stress fibers and focal adhesions (Acuto and Cantrell, 2000). However, almost any coordinated interaction of a cell with its environment involves a large number of cytoskeletal movements. Accordingly, Rac1/2, RhoA, RhoG, and Cdc42 are all involved in lymphocyte extravasation, chemotaxis, phagocytosis, and the formation of immunological synapses (Heasman and Ridley, 2008; Mulloy et al., 2010; Niedergang and Chavrier, 2005; Rougerie and Delon, 2012). The activation of each of these GTPases must be precisely controlled both spatially and temporally to accomplish any one of these processes. For instance, phagocytosis of large particles involves the initial activation of Cdc42 at the tip of the phagocytic cup, followed by Rac1 activation forming the walls surrounding the particle, and finally Rac2 activation at the base of the cup during the completion of phagocytosis (Hoppe and Swanson, 2004; Swanson and Hoppe, 2004).

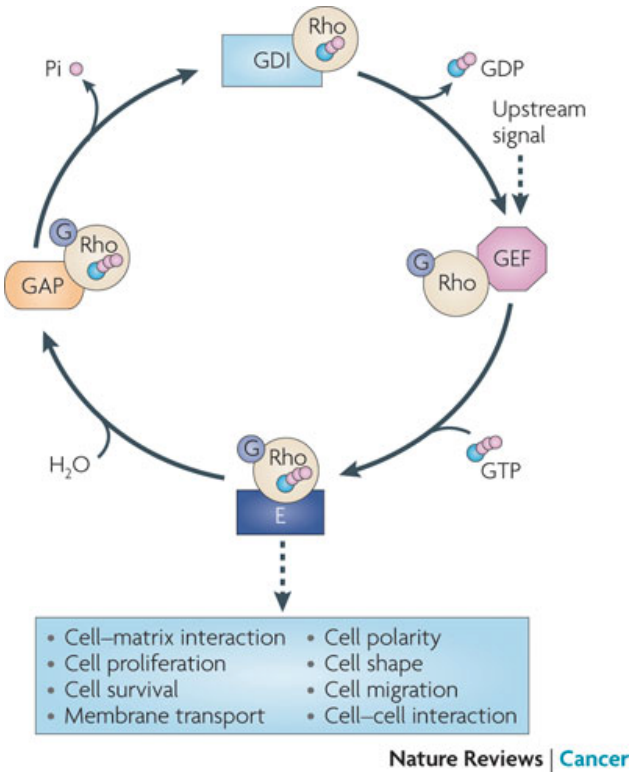

Figure 8: GTPase activation cycle

An overview of the cycle of regulation and activation of most Rho GTPases. From the top, GTPases are typically held in the cytosol of cells in an inactive, GDP-bound state by a guanosine nucleotide dissociation inhibitor (GDI). These GDIs keep the GTPase from releasing GDP, and from inserting into a membrane. Activating stimuli leads to the release of the GTPase from the GDI into a membrane. The GTPase can then encounter a GEF (such as Vav1) that catalyzes the release of GDP and acquisition of a GTP, thus activating the GTPase. Active GTPases then go on to bind and activate downstream effectors. In the case of Rho GTPases, a number of the roles of the effectors are listed in the blue box. The eventual hydrolysis of GTP to GDP by the GTPase is greatly accelerated through the action of GTPase activating proteins (GAPs). Once the GTPases are inactive/GDP bound, GDIs can again remove them from the membrane and hold them in the cytosol, ready for the next cycle. Graphic is from (Vigil et al., 2010).

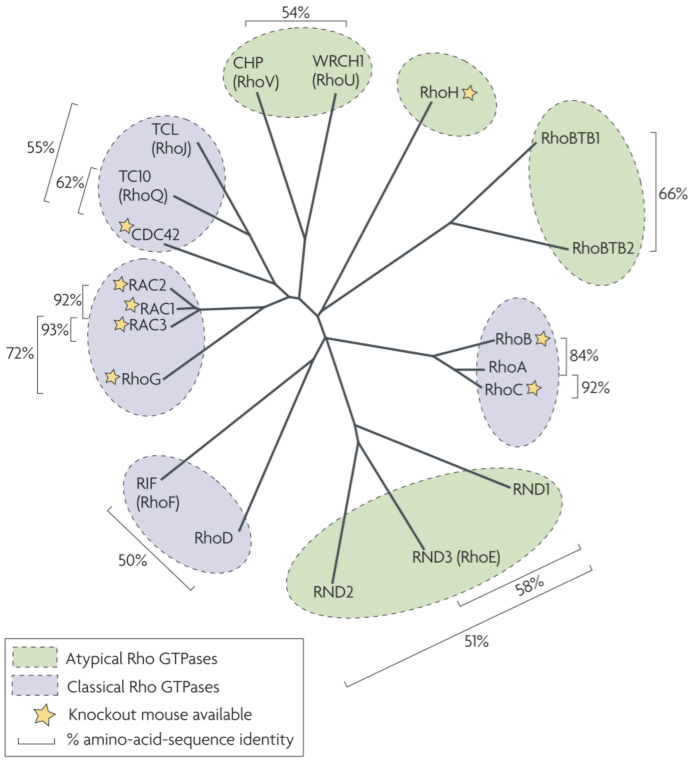

Figure 9: Rho GTPase subfamilies

Phylogenetic tree of the Rho family of small GTPases. The 'classical Rho GTPases' are known to undergo the activation cycle as described above. 'Atypical Rho GTPases' may not be activated by GEFs. Of note for this thesis, the Rac isoforms share a large degree of sequence identity, along with RhoG. Cdc42 is from a different subset, and is the only member of this subset highly expressed in T cells. RhoA is in a third subset of the Rho GTPase family. Diagram is from (Heasman and Ridley, 2008)

4.6 Rho GTPases in T cell signaling

Our understanding of the roles that Rho GTPases play in T cell activation is far from complete, but their importance is clear. Most research has focused on the most prominent of these Rho family GTPases: Rac1, Rac2, Cdc42, and RhoA. Mouse knockout models of these GTPases were not straightforward to develop, as total knockout of Rac1, Cdc42, or RhoA are embryonic lethal (Mulloy et al., 2010), and conditional knockouts of these GTPases in lymphocytes have been a fairly recent development. Direct assessment of these major Rho GTPases has shown that all of them have roles downstream of TCR ligation (Cdc42: Makrogianneli et al. (2009), Rac1: Ku et al. (2001); Tiede et al. (2003), Rac2: Yu et al. (2001) RhoA: Costello et al. (2000)) and can accumulate at the immunological synapse (IS) (Labno et al., 2003; Singleton et al., 2009; Zeng et al., 2003). However, active Rac, RhoA, and Cdc42 all show different dynamics of recruitment to the IS, and different spatial patterns once there (Singleton et al., 2009). These differences suggest that a diverse array of proteins involved in the GTPase activation cycle are at work in the IS to control the individual Rho family members. As the majority of my work with Rho GTPases has involved Rac and Cdc42, I will limit most of my discussion to these two.

4.6.1 Roles of Rac1 and Rac2 in T cell development and function

Rac1 and Rac2 have long been appreciated as being activated downstream of TCR ligation, and for playing numerous roles in changes in the morphology of T cells after stimulation. These two GTPases have a high degree of redundancy in T cells, as major defects in development and activation are only seen in mice with a double knockout of Rac1 and Rac2 (Guo et al., 2008; Mulloy et al., 2010; Walmsley et al.,

2003). Developing T cells in these Rac1 and Rac2 KO mice accumulate in the thymus at checkpoint stages that require productive TCR ligation to progress. The T cells that make it to the periphery have severe defects in T cell proliferation and IL-2 production after TCR stimulation (Guo et al., 2008). These results show that Rac1 and Rac2 are necessary for functional TCR signaling. Rac2 has also been directly implicated in supporting calcium signaling in T cells (Yu et al., 2001). The importance of Rac GTPases is not limited to T cells, as the double knockout mice have defects in every other hematopoietic cell subset investigated (Mulloy et al., 2010).

4.6.2 Roles of Cdc42 in T cell activation

While Rac1 and Rac2 appear to support strong TCR signaling, the role of Cdc42 activation in T cells is less straightforward. Cdc42 is activated downstream of TCR ligation in Jurkat and primary T cells (Cannon et al., 2001; Guo et al., 2010; Phee et al., 2005). Early genetic manipulation showed that Cdc42 is involved in T cell activation, as a knock-in of active Cdc42 (on top of endogenous) leads to completely dysregulated T cell development and function (Na et al., 1999). Recent studies using T cell conditional knockouts of Cdc42 report that these mice experience both blocks in T cell development in the thymus and hyperproliferation of stimulated peripheral T cells (Guo et al., 2010; Guo et al., 2011). I examine these studies further in the Discussion Section of this thesis in light of my results; but by way of an introduction, the authors conclude that Cdc42 appears to be part of a regulatory system for T cells. Not only do the Cdc42 T cell knockouts have very different phenotypes than Rac1/2 knockouts, but these GTPases appear to be activated with different temporal dynamics. Cdc42 shows

activation within the first 30 seconds of TCR ligation, while strong Rac1 activation takes closer to 2 minutes to appear (Phee et al., 2005).

4.6.3 Effects of Rho GTPases on immune cell calcium signaling

Surprisingly little is known about the effects of Rho family GTPases in the initiation of calcium influx into T cells, or immune cells in general. Conventional wisdom holds that these GTPases are mostly cytoskeletal regulators, which probably limits the inclusion of them in studies of calcium signaling. However, precise coordination of the cytoskeleton is essential for regulated calcium entry (Burkhardt et al., 2008; Rivas et al., 2004). For instance, the STIM proteins found on the ER membrane must be brought into proximity with the plasma membrane bound Orai calcium channels to initiate the major calcium influx into the cytosol (Figure 6), and this positioning requires the Rac1/2 effector WAVE (Babich and Burkhardt, 2013). Loss of the WAVE protein results in severely diminished calcium responses to TCR ligation (Nolz et al., 2006). Accordingly, disrupting Rac1 signaling also inhibits these calcium responses (Arrieumerlou et al., 2000). Increased levels of intracellular calcium also activates a number of proteins that directly affect the cytoskeleton, so the two systems have substantial crosstalk (Babich and Burkhardt, 2013).

The most direct links between Rho GTPases and regulators of calcium signaling involves Rac proteins. Active Rac1 and Rac2 have been shown to directly bind and assist in the activation of Plcγ2 and Plcβ2, helping to stimulate the production of IP3, and thus facilitating the opening of calcium channels (Bunney et al., 2009; Illenberger et al., 1998; Walliser et al., 2008). However, in T cells, Plcγ1 is the main Plc family isoform, and no interaction between Plcγ1 and Rac proteins are found in

these studies. Cdc42 is linked to the activation of Plcβ2 (Illenberger et al., 1998); but again, this isoform is not thought to contribute to calcium signaling downstream of TCR ligation.

There are also reports that Rac1 influences the activity of the Phosphatidylinositol-4-Phosphate 5-Kinase (PIP5K) kinase PIP5KIα (Halstead et al., 2010; van Hennik et al., 2003). This kinase generates PI(4,5)P2 at the plasma membrane, the required material for Plcγ proteins to hydrolize and produce IP3. Therefore, active PIP5K is important to supply the starting materials for initiating calcium mobilization in the cell. Although these finding suggest Rac1 has important roles in T cell calcium signaling, to the best of my knowledge, no in depth examination of the mechanisms by which Rac1 interacts with this pathway has been performed.

Even less is known about the impact of Cdc42 on T cell calcium signaling. However, studies in other immune cell types have found roles for Rho GTPases in the initiation calcium influx. Both CA Cdc42 and Rac1 can increase calcium influx and the ensuing degranulation in mast cells downstream of Fcε activation (Hong-Geller and Cerione, 2000; Hong-Geller et al., 2001). The mechanism of this enhancement is unclear, but may involve activation of PI5K (Wilkes et al., 2014). Cdc42 appears to be necessary for a full calcium influx in B cells, as Cdc42 KO primary murine B cells have a diminished calcium response downstream of BCR stimulation (Burbage et al., 2014), and overexpression of DN Cdc42 inhibits NF-AT activation in B cells (Doody et al., 2000).

4.7 Rho GTPases in disease

Discussion of the RAS superfamily of GTPases in human pathology is usually dominated by the well-established role of the three RAS genes in cancer (KRAS, HRAS, and NRAS), as mutations in these three that lead to unregulated activation occur in around 30% of cancers. In contrast, mutations in the Rho subfamily of GTPases are rarely found in cancerous tissue (Vigil et al., 2010), although the activating mutants of RhoA and Rac1 have recently been discovered in lymphomas and melanomas, respectively (Davis et al., 2013; Kataoka et al., 2015; Palomero et al., 2014). Another recent discovery is that a splice variant of Rac1, called Rac1b, while not being transforming on its own, synergizes with oncogenic K-RAS to drive tumor growth (Zhou et al., 2013). Notwithstanding these cases, Rho GTPase mutations are still rare in cancer. However, these proteins are heavily involved in tumorigenesis and invasion (Ellenbroek and Collard, 2007; Vega and Ridley, 2008; Zhuge and Xu, 2001). The oncogenic mutations that drive the dysregulated activation of these GTPases are instead found in proteins that regulate GTPase activation, including GEFs such as Vav.

Due to the connections between aberrant Rho GTPase activation and oncogenesis, methods of targeting these active GTPases are the subject of active investigation. For example, Cdc42 is currently being investigated as a target for cancer therapy (Arias-Romero and Chernoff, 2013). One recent study shows that the use of a small molecule inhibitor of Cdc42 improved the survival of mice in a model of breast cancer by reducing the development of tamoxifen resistance in these cells (Chen et al., 2013). As Rho GTPases are critical for the normal functioning of many tissue types, a

global inhibition of one of these GTPases is probably too drastic to use as a therapy. However, with an increased understanding of which GEF-GTPase interactions drive different cancers, targeting this interaction could provide a much more precise tool to deploy.

4.7.1 The GEF-GTPase interaction as a target for therapy

The feasibility of selectively blocking the activity of a GEF has been demonstrated, albeit unwittingly, by the use of Brefeldin A. This small molecule was isolated in the 1950s from a fungus, and is still widely used in research to block the transport of proteins (especially cytokines) from the ER to the Golgi apparatus. Much more recently, the mechanism of action of Brefeldin A has been identified as blocking the activation of an Arf GTPase by an Arf GEF (Vigil et al., 2010). This mechanism has served as a proof-of-concept for researchers, and has spurred more research into targeting GEF-GTPase interactions. Newer discoveries have involved the interaction between Rho GEFs and GTPases. For example, the small molecule NSC23766 greatly reduces the activation of Rac1 by the GEFs Trio and TIAM1 by interfering with the binding of Rac1 specifically to these catalytic pockets. Other GEFs, such as Vav1, have a different method of activating Rac1, and are unaffected by this drug (Gao et al., 2004). This inhibitor was created at least partially by rational design by examining the structures of Rac1 interacting with catalytic surfaces; and its design is being further refined to increase affinity and alter specificity (Montalvo-Ortiz et al., 2012).

With our increasing ability to screen and design small molecules that can target specific GEF-GTPase interactions, it becomes imperative that we understand the roles of different GEFs in both the normal function of tissues and in pathology. As I have

discussed in this Introduction, the Vav family of GEFs is necessary for mounting an effective immune response. They are also involved in oncogenesis and metastasis, at least partly by GTPase activation. Illuminating the mechanisms by which different Vav isoforms contribute to each beneficial and pathological process could allow us to selectively target, say, the dysregulated activation of Rac1 by Vav3 in lymphomas (Colomba et al., 2008), while avoiding the overall immunosuppression that a global inhibition of all Vav isoforms, or of Rac1, would cause.

4.8 Models of Vav function

4.8.1 Reports of Vav GEF specificity

In order to fully understand the contributions of different Vav isoforms to health and disease, its critical to understand which Rho family GTPases these isoforms activate. Somewhat surprisingly, there is no consensus on this issue. Vav1 has been reported to activate Cdc42 in some studies (Han et al., 1997a; Olson et al., 1996), but other studies see no such activity (Aghazadeh et al., 2000; Patel et al., 2002). And RhoA is reported to be the main substrate for Vav2 in one report (Schuebel et al., 1998), but to be almost unaffected by Vav2 in another report (Jaiswal et al., 2013). As is often the case, this confusion stems at least somewhat from the imprecision of the available assays.

4.8.2 Assays used to determine GEF catalytic specificity

Most studies of GEF-GTPase specificity use either pull-down or *in vitro* activations assays. No antibodies exist (or are commonly available) that can used to determine the activation state of GTPases in a Western blot in the same way we can

use specific phospho-antibodies to assess protein activation. As a result, pull-down assays were developed to determine *in vivo* GTPase activation in cell populations.

GTPase pull-down assays typically involve incubating stimulated cell lysates with purified proteins that can only bind to active, GTP-bound GTPases. After the rest of the cell lysates are washed away, the amount of bound GTPase per condition can then be assessed by Western blot as a readout for activation. Reports using these assays typically agree that Vav proteins increase stimulus-driven Rac1 activation (Faccio et al., 2005; Hamann et al., 2007; Kaminuma et al., 2001; Liu and Burridge, 2000; Movilla and Bustelo, 1999). However, these studies differ on their assessment of the activation of Cdc42, RhoA, or RhoG by the various Vav isoforms. One difficulty with the pull-down assays is the difficulty in differentiating direct vs. off-target effects of GEF manipulation on GTPase activation. For instance, a Vav1 knockdown could lead to the loss of Rac1 activation due to either the loss of Vav1 itself, or the destabilization of signaling structures, such as SLP-76 microcluster, that may be required for the function of other GEFs. These assays also give no indication of the subcellular localization of the GEF-GTPase activation.

The other common type of assay for GTPase activation by GEFs involved combining purified GEF and GTPase fragments *in vitro*. Typically these assays only use fragments of the GEF, such as only the DH alone or the DH-PH-C1 portion of Vav proteins, due to difficulties in purifying and activating full-length proteins. Exchange rates can then be determined by monitoring the loading of GTP analogs into, or release of GDP analogs from, the GTPase by using a molecule that changes in fluorescence when GTPase-bound (i.e. MANT-GTP). These assays can be excellent for determining

if GEFs are capable of activating isolated GTPases, and to measure the kinetics of these interactions. However, these assays are limited by the *in vitro* environment. The GEF and GTPases are often purified from bacteria, so may lack important mammalian modifications. At a minimum, the GTPase are usually truncated to remove the C-terminal prenylation motif and are assessed without the presence lipid bilayers, both of which can be critical for GEF-GTPase interactions (Hamann et al., 2007; Skowronek et al., 2004). Overall, in removing these proteins from a cellular environment, *in vitro* experiments lack the influences of phosphorylations, methylations, ubiquitinations, and sumoylations that affect GTPase activation, as well as the presence of GDIs, GAPs, and other proteins that can alter the availability of the GTPase to the GEF. Therefore, these assays cannot reflect the fact that a GEF can activate different GTPases depending on the cell type, or localization within the cell (Rossman et al., 2005). In this thesis, I present a different method for assessing GEF and GTPase interactions. We developed an imaging assay in our lab that can determine the co-localization of GEFs and GTPases within a cell. I believe that this assay can complement standard GTPase activation assays and give more insight into the actual *in vivo* interactions of GEFs and GTPases. I hope this new approach to determining GEF specificity will give researchers a valuable experimental tool.

4.8.3 Jurkat cells as a model of T cell signaling.

For both the GEF-GTPase interaction assays and for calcium assays used throughout this thesis, the model system I used is the Jurkat line of immortalized human T cells. Therefore, the strengths and limitations of these cells must be kept in mind. Jurkat T cells have been a staple of research on T cell signaling since the 1980s

(Abraham and Weiss, 2004). The transforming mutations in Jurkat cells have been at least partially characterized over time. These cells lack the phosphatase PTEN, which converts membrane-bound PI(3,4,5)P3 into PI(3,4)P2 (Sakai et al., 1998). As a result, Jurkat have high constitutive levels of PIP3 on the plasma membrane, which constitutively recruits certain PH-domain-containing signaling molecules to the PM. One of the molecules recruited and activated is Akt (Protein kinase B), which is a central player in the cellular processes that lead to increases in cell metabolism, growth, and division. The high basal activity of Akt in Jurkat is a key component of the transformed nature of these cells (Seminario et al., 2004). The production of PIP3 in primary T cells is positively regulated by the activation of the kinase PI3K, which is activated by co-stimulatory ligation, notably by CD28. Thus, Jurkat cells can be thought of as in a constant state of co-stimulation, and may not be a good model of signaling involved in this aspect of T cell activation. However, the state of PTEN in Jurkat cells does not seem to affect calcium signaling in these cells (Seminario et al., 2004).

4.8.4 Calcium signaling in Jurkat T cells

Jurkat T cells were the model used to first establish the link between TCR activation and increases in intracellular calcium (Imboden and Stobo, 1985; Imboden et al., 1985). The Jurkat cell model also closely resembles murine primary T cells in many aspects of calcium signaling. Vav1 is required for a robust calcium influx in both primary murine T cell and Jurkat cells. In particular, the difference in the calcium response of Vav1 KO and WT mice resembles the difference between the 'parental' E6 Jurkat line and the Vav1 targeted KO line: J.Vav1 (Figure 10).

As well, the residual calcium influx in both Vav1 KO models is reduced to almost nothing with the additional loss of Vav3 (Charvet et al., 2005; Fujikawa et al., 2003). However, the limitations of all model systems must be taken into account, and Jurkat cells have some obvious differences in terms of calcium signaling. Probably the most striking difference is that Jurkat cells are quite sensitive to TCR ligation by antibodies. To achieve the level of calcium influx in primary cells that can be achieved with mid-nanomolar concentration of anti-CD3 in Jurkat usually requires the use of low micromolar concentrations of both anti-CD3 and anti-CD4, along with a method for crosslinking these antibodies (personal observations and conversations). The reasons for this sensitivity are not clear, but may be due in part to higher levels of both expression activation of the Tec kinase Itk, which leads to much greater phosphorylation of Plcγ1, the major enzyme responsible for calcium release in T cells (Bartelt et al., 2009; Shan et al., 2000).

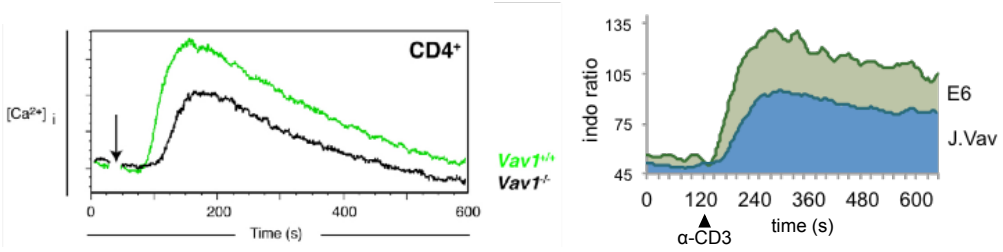

Figure 10: J.Vav1 Jurkat cells serve as models for primary T cells

Left: Differences in calcium response to TCR ligation in primary murine CD4+ cells from either WT (green) or Vav1 KO (black) mice from Ksionda 2012 (Ksionda et al., 2012). **Right:** Differences in calcium response after TCR ligation in parental E6 Jurkat (green line and shading) vs. Vav1 KO, 'J.Vav1' Jurkat (blue line and shading). Both sets of experiments were performed using the calcium-sensitive Indo dye and anti-CD3 antibodies.

4.8.5 Methods for determining expression-dependent effects on calcium signaling

One of the major strengths of the Jurkat T cell systems is relative ease of reliably expressing moderate to high levels of exogenous proteins, and I take full advantage of this feature in my calcium assays. As our lab's method of presenting the results of calcium assays is not common, and as the presentation of these results constitutes a large portion of my thesis, I present this particular method here rather than somewhat buried in the Methods section. To assess the effects of different proteins on calcium signaling, I expressed plasmids by transient transfection of fluorescently-tagged proteins into J.Vav1 (for most experiments), or E6 cells. After an overnight recovery, each condition displays a range of fluorescence that correlates to the levels of exogenous protein expression. The cells were then loaded with a calcium-sensitive dye (Indo-1), and monitored for changes in intracellular calcium after TCR stimulation using flow cytometry. This method allowed for gating on cells expressing no protein construct (null), moderate amounts of the construct (low), and high levels (high) within the same tube. These cells are experiencing the exact same stimulation conditions, only varying by level of exogenous protein. The responses for each category could then be graphed and quantified, as in Figure 11. The residual calcium response to TCR ligation in J.Vav1 cells is a useful feature in this setup, as it allows differentiation of constructs that have no effect on calcium from those that actively inhibit the calcium responses in J.Vav1 cells.

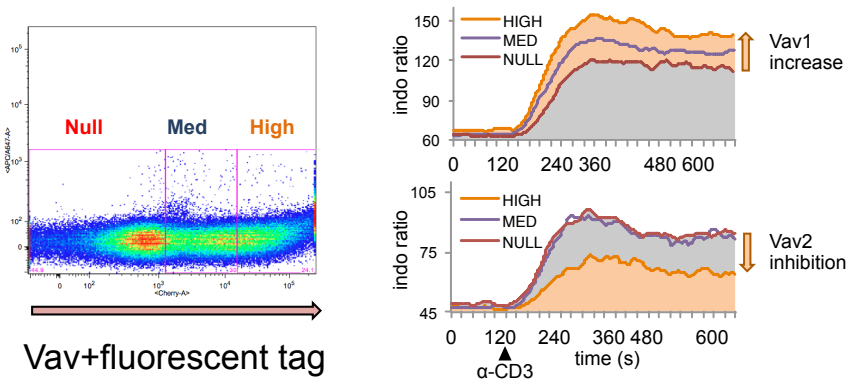

Figure 11: Level-dependent effects of constructs on calcium signaling

J.Vav1 cells expressing mYFP tagged Vav1 or Vav2 were assessed for calcium influx as in Figure 10. **Left:** J.Vav1 cells were transfected with fluorescently tagged Vav isoforms and gated for no expression (Null), moderate expression (Med), or high expression (High) of the exogenous protein as in this example. **Right:** Responses of untransfected cells (brown line, gray shading) superimposed with moderate expressing (blue line), and high expressing (orange line, orange shading) cells are superimposed.

4.9 Summary and Goals

Increasing our understanding of the mechanisms by which Vav proteins initiate downstream signaling cascades is necessary to be able to develop tools to tailor immune responses and to combat Vav-driven tumors growth and invasion. The three Vav isoforms are differentially expressed and play both unique and overlapping roles in immune cells, stromal cells, and cancerous tissue. A full appreciation of the differences in these isoforms can lead to therapies that target individual Vav family members and therefore different immune cell subsets or tumors.

The best-characterized Vav isoform is the first to be discovered, Vav1. And the roles of Vav1 have been studied most extensively in T cells. However, the mechanism of one of the major functions of Vav1, that of supporting a strong calcium influx on T cell activation, has yet to be understood. My thesis studies began as an investigation of this mechanism. I initially assumed I would find a binding partner of Vav1 that would explain why Vav1 is necessary for calcium signaling in T cells. However, my investigations led me to an examination of the signaling differences between Vav1 and Vav2, and led to the discovery of major differences in the catalytic specificities of these isoforms. These findings pave the way for both understanding and targeting different Vav isoforms in immune cells and tumors. The work I present here touches on the structure of Vav proteins, the calcium signaling pathway in T cells, and the activation and function of the Rho family of small GTPases.

5 Materials and Methods

5.1 Reagents

5.1.1 Antibodies

Jurkat cell stimulations were performed with either soluble (calcium assays) or plate-bound (imaging) anti-CD3ε clone OKT3 (BioExpress). Some imaging conditions used unlabeled anti-CD43 (555474/1G10, BD Pharmingen). Probing Western blots was performed with anti-Vav1 (07-192, EMD Millipore), anti-Vav2 (ab52640, Abcam), anti-Vav3 (ab52938, Abcam), anti-GFP (JL-8, Clontech), and anti-Erk1/2 (4695, Cell Signaling), anti-PLCγ1 (2822, Cell Signaling Technology), anti-Rac1 (ARC03, Cytoskeleton), anti-Cdc42 (2466, Cell Signaling), anti Flag (F3165/'M2', Sigma), and anti-RFP (ACT-CM-MRRFP10, Allele Biotech) primary antibodies. Secondaries for Westerns were horseradish peroxidase-conjugated anti-mouse (31432, Thermo) and anti-rabbit (31462, Thermo) antibodies.

5.1.2 Inhibitors

Cdc42 inhibition was performed using the small molecules ZCL278 (ApexBio) (Friesland et al., 2013) and ML141 (#4266, Tocris)(Bologa et al., 2010). ZCL278 was resuspended in DMSO to 50 mM and used at 100 μM final concentrations in the assays presented here. ML141 proved to fluoresce in a variety of channels when excited by a number of laser wavelengths, making it difficult to use for flow cytometry based assays. Rac1 inhibition was achieved using the pan-Rac inhibitor EHT 1864 (#3872, Tocris) (Désiré et al., 2005). This compound was resuspended in DMSO and used at final concentrations between 15 uM and 50 uM in assessing its impact on calcium signaling in my flow cytometry assays.

5.1.3 Fluorescent reporters

For flow cytometry calcium response assays, the majority of the experiments presented here were performed with the calcium-sensitive dye Indo-1 AM (Thermo Fisher / Molecular Probes, I1223). For experiments that required the use of other fluorescent channels, another calcium-sensitive dye, Fluo-4 (Thermo Fisher / Molecular Probes, F14201) was used. Reactive oxygen species generation was monitored by flow cytometry with the ROS reporter 6-carboxy-2',7'-dichlorodihydrofluorescein diacetate (DCFDA) (Thermo Fisher / Molecular Probes, C400).

5.1.4 Cell culture

Jurkat cells were maintained in RPMI 1640 containing phenol red (GE Healthcare and Lonza), supplemented with 10% FBS (Atlas Biologicals), 20mM L-Glutamine (Lonza), and 10µg/mL ciprofloxacin, (Complete RPMI). Human 293T cells were maintained in DMEM (Cellgro) supplemented with 10% FBS, 2s0 mM L-glutamine, 100 U/ml penicillin, and 100 U/ml streptomycin (Complete DMEM).

5.1.5 Cell staining

For fluorescent calcium assays, cells were labeled in ‘Solution 1:’ Hanks balanced salt solution (HBSS) supplemented with 5 mM dextrose, 1.25mM $CaCl_2$ (Sigma), 0.9 mM $MgCl_2$ (Sigma), and buffered with 10 mM HEPES pH 7.0. Cells were stimulated in ‘Solution 3:’ HBSS supplemented with 5 mM dextrose, 1.25mM $CaCl_2$ (Sigma), 0.9 mM $MgCl_2$ (Sigma), 0.05% BSA (fraction V, Thermo Fisher), and buffered with 10 mM HEPES pH 7.4. To check for ER stores release, modified versions of Solution 3 were used without calcium.

5.1.6 Cell selection

Lentivirally infected cells were selected on the basis of puromycin resistance using, typically, 1 μg/ml of puromycin (Thermo Fisher, MT-61-385-RA).

5.1.7 Cell lysate preparation and Western blotting

Cell lysates were typically prepared using the Lab Standard Lysis Buffer: 50 mM Tris-HCL, pH 8.0, 150 mM NaCl, 2 mM tetrasodium EDTA, 1% Triton X-100, 10 mM NaF, 1 mM Na_3VO_4, a Complete Protease Inhibitor Cocktail (Roche), 25 μg/mL Pepstatin A, and 1 mM DTT. Lysates were boiled in LDS Sample Buffer (Thermo Fisher, NP0007), initially at 4X, supplemented with dithiothreitol (DTT) to 3X, and then added to lysate to 1X. Lysates were run on run on 4-12% Bis-Tris Protein Gels (Life Technologies), using MOPS Running Buffer (Thermo Fisher, NP0001). Precision Plus Protein Standard (Bio-Rad, #161-0375) was used to track molecular weight. Proteins were transferred using transfer buffer (Thermo Fisher, NP0006). Signal was collected on film (Kodak) after treatment of the membrane by chemiluminescence reagents (Super Signal; Thermo).

5.2 Calcium assay

5.2.1 Flow cytometry-based assessment of intracellular calcium

For the calcium assays, Jurkat cells were counted for live cell density, spun down, washed once in 37°C PBS, and resuspended in Solution 1 (see Cell Staining) containing 50μg/ml of Indo-1. Cell were incubated at 37° C, in 100ul per condition, at a density of $1.5x10^7$ cells/ml. After 30 minutes, 100ul of Solution 3 was added and incubation continued for 30 more minutes. Cells were then washed 2X with 500ul of Solution 3 and brought up in 500ul of Solution 3. Samples were then placed on ice in

the dark until reading. The procedure for loading with Fluor-4, the alternate calcium-sensitive dye, was essentially the same, except the cells were incubated with Fluor-4 (Molecular Probes) in the place of Indo-1.

Individual samples/conditions were removed from ice and added to 500ul of room temperature Solution 3 for 5 minutes. Cells were then moved to a container maintained at 37° C by a circulating water bath for 5 more minutes before collecting data, and were maintained at this temperature for the duration of the collection. Calcium levels were monitored on a BD LSR II flow cytometer. Basal calcium levels were collected for 2 minutes by recording the emission of Indo-1 dye when excited by a 355nm laser: the ratio of calcium-bound Indo-1 emission (505nm long-pass filter, 525/50nm bandpass) to calcium-bound (405/30nm bandpass filter). If Fluor-4 was used instead, the fluorescence of the 'FITC' channel (488nm excitation, 514 nm 506 emission) was monitored instead to assess the change from calcium-free Fluor-4 (high levels of FITC emission) to calcium-bound (low FITC emission).

Cells were stimulated at 2 minutes (or as indicated) by removing the tube and injecting 10µl of 3µg/ml OKT3 for a final concentration of 30ng/ml OKT3 (unless otherwise noted), lightly vortexing, and then replacing the tub. Cells were then monitored for an additional 10 minutes. Initial assessments of the ability of cells to influx calcium involved an addition of the calcium ionophore ionomycin to a final concentration of 10µM at the 12 minute mark and collecting 2 more minutes of data. If ionomycin, or other DMSO suspended reagents were used, the LSR II was cleaned between reads by running a 70% ethanol solution 3X for 30 seconds each time and

wiping the metal sip tube of the cytometer clean between washes. Deionized H_2O was then run for at least 30 seconds before the next sample was collected.

5.2.2 Inhibitor effects on calcium influx

For the Cdc42 inhibitor calcium assays, cells were prepared as above, read for 60 seconds, and then brought to 100μM of ZCL278 by adding 2 μl of the stock solution in DMSO, or 2 μl of DMSO alone. The effects of the inhibitor on basal calcium levels were monitored for 5 minutes, and then the cells were stimulated with OKT3 and monitored for 6 additional minutes.

5.3 Molecular biology

5.3.1 Construct creation

The hs.flag.Vav1.yfp construct was from ML Schmitz, and the ΔCH Vav1.yfp and all other Vav1 chimeras were created from this starting material. pC.HA Vav2 was a gift from Joan Brugge (Addgene plasmid # 14554) (Moores et al., 2000) and all Vav2 mutants and chimeras were created from this starting material. The vectors encoding mRFP1 and TagRFP-T (here called TRT) were provided by R. Tsien (Shaner et al., 2004; Shaner et al., 2008). The placental Cdc42 isoforms were created from the curated sequence: the C-terminus was ordered from Integrated DNA Technologies (idtdna.com) as a gBlock fragment, and cloned into HS Cdc42 isoform1 (brain) constructs using the Gibson Assembly Cloning Kit (New England BioLabs)(Gibson et al., 2009). The HS Cdc42 isoform1 (brain) constructs YFP-Cdc42(V12) (plasmid #11399), YFP-Cdc42(V12) (plasmid # 11399), and YFP-Cdc42(N17) (plasmid # 11400) were gifts from Joel Swanson (Addgene plasmid # listed after each) (Hoppe and Swanson, 2004). HS Cdc42 isoform2 (Q61L) was created by mutagenesis from

the WT construct. HS YFP-Rac1 (plasmid #11391), YFP-Rac1(L61) (plasmid #11401), YFP-Rac1(N17) (plasmid # 11395), YFP-Rac2 (plasmid #11393), and YFP-Rac2(V12) (plasmid #11397), were gifts from Joel Swanson (Addgene plasmid # listed after each) (Hoppe and Swanson, 2004). HS pcDNA3-EGFP-RhoA-wt (plasmid # 12965), and pcDNA3-EGFP-RhoA-T19N (plasmid # 12967) were gifts from Gary Bokoch (Addgene plasmid # listed after each) (Subauste et al., 2000). HS RhoG(V12) and RhoG(N17) were gifts from R. Isberg (Mohammadi and Isberg, 2009). The mCerulean3 construct was created in-house from the sequence developed by the M. Rizzo lab (Markwardt et al., 2011).

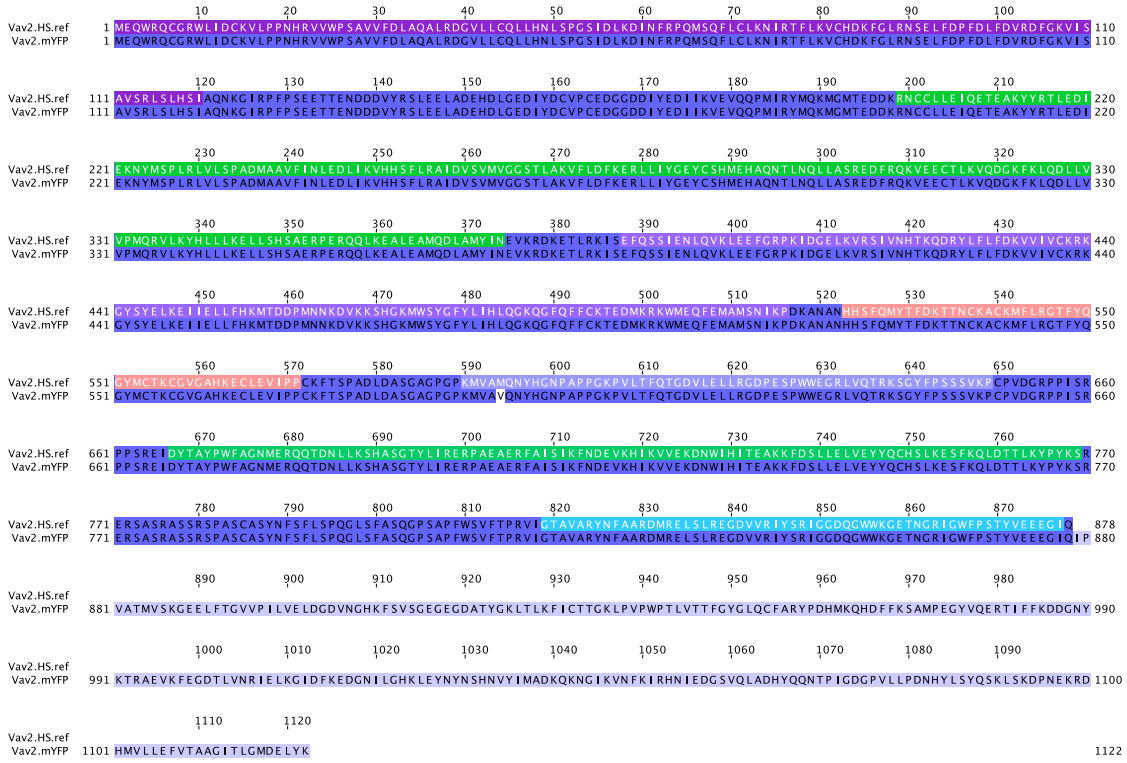

Figure 12: Sequence alignment of the CH domain deletions and chimeras used

Alignment of the reference amino acid sequence of Homo sapiens Vav2 from NCBI (Vav2.HS.ref) with the sequence of the Vav2.mYFP sequence used in my assays. The top row showing the reference sequence is colored by domains, from upper left: the CH domain in purple, the DH domain in green, the PH domain in lighter purple, the C1 domain in orange, the nSH3 in lightest purple, the SH2 in green, and the cSH3 in light blue. The Vav2.mYFP sequence is colored dark blue for sequence identity, white for mismatch, and light blue for extra residues. Of note, there is one amino acid disparity at residue 594, but this is in the nSH3 domain, which does not play a role in the calcium phenotypes of Vav2 reported here. The trailing amino acids in my construct are the linker and mYFP portion.

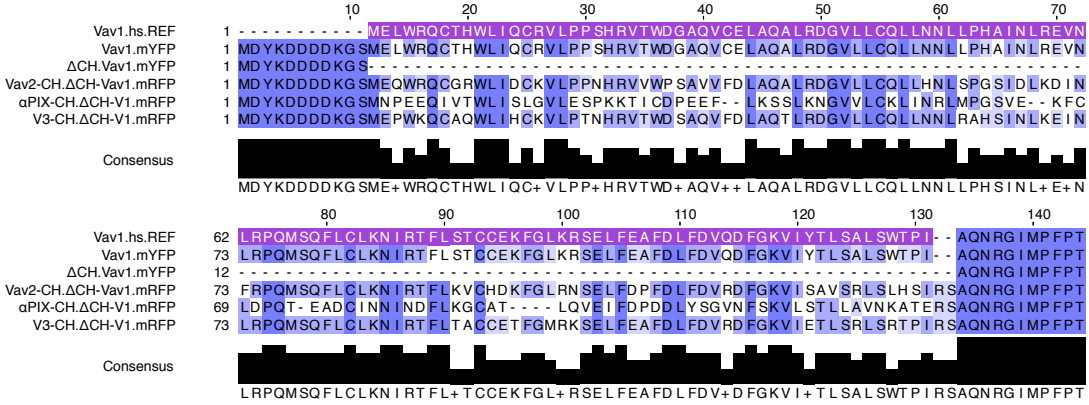

Figure 13: Alignments of Vav CH domain mutants

Sequence alignments of the N-terminus of Vav CH domain chimeras used in this report. The top sequence is the NCBI reference sequence, followed by the Vav1.mYFP used in this thesis, and then the CH domains deletions or addbacks from other proteins. The leading 11 amino acids are a 'Flag-tag.' Construct sequences are colored in dark blue to white for perfect consensus to none. A histogram depiction of the consensus sequence is included underneath.

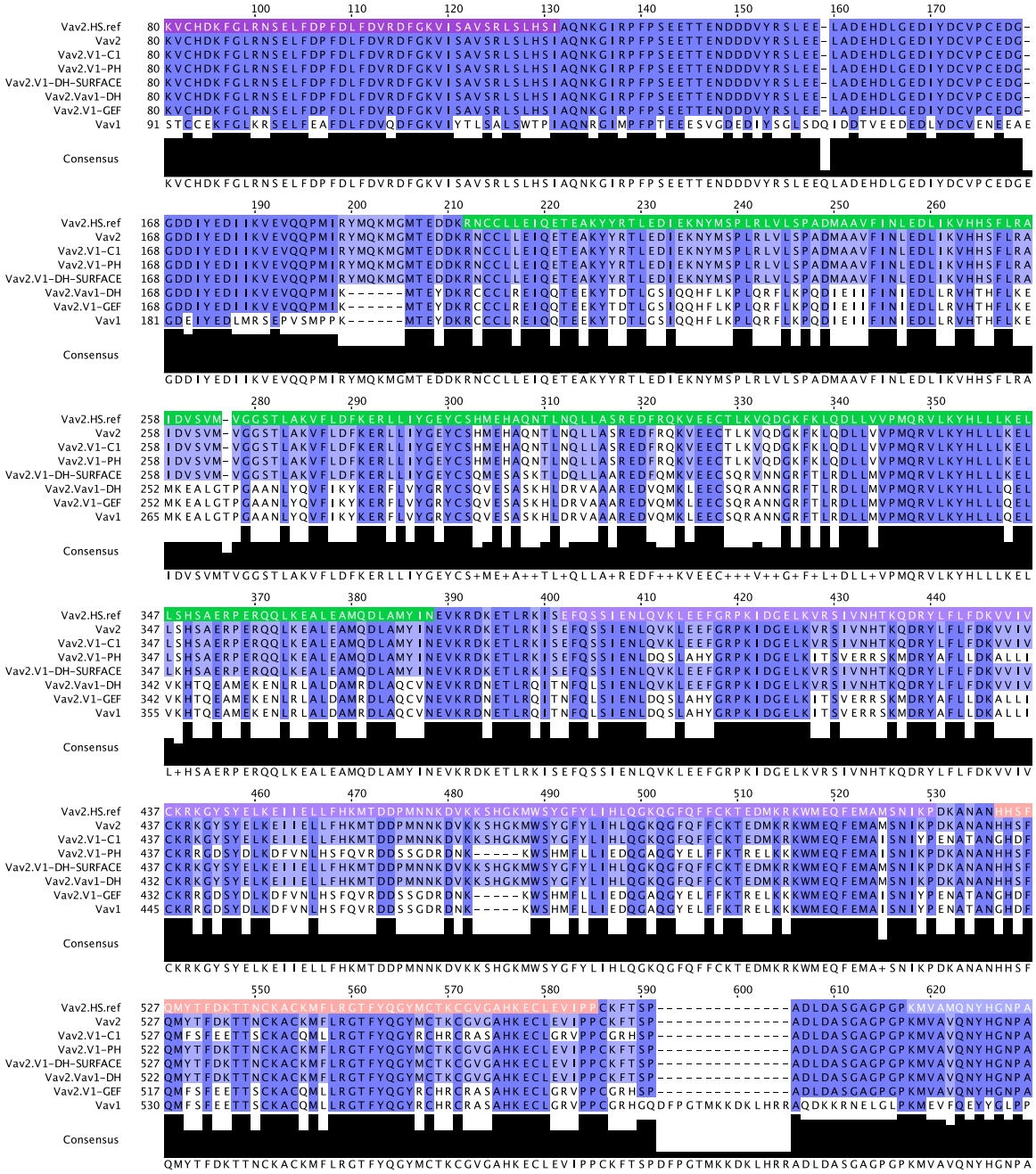

Figure 14: Alignment of Vav1 and Vav2 constructs that contain mutations in the catalytic core

Sequence alignments of the constructs containing the central, GEF swaps. The Vav2 reference sequences is at the top, and the Vav1.mYFP construct at the bottom. Color coding of the constructs is as in Figure 13.

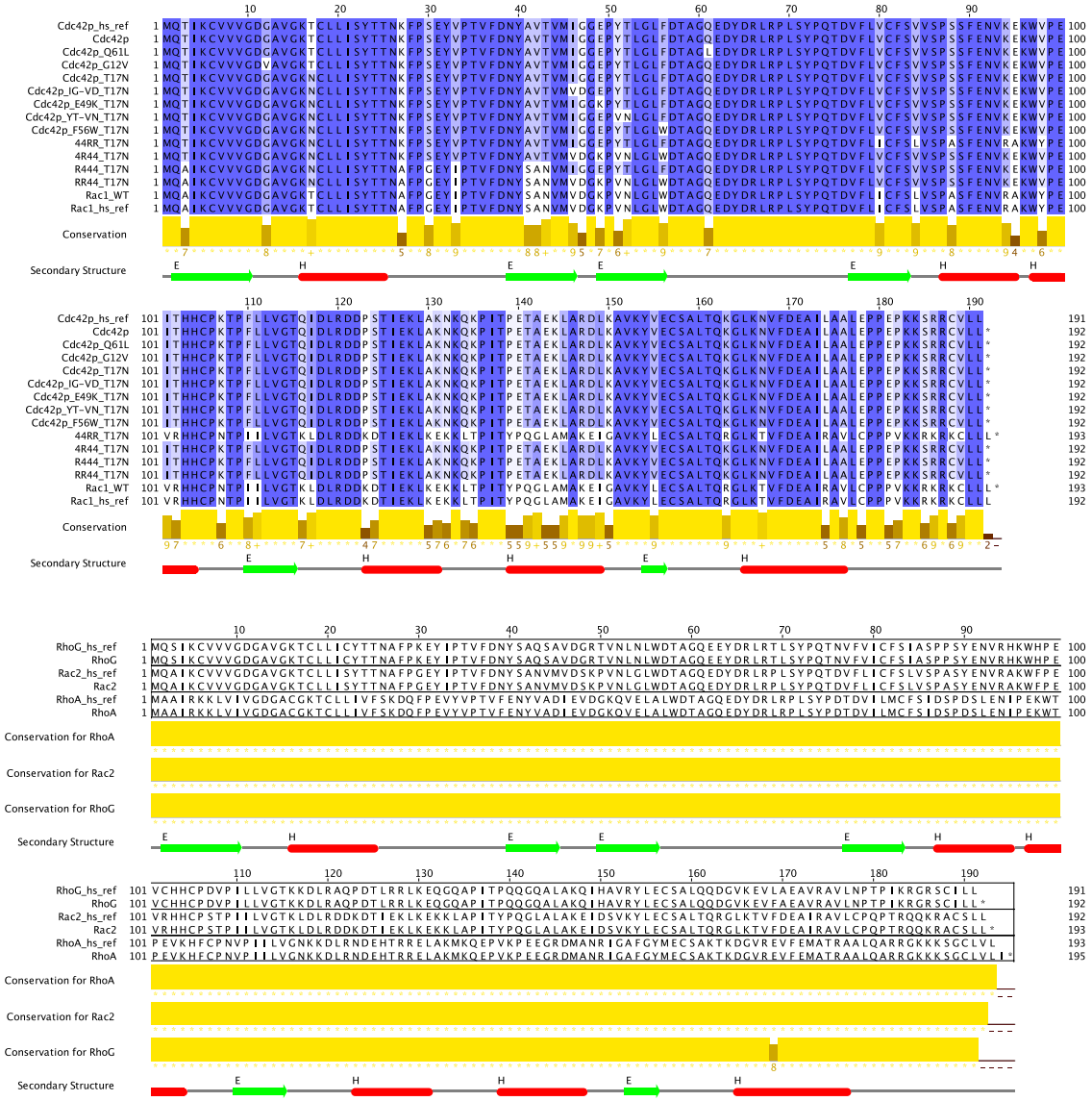

Figure 15: Sequences of major GTPases used

Upper: Cdc42 and Rac1 sequences and section swaps aligned. The Cdc42 isoform 1 (placental) reference sequence is included at the top, and the Rac1 at the bottom. Alignment is color coded as in Figure 13. A consensus histogram is included underneath, as is a representation of the helixes (in red) and sheets (in green) of the GTPases. **Lower:** Alignments of the reference sequences for Homo sapiens RhoG, Rac2, and RhoA with the wild type constructs used as the basis for mutants in this assay. Sequences are not color-coded, as no discrepancies exist, which is shown by the yellow conservation histograms for each pair.

5.4 Western blotting

Western blotting was performed by lysing cells at a concentration of $25x10^6$ cell/ml in lab standard lysis buffer. Cells were washed in PBS prior to lysis to remove serum protein. After lysis buffer was added, the cells were gently resuspended in the buffer and incubated on ice for 10 minutes. After incubation, cells were spun down at high speed at 4° C for 10 minutes. The supernatant was removed, sample buffer was added, and the sample was boiled for 5 minutes. Samples were run out on 4-12% gels, and transferred to PVDF membranes using a semi-dry technique and applying 10V for 1 hour. Membranes were blocked with 1% BSA before primary and secondary antibodies were applied. Chemiluminescence was detected by film or using a Bio-Rad Gel Doc.

5.5 Transfections and Transductions

5.5.1 Transient Transfections

Transient transfections were performed using Jurkat cells at a density of between $5x10^5$ and $1x10^6$ cells/ml. These cells were spun down, washed 1X in RPMI 1640 with no supplements, and resuspended at a density of $40x10^6$ cells/ml in complete RPMI. Typically either 300µl ($12x10^6$ cells) or 100µl ($4x10^6$ cells) of cells were used for transfection. These cells were combined with plasmid DNA at a maximum of 10µg/100µl of cells, or 10% total volume of plasmid prep. Cell/DNA mix was moved to a 4 mm gap cuvette and electroporated by delivering one 300V, 10ms pulse using a BTX ECM 830 square wave electroporator. Cells were allowed to recover for 10 minutes, then moved to complete RPMI at a normal growth density and incubated overnight.

5.5.2 Lentiviral transduction

Lentivirus was packaged using 293T cells. The day before transfection, cells were plated in 10 cm plates to be at around 40-50% confluency on the day of transfection. Each plasmid was packaged using approximately 5µl of fresh miniprep DNA, 1.5 µg of the packaging plasmid psPAX2 and 0.5 µg of the pseudotyping plasmid pMD2.G in 40µl of serum-free DMEM 18µl of FuGENE 6 Transfection Reagent (Roche), and 142µl of serum-free DMEM. Plasmids were combined and added to cells as per the FuGENE instructions. After 12-15 hours the 293T media was replaced with complete DMEM. Supernatants containing lentivirus were collected 66-72 hours post 293T transfection. Lentiviral supernatants were filtered through 0.2µm filters to remove 293T cells and other contaminants. Virus was either used at this concentration (1X), or concentrated to 5X or 10X by centrifugation using Amicon Ultra filters (EMD Millipore). To transduce Jurkat cells, lentiviral supernatant, log-phase cells, and fresh complete RPMI were mixed in a 1:1:1 ratio. Fluorescent protein expression or protein knockdown was then tracked over the following days, and cells were selected on the basis of puromycin resistance if applicable.

5.6 Imaging

5.6.1 Plating cells for imaging

Cells were stimulated and imaged in glass bottomed 96-well. Imaging plates were prepared by activating with 0.01% poly-L-lysine in purified H_2O for 15 minutes, then thorough drying. Plates were then coated with 10µg/mL OKT3 (anti-CD3ε) in PBS by incubating at 37°C for 1 hour, washing 3X with PBS, and then blocking with

1% BSA in PBS for 45 minutes at 37°C as and washing 3X in PBS as described (Bunnell et al., 2003). To image cells expressing DN RhoG (see Results for discussion), 10μg/mL anti-CD43 in PBS was added after OKT3 coating and before blocking, as described (Nguyen et al., 2008). For fixed cell imaging, cells were injected into wells in complete media and incubated for 7 minutes at 37°C and 5% CO_2. Cells were then fixed by addition of paraformaldehyde to a concentration of 1%, and incubation for 25 minutes at 37°C. Wells were then rinsed into PBS. Live cell imaging was performed at 37°C in complete media buffered with 25mM HEPES, pH 7.4. Cells were imaged continuously for 5 minutes shortly after landing and spreading.

5.6.2 Confocal imaging

Image acquisition was performed using a spinning-disc confocal microscope, consisting of a 40x Plan-Neofluar oil immersion objective lens (NA 1.3; Carl Zeiss), a 2.5x expanding lens, a spinning-disc confocal head (CSU-10; Yokogawa Corporation of America), and an Axiovert 200M stand (Carl Zeiss). All images presented here were collected using an intensified CCD (ICCD) camera (XR MEGA-10; Stanford Photonics). For live cell imaging, the cells were held at 37° C.

5.7 Analysis and Quantification

5.7.1 Image collection

Confocal images were acquired using the NIH-funded open-source Micro-Manager software package (Edelstein et al., 2010). Movies and kymographs were processed with iVision software (BioVision Technologies) using scripts developed in-house and described previously (Ophir et al., 2013; Sylvain et al., 2011). Fixed image

analysis was performed using NIH ImageJ and Fiji (Schindelin et al., 2012; Schneider et al., 2012).

5.7.2 Image quantification

To validate and present my findings on microcluster co-localization, I used a combination of ImageJ scripts written in the internal ImageJ language, and plugins from the University of Sussex's GDSC resources for ImageJ (http://www.sussex.ac.uk/gdsc/intranet/microscopy/imagej/gdsc_plugins). Cluster identification was performed using the version 1.01 GDSC plugin FindFoci (Herbert et al., 2014). Co-localization was quantified by using GDSC's Match Calculator to determine the fraction of clusters in the SLP-76.YFP channel that overlap with clusters in the TRT.GTPase channel. I defined 'overlapping' as having a cluster peak in one channel that occurs within 3 pixels, or 300nm at our resolution, of clusters in the other channel. Numbers reported here are the 'F1' output of the plugin, which represents a weighted average of the fraction of co-localized clusters. FI is defined as: $2/((1/R1) + (1/R2))$, where R1 is the fraction of points in RFP that also occur in YFP, and R2 is the fraction of points in YFP that also occur in RFP. The plugin outputs for every cell in every experiment analyzed were imported into an Excel spreadsheet. F1 values for each condition were averaged across cells, and are presented as boxes enclosing the 2nd and 3rd quartiles. Whiskers encompass the minimum and maximum observed values. Graphs were created and formatted in Microsoft Excel for Mac 2011 (Microsoft).

5.7.3 Calcium assay analysis and quantification

Flow cytometry data was collected on a BD LSR II using Diva software. Data was exported for analysis using FlowJo software (version 8.8.7). For transiently-transfected cells expressing a fluorescent construct, cells were gated on null, medium, and high expression of the transfected construct. Each gate was analyzed for the kinetic data of the increase in intracellular calcium, defined as 100*((calcium-bound Indo-1 emission)/(calcium-free Indo-1 emission)). The kinetic data was based on the mean cell value. This kinetic data was exported to Microsoft Excel. In Excel, for each of the three populations present within a single sample, the raw area under the curve (AUC) was calculated for the period of stimulation. The raw AUC was corrected by removing the baseline, calculated using the average calcium baseline during the prestimulation period. The percent change is calculated by taking the baseline corrected AUC of the low or high expressors, subtracting the baseline corrected AUC of the corresponding null expressors, and dividing by the AUC of the null expressors, e.g.: 100*(((AUC high expressor)-(AUC null expressor))/(AUC null expressor)). These values were graphed in Excel to show average value for each condition over all experiments, plus or minus S.E.M. The *p* values were computed using an unpaired, unequal variance, two tailed, Student's t-Test in Excel.

6 Results

6.1 Vav family members in Jurkat calcium signaling

6.1.1 Vav1 and Vav3 support TCR induced calcium entry

In order to establish the foundation for my examination of the roles of Vav proteins in T cell calcium signaling, I assessed the effects of expressing each human Vav isoform in my model system of Vav1-deficient Jurkat T cells (J.Vav1). As our lab and others have noted, the addback of exogenous WT Vav1 into Vav1-deficient Jurkat cells increases the peak and sustained levels of cytosolic calcium entry into the cells after TCR ligation (Cao et al., 2002; Sylvain et al., 2011) (Figure 16). The presence of endogenous Vav3 in J.Vav1 cells is responsible for the residual calcium response of this cell line (Charvet et al., 2005), so it is not surprising that the overexpression of exogenous Vav3 increases the calcium response of these cells when stimulated (Figure 16). However, it is notable that Vav3 cannot improve the calcium response to the extent that Vav1 can, even when they are expressed to comparable levels (see below for a level comparisons).

Although to different extents, both Vav1 and Vav3 support calcium signaling in Jurkat T cells in a dose-dependent manner. In contrast, high levels of Vav2 potently inhibit TCR stimulated increases in cytosolic calcium (Figure 16). This observation is in line with reports showing that Vav2 expression inhibits NF-AT activation in Jurkat cells (Doody et al., 2000; Tartare-Deckert et al., 2001), and verifies that these effects on NF-AT are due to alterations in calcium signaling. The inhibition of calcium signaling by Vav2 does not manifest unless the protein is expressed at high levels,

suggesting that the exogenous Vav2 must out-compete endogenous Vav3 in the TCR signaling cascade before its inhibitory effects predominate.

Protein overexpression can have off target consequences. I determined that the cells expressing high levels of Vav2 are not simply unresponsive to all stimuli in a few ways. The first observation is that both Vav1 and Vav3 improve T cell calcium signaling in a dose-dependent manner; so the cells are able easily tolerate this level of protein expression. As well, Vav2 high expressors responded to ionomycin treatment (data not shown), showing that they can influx calcium. These cells can also respond to TCR signaling. High levels of Vav2 increase the upregulation of the early activation marker CD69 in J.Vav1 stimulated overnight with anti-CD3 (data not shown). Therefore, high levels of Vav2 expression can support certain signaling pathways downstream of TCR activation.

The relative amount of Vav2 protein expressed in the high expressors is also within the bounds of the normal ratios of Vav proteins in T cells. I used quantitative Western blotting in combination with flow cytometry to determine the levels of Vav2 expression represented in the 'High' gates of the calcium assays. As shown in Figure 18, the amount of Vav2 expressed in a typical 'High' population is equal to approximately six times (6X) the amount of Vav1 expressed in the parental Jurkat T cell line (E6). Expression varied somewhat between experiments, but I estimate the range of Vav2 Jurkat T cells to be between 5 – 10X the 'normal' levels of Vav1. This amount of overexpression is consistent with a dominant negative molecule having to fully displace the 'normal' molecule (Vav3 in this case) to fully inhibit signaling.

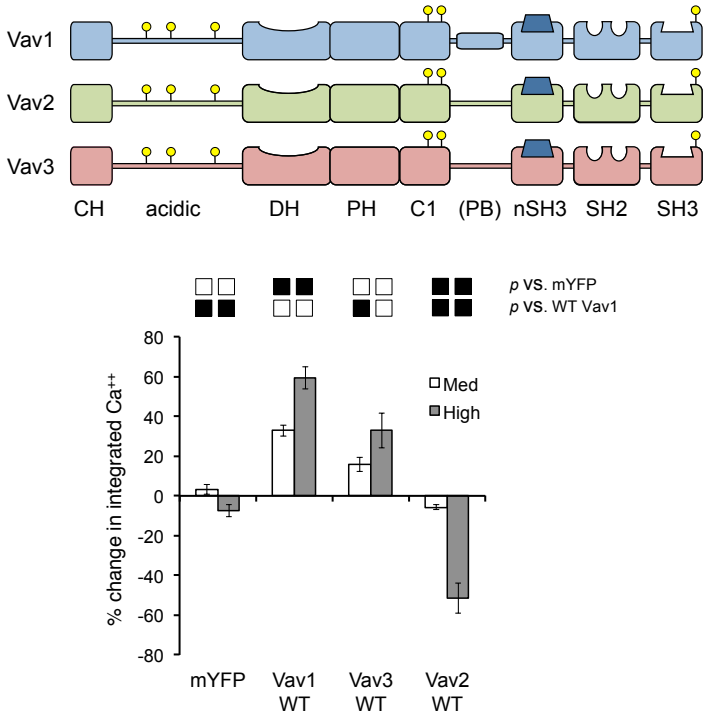

Figure 16: Vav1 and Vav3 support calcium signaling in Jurkat while Vav2 inhibits calcium influx.

Upper: Vav chimeras used in this figure. All fluorescent protein tags for Vav constructs are C-terminal (not shown). **Lower:** Quantification of calcium influx data for the indicated mYFP-tagged Vav chimeras. Jurkat lacking endogenous Vav1 (J.Vav1 cells) were loaded with the calcium-sensitive dye Indo-1. Calcium responses were continuously monitored by flow cytometry. Cells were stimulated at 2 minutes using 30 ng/mL OKT3 (anti-CD3ε). Graphs depict the percentage change in the integrated calcium responses of the moderate and high mYFP expressing populations relative to the non-expressing population within the same sample. Graph represents an average of experiments, and error bars show SEM ($n \geq 3$ for all constructs, except $n=2$ for Vav3). Small boxes depict *p* values for comparisons between chimeras expressed at similar levels. Black boxes represent *p* of < 0.05, white boxes are > 0.05.

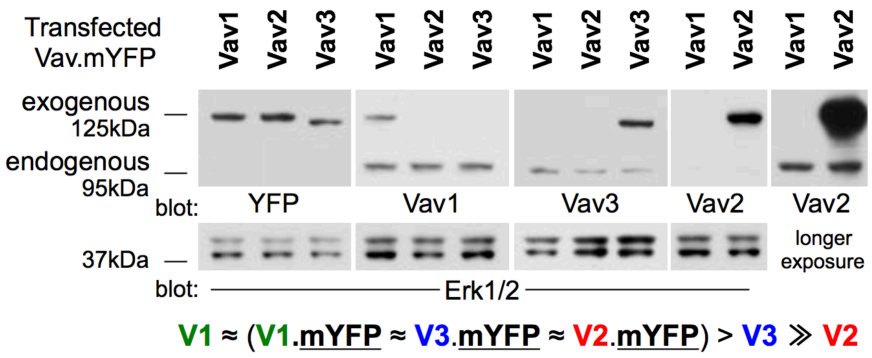

Figure 17: Vav family expression in Jurkat cells

'Transitive' western blots were performed to determine the relative abundances of endogenous Vav1, Vav2, and Vav3 in the parental E6.1 Jurkat line by comparison with mYFP-tagged exogenous constructs expressed at similar levels (top left panel). Each vertical panel is from a different gel with the same lysates. The loading controls are from the same lanes as the panels above them. The last two panels in the upper right are the same blot with different exposure times to reveal the signal from the endogenous proteins. The blots shown are from one experiment, representative of two.

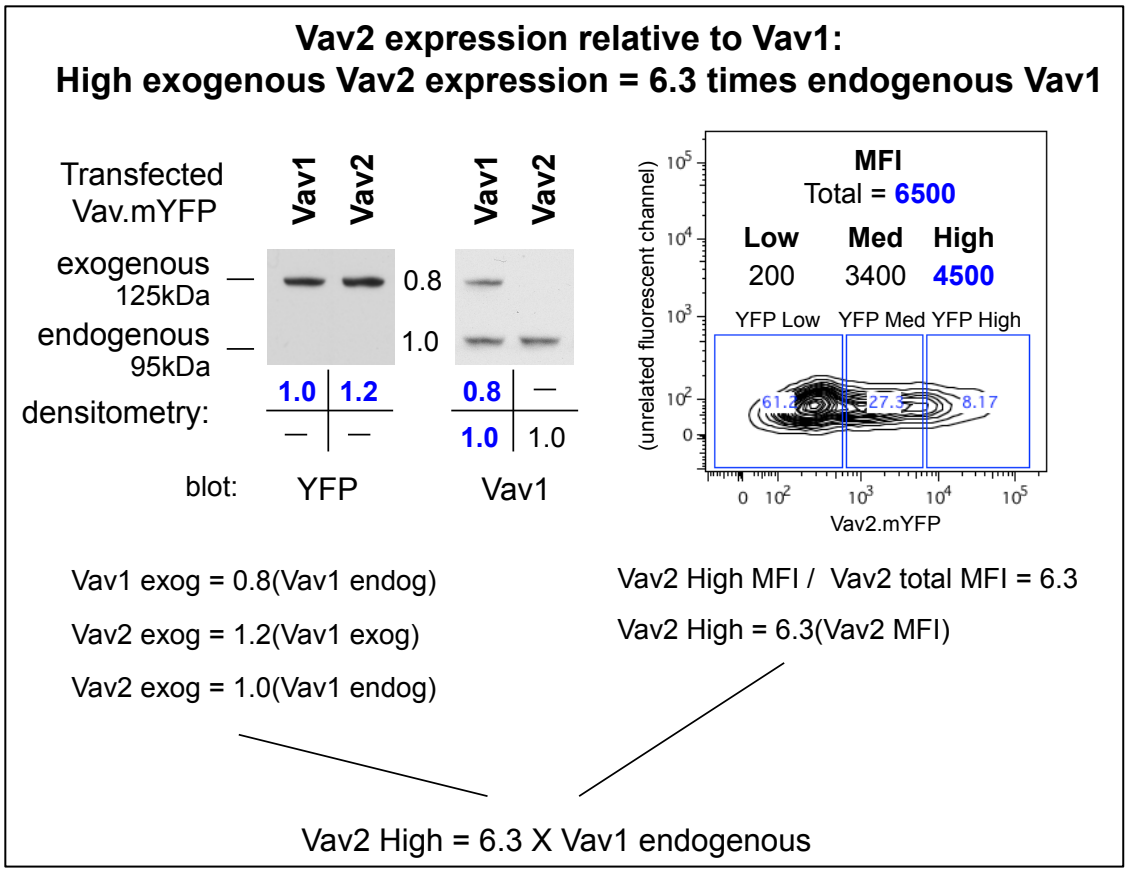

Figure 18: Relative amounts of Vav2 expression

Determining the levels of Vav2 overexpression needed to see the effects on calcium signaling from this construct. **Left:** Relevant Western blots from Figure 17. Densitometry data is listed below for the bands, normalized to endogenous (right) or exogenous (left) Vav1. Below shows a transitive comparison of the levels of expression, concluding that the average Vav2.mYFP protein level is the same as endogenous Vav1. **Right:** Expression, by flow cytometry, of the same Vav2.mYFP expressing cells shown in the Western blot. The gating on null, medium, and high expressors is representative of gatings for calcium assays. Below: Average mean fluorescence intensity (MFI) is proportional to the average amount of protein shown in the Western. High expression by flow cytometry is approximately six times the average expression. Therefore, the high levels of Vav2 protein expression that inhibits calcium signaling in Jurkat T cells is in the realm of six to ten times the level of Vav1 in parental (E6) Jurkat.

6.2 The CH domains of Vav1 and Vav2 support calcium signaling

Early in my investigations, the portion of Vav2 responsible for the inhibition of TCR induced calcium influx seemed fairly obvious. It is well known that Vav1 requires the presence of an intact N-terminal CH domain to support calcium signaling (Billadeau et al., 2000; Sylvain et al., 2011; Wu et al., 1995; Zhou et al., 2007). Accordingly, a Vav1 construct lacking this CH domain (ΔCH Vav1) inhibits calcium entry into J.Vav1 cells when expressed at high levels (Figure 19). Furthermore, the calcium influx inhibition by ΔCH Vav1 is nearly identical to that of Vav2 (Figure 19). Therefore, my first hypothesis was that the CH domain of Vav2 could not support T cell calcium signaling. Moreover, two papers (from the Cao lab) were published while I was beginning my investigations that suggested the Vav2 CH was the portion of Vav2 responsible for inhibiting T cell calcium signaling (Li et al., 2012; Zhou et al., 2007).

My plan was to use the Vav2 CH domain as a negative control for experiments examining the positive role of the Vav1 CH in T cell calcium influx. To my surprise, I found that a replacing the entire CH domain of Vav1 (amino acids 1-120) with that of Vav2 created a construct perfectly capable of supporting calcium influx downstream of TCR activation (Figure 19, Vav1.Vav2-CH). Furthermore, not just any CH domain can support calcium signaling in this assay, as a Vav1 construct expressing a CH domain from a distantly-related GEF, αPIX, was a strong dominant negative in these experiment (Figure 19, Vav1.αPIX-CH). My Vav2-Vav1 chimeric construct differs from that reported in Li et al. in that their construct only replaced the first 20 amino acids of Vav1 with the Vav2 equivalents instead of the entire domain. This partial

domain mutation could result in a misfolding of the domain as a whole. I further examine the discrepancies between the findings in Li *et al*. with mine in the Discussion. It is also worth noting that both Vav2 and Vav1 enhance calcium signaling in B cells, and that a Vav2 construct lacking a CH domain is not able to enhance B cell calcium signaling in a B cell line (Doody et al., 2000). Therefore, an intact Vav2 CH domain is able to support calcium signaling in B cells and in Jurkat T cells. I then turned my attention away from the Vav2 CH domain to determine which other portions were responsible for its inhibition of calcium signaling in Jurkat cells.

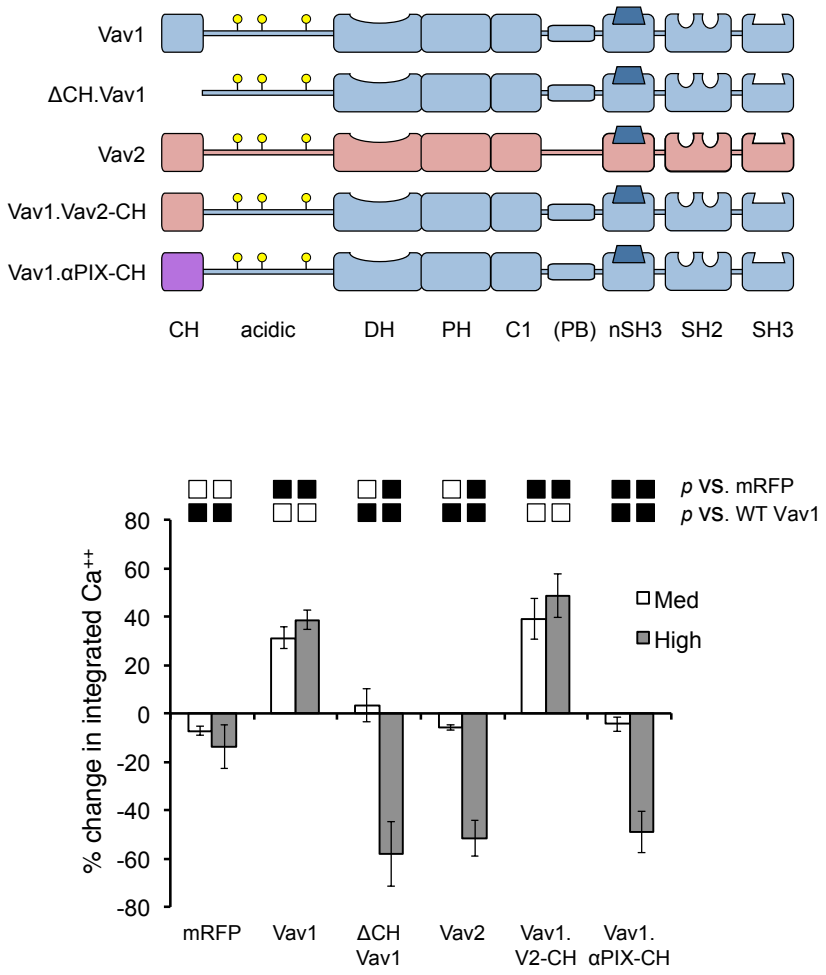

Figure 19: Vav1 and Vav2 CH domains support calcium signaling

Upper: Schematic of the Vav CH domain swaps used in this figure. Vav1 domains are represented in blue, Vav2 in red, and the one αPIX domain in purple. **Lower:** Quantification of calcium influx data for the indicated mRFP-tagged Vav chimeras, except for Vav2, which was YFP-tagged, but is included here for comparison to the ΔCH and αPIX CH Vav constructs. Experiments and calculations were performed as in Figure 20. Plots depict the mean ±SEM of n≥3 experiments per condition.

6.3 The catalytic core of Vav2 inhibits calcium signaling downstream of TCR ligation.

In order to determine which domains of Vav2 could be responsible for the inhibition of calcium signaling by full-length Vav2, I continued the strategy of domain swaps of Vav2 into Vav1. The scaffolding domains of the C-terminus of Vav proteins have been reported to bind dozens of proteins, some of which only bind to specific isoforms (Bustelo, 2012). Additionally, our lab has shown that point mutations in either of the Vav1 SH3 domains results in a construct that can no longer support robust calcium influx in T cells (Sylvain et al., 2011). However, I found that replacing the SH3-SH2-SH3 portion of Vav1 with that of Vav2 created a construct that supported strong calcium signaling in our system (Figure 20, Vav1-Vav2 323). Therefore, the differences in the binding partners of the Vav2 and Vav1 C-terminal domains are not relevant for calcium signaling.

Less is known about the scaffolding properties of the central, catalytic portion of Vav proteins. It is well established that the three domains (DH-PH-C1) form a higher-order structural unit (Chrencik et al., 2008; Rapley et al., 2008), and that the removal of either the PH or C1 domains diminishes the GEF activity of the DH domain. In order to not disrupt the overall structure of this portion of Vav2, I moved these three domains as a single unit from Vav2 into Vav1. This Vav1-Vav2 GEF chimera exhibited the same degree of calcium signaling inhibition as WT Vav2 (Figure 20). This striking result led me to re-evaluate my assumptions about the catalytic roles of Vav proteins in T cell calcium signaling.

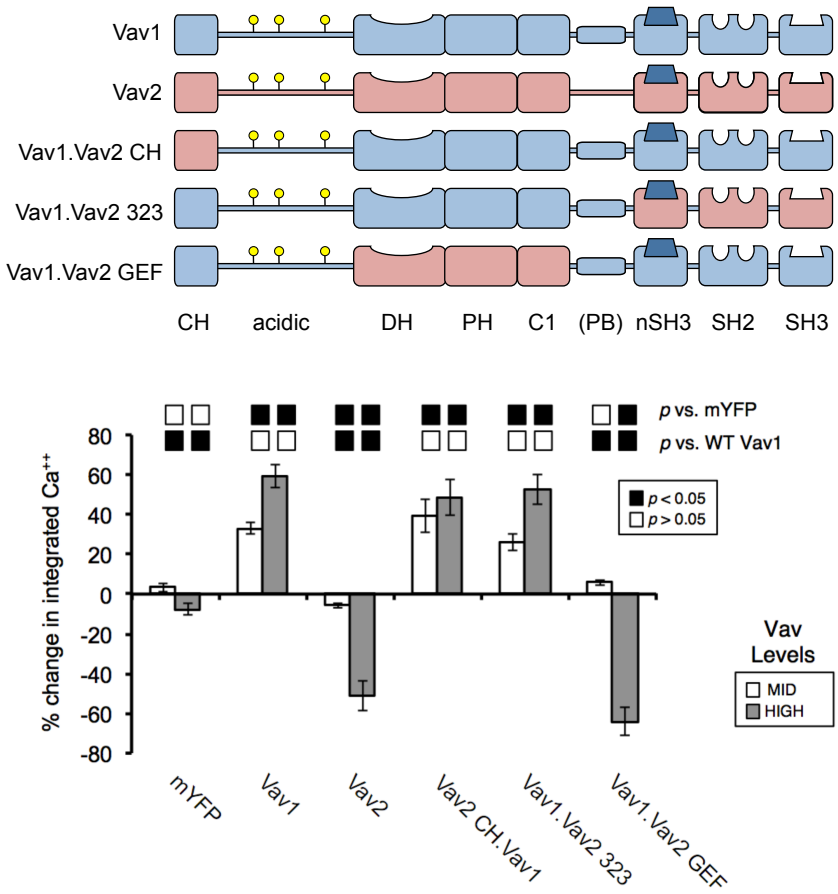

Figure 20: The catalytic core of Vav2 conveys calcium inhibition into a Vav1 chimera

Upper: Vav chimeras used in this panel. Pertinent domain swaps are depicted, with Vav1 regions in blue and Vav2 in red. **Lower:** Calcium profiles of cells expressing mYFP-tagged Vav chimeras. Experiments were performed and quantified as in Figure 16. Plots depict the mean ±SEM of n≥3 experiments per condition.

6.3.1 Effects of terminating the GTPase exchange ability of Vav2

As Vav1 supports calcium signaling purely through structural functions (Saveliev et al., 2009; Sylvain et al., 2011), I had been working with the hypothesis that the signaling differences between Vav1 and Vav2 were solely due to differences in binding partners, not catalytic specificity. However, discovering that the Vav2 catalytic regions conveyed calcium inhibition led me, with suggestions from my committee, to determine if Vav2 is activating a GTPase that inhibits calcium signaling. In order to test this hypothesis, I used the pair of point mutations that have been shown to block the GEF activity of Vav1 without altering the folding of the DH domain. The mutations in Vav1 are Leu^{334} to Ala and Lys^{335} to Ala (LK-AA) (Saveliev et al., 2009). This Leu and Lys amino acid pair is highly preserved throughout DH domains, and makes contacts with the critical switch II region of Rho GTPases to facilitate nucleotide exchange. The amino acids surrounding L^{334} and K^{335} are highly conserved between Vav1 and Vav2, both in the linear sequence, and on the predicted exposed surface of the folded protein (Figure 21). I therefore created catalytically inactive, LK-AA versions of WT Vav2 and the construct with the Vav2 GEF into Vav1. Both of these constructs showed a reduced ability to inhibit calcium signaling in J.Vav1 cells compared to their catalytically competent counterparts (Figure 22, Vav2 LK-AA and Vav1.Vav2-GEF LK-AA). Of note, these constructs are still somewhat inhibitory, suggesting that the Vav1 GEF also has non-catalytic functions that are critical to boosting calcium signaling in Jurkat T cells. However, these results show that the catalytic activity of Vav2 leads to a suppression of calcium signaling in Jurkat cells, and added a new avenue to my investigations.

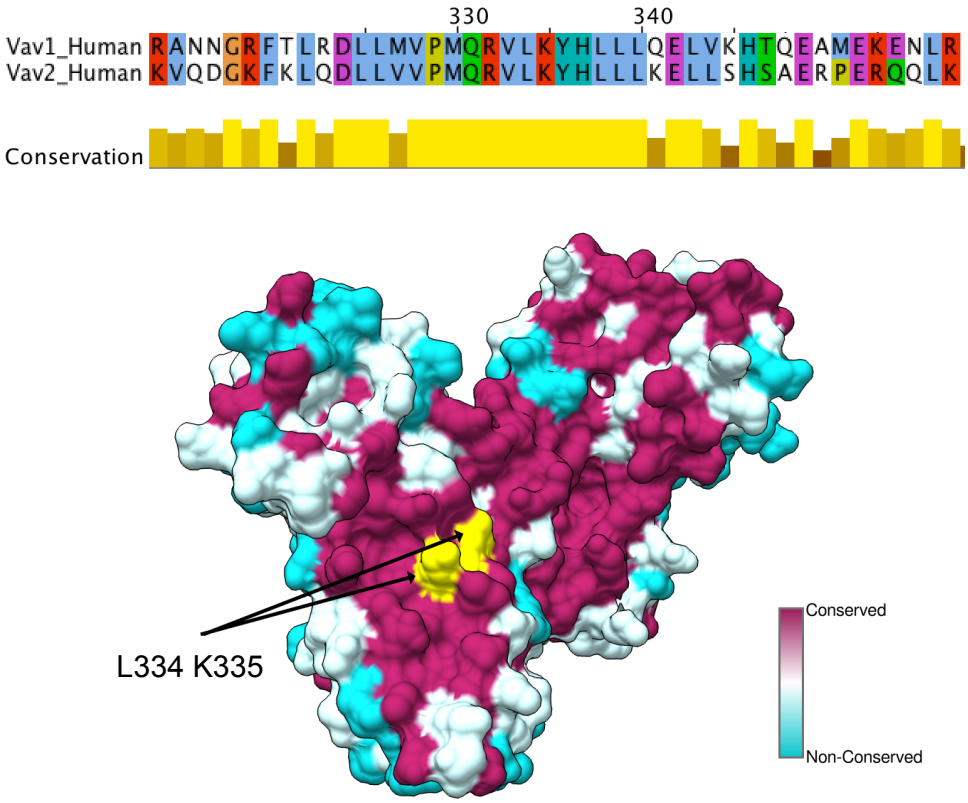

Figure 21: Vav1 and Vav2 amino acid conservation around the critical LK residues

Upper: Aligned amino acid sequences from Homo sapiens Vav1 and Vav2. The portion shown is centered on Leucine 334 and Lysine 335 (L^{334}, K^{335}). Sequences are colored using the ClustalX scheme. The 'Conservation' bar below shows the high degree of identity and conservation surrounding these LK residues. **Lower:** Surface representation of the crystal structure of the DH-PH-C1 portion of Vav1. The surface facing out includes the catalytic pocket of Vav1 that contacts Rac1. The L^{334} and K^{335} residues are highlighted in yellow. The rest of the surface is colored according to the degree of amino acid conservation with the Vav family of proteins. High conservation / identity is colored in maroon, moderate in white, and low conservation in blue. The surface of the catalytic pocket around the LK residues is highly conserved in both the linear sequence and the folded, 3D structure.

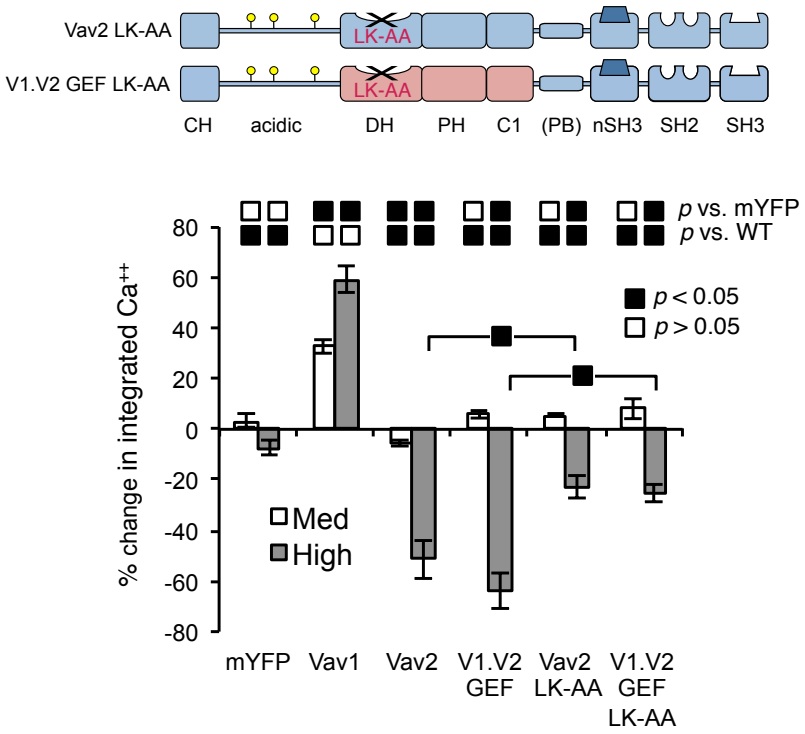

Figure 22: Vav2 catalytically inhibits Jurkat T cell calcium signaling

Upper: Schematic of Vav chimeras used in this panel. The site of the LK-AA mutation is indicated in the DH. Pertinent domain swaps and the GEF-inactivating LK-AA mutation are depicted. **Lower:** Calcium profiles of cells expressing mYFP-tagged Vav chimeras that contain either an intact or a catalytically inactivated GEF core derived from Vav2. Experiments were performed and quantified as in Figure 16. Plots depict the mean ±SEM of n≥3 experiments per condition.

6.3.2 Inhibition of calcium signaling by ΔCH Vav1 is not catalytic

After discovering that the catalytic activity of Vav2 inhibits calcium influx downstream of TCR ligation, I next turned my attention back to the similar inhibition by the Vav1 mutant that lacks a CH domain (ΔCH Vav1). I hypothesized that the CH domain may be imparting GTPase specificity on Vav1, and perhaps the unregulated GEF activity of the ΔCH Vav1 was responsible for inhibiting calcium signaling in T cells. However, this theory proved baseless. I rendered the ΔCH Vav1 construct catalytically dead using the LK-AA mutation, and found that both active and catalytically dead ΔCH Vav1 are equivalent in their affect on calcium influx in Jurkat (Figure 23). Therefore, the mechanism by which Vav2 inhibits calcium signaling in Jurkat T cells is partially separate from the mechanism of inhibition by ΔCH Vav1.

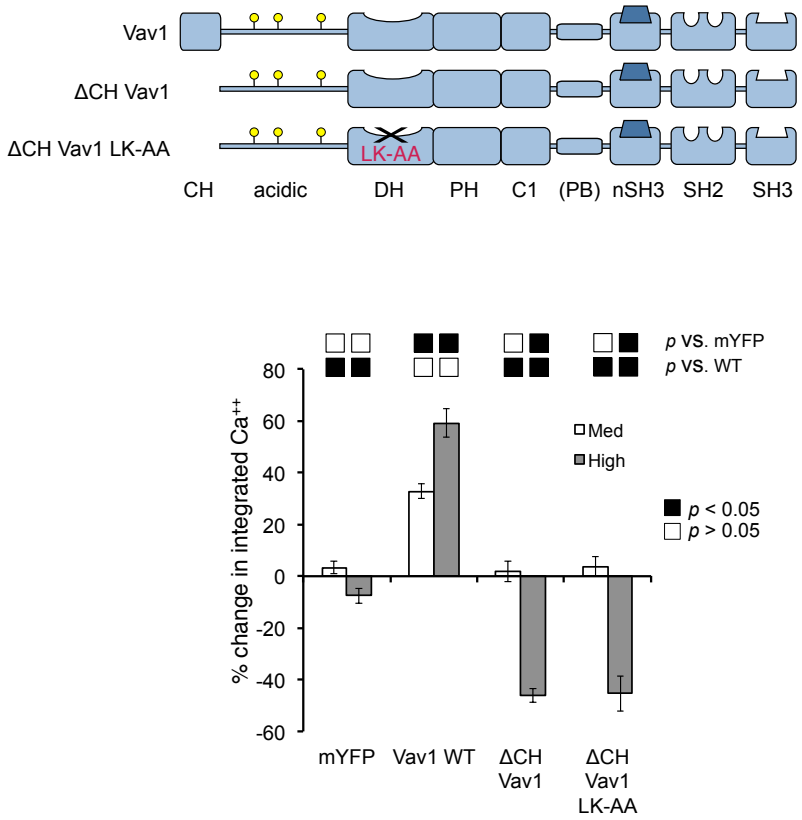

Figure 23: ΔCH Vav1 does not require catalytic activity for calcium inhibition

Upper: Schematic of Vav chimeras used in this panel. The site of the LK-AA mutation is indicated in the DH. **Lower:** Calcium profiles of cells expressing mYFP-tagged Vav chimeras that contain either an intact or a catalytically inactivated GEF on the ΔCH Vav1 construct. The previously shown WT Vav1 and ΔCH Vav1 are shown for comparison purposes. Experiments were performed and quantified as in Figure 16. Plots depict the mean ±SEM of n≥3 experiments per condition.

6.4 Calcium profiles of Rho family GTPases

6.4.1 Determining the Calcium phenotype of Rho Family GTPases

In order to reconcile my findings that Vav2 catalytically inhibits calcium signaling in Jurkat cells with the positive impact of Vav1, I needed to establish two things. First, one of the GTPases that Vav2 activates must inhibit calcium influx in Jurkat when it is active. Second, that GTPase must be a target of Vav2 and not Vav1. To address the first question, I investigated the impact of Rho family GTPases on calcium signaling. However, as there are at least 25 members of the Rho GTPase family (Tybulewicz and Henderson, 2009), I first established which ones were possible candidates. Using a phylogenetic trees that group Rho GTPases into subfamilies, I found that only three of these subfamilies contain GTPases that have been reported to be activated by one of the Vav isoforms (Figure 24, subfamilies shown in white have at least one member that can be activated by a Vav isoform). As well, some of these GTPases are atypical and are not activated by GEFs (RhoH and RhoBTB1-3) (Tybulewicz and Henderson, 2009). I also examined which Rho family GTPases were expressed at high levels in either CD4+ or CD8+ T cells (Figure 24, in red). GTPases that were both high expressors and in subfamilies that have been implicated as potential Vav GEF targets were selected for screening (Figure 24, marked blue).

To determine the impact on calcium signaling of the selected GTPases, I obtained, created, or used pre-existing constructs with activating mutations. There are two well-characterized single amino acid mutations that lock Rho family GTPases in

an active state: G12V or Q61L (Rac1 numbering). I expressed fluorescently tagged versions of these constitutively active (CA) GTPase mutants by transient transfection into J.Vav1 cells. These cells were stimulated, and their calcium responses were assessed.

6.4.2 Cdc42 strongly inhibits Ca++ influx in J.Vav

All of the members of the Rac1 subfamily tested, Rac1, Rac2, and RhoG, increased the level of calcium influx after TCR ligation when expressed as CA mutants (Figure 25). While these increases were not necessarily dramatic, they were consistent, and were also the result of overexpression on top of the endogenous forms that are presumably still being activated. These results suggest that the Rac1 subfamily of proteins have underappreciated roles in T cell calcium signaling, and would benefit from further study. Active RhoA appeared to exert a mild inhibition, but the effect was not significant. In contrast, high levels of CA Cdc42 dramatically inhibited calcium influx after TCR ligation (Figure 25). These findings pointed to Cdc42 as the most likely target of Vav2 that suppresses calcium signaling in Jurkat T cells.

Subfamily	Expression in T CD4	CD8	Tested
Rac1	5.3	5.3	
Rac3	4.1	4.0	
Rac2	5.8	5.8	
RhoG	5.2	5.2	
Cdc42	5.2	5.3	
RhoJ	3.7	3.6	
RhoQ	3.4	3.5	
RhoU	4.1	4.0	
RhoV	3.5	3.4	
RhoH	4.8	4.9	
RhoHBTB1	3.8	3.7	
RhoHBTB2	4.5	4.6	
RhoHBTB3			
Miro1			
Miro2			
RhoA	5.3	5.5	
RhoC	3.9	3.8	
RhoB	3.9	3.5	
RND1			
RND2			
RND3			
RhoD			
RhoF			

Figure 24: Rho family GTPases: Subfamilies and T cell expression

An explanation of the decision process for which GTPases I chose to investigate. The left column splits the Rho family into subfamilies as determined by phylogenetic analysis. White backgrounds denote subfamilies that have members linked to Vav GEFs in at least one published report. Grey backgrounds are subfamilies that either do not interact with GEFs, such as the RhoH group, or have no evidence of connections with Vav proteins. The central column represents expression of the individual GTPases in splenic naïve CD4+ CD25-, or CD8+ murine T cells, as reported by Immgen.com (Heng and Painter, 2008). The numbers are relative numbers based off of the absolute values reported at Immgen.com. GTPases with a relative expression of 4.5 or higher are highlighted in red. The far right column indicates, in blue, which GTPases meet the criteria of strong expression in T cells and a potential interaction with Vav GEFs.

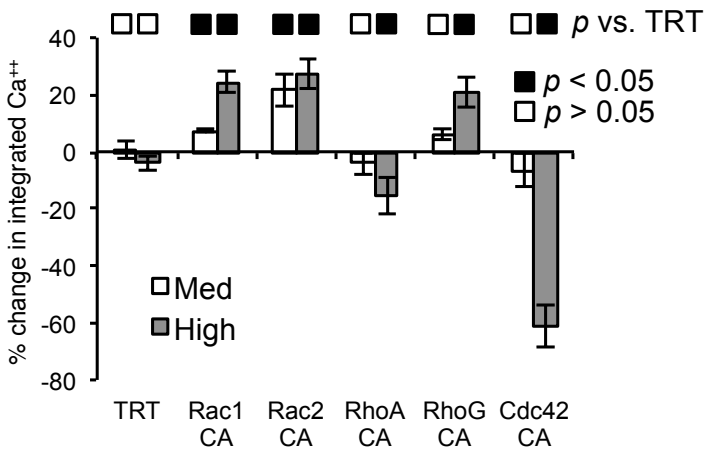

Figure 25: Calcium profiles of select active Rho family GTPases

Calcium profiles of cells expressing the indicated levels of 3xFlag.TRT-tagged, constitutively active (CA) GTPase constructs. Experiments were performed and quantified as in Figure 16. Plots depict the mean ±SEM of n≥3 experiments per condition, with the following exceptions: Rac2 CA (n=2), RhoA CA (n=2).

6.4.3 Calcium inhibition is common to Cdc42 isoforms and CA mutants

It is poorly appreciated that Cdc42 has two isoforms with different tissue distributions. Many of the papers that express exogenous Cdc42 constructs in hematopoietic cells fail to report the isoform used, and the practice of sharing plasmids between labs can propagate the unwitting use of the uncommon isoform. Oddly, Isoform 2 has been chosen as the 'canonical' sequence of Cdc42, even though this isoform has only been found in brain tissue. However, hematopoietic cells exclusively express isoform 1, the 'placental isoform.' The isoforms differ in their C-terminus, and experience different post-translational modification (Figure 26).

As a result, the two isoforms can have different intracellular localizations in the same cell type, and activate different pathways (Wirth et al., 2013). I initially used the brain isoform (isoform 2) for my experiments, but switched to the placental isoform (isoform 1) on discovering that only isoform 1 is expressed in T cells, and verified all of my initial results with the new isoform. I found that both isoforms have similar impacts on calcium signaling in stimulated Jurkat cells. I also tested both activating mutations, G12V and Q61L, to make sure the inhibition of calcium signaling was not specific to one of these mutations, and found both inhibited calcium signaling in Jurkat T cells (Figure 27).

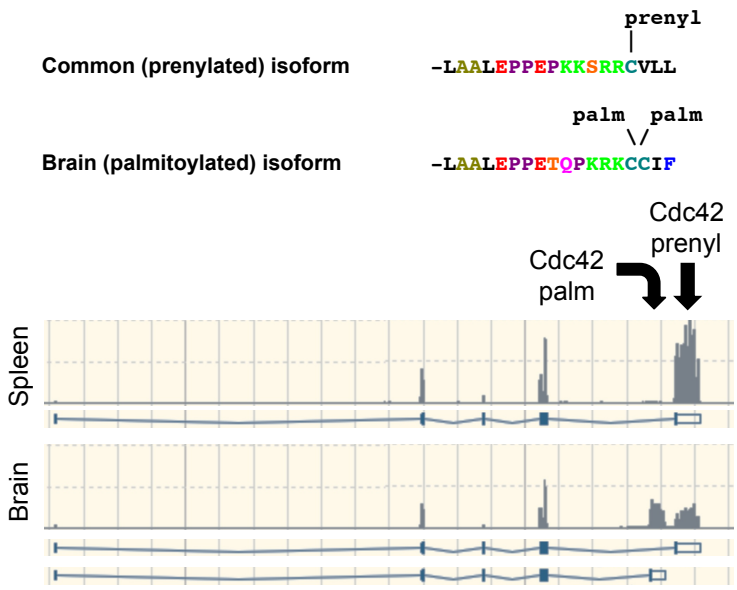

Figure 26: Cdc42 isoform differences and expression pattern

Upper: C-terminal amino acid sequence differences between the two Cdc42 isoforms, and the resulting post-translational modifications. Isoform 1 is the 'placental,' common isoform that is prenylated. Isoform 2, or the 'brain' isoform, is palmitoylated. **Lower:** RNASeq expression profiles of the two isoforms in murine hippocampus (brain) and spleen. The spleen only expresses the prenylated isoform. Data acquired from Ensembl release 80 (Flicek et al., 2014).

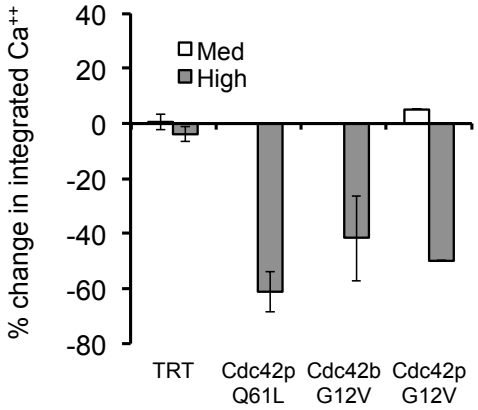

Figure 27: Both Cdc42 isoforms and CA mutations inhibit calcium signaling

Calcium profiles of J.Vav cells transfected with either a TRT control or the indicated activating (CA) Cdc42 constructs. Cdc42p is the 'placental,' or isoform 1, of Cdc42 that is found in hematopoietic cells, and Cdc42b is the 'brain,' or isoform 2, found primarily in the CNS. Q61L and G12V are the amino acid mutations widely used to maintain GTPase in the GTP-bound, active state. Calcium responses to TCR stimulation were collected and quantified as in Figure 1D. Data is from n≥3 for YFP, Cdc42p Q61L, and Cdc42b G12V, and n=1 for Cdc42p G12V.

6.5 Determining the GTPase specificity of Vav isoforms

6.5.1 Designing an *in vivo* assay for GEF specificity

Given the similarity in the effects of both Vav2 and active Cdc42, I hypothesized that Vav2 catalytically inhibits calcium signaling in Jurkat T cells by activating Cdc42. However, as catalytically active Vav1 enhances calcium influx in our model, this hypothesis only makes sense if Vav2 and Vav1 have different catalytic specificities. Unfortunately, as discussed in the Introduction, my examination of the literature yielded no clear information on differences between GTPase targets of Vav1 and Vav2. Therefore, I had to establish these differences in our model system. Due to the limitations of the commonly used GTPase activation assays (again, see the Introduction), we decided to turn to imaging techniques to determine GTPase interactions with Vav isoforms. In the development of this technique, we were aided by the ability to clearly visualize the pool of active Vav1 in T cells in the SLP-76 microcluster (Sylvain et al., 2011). Therefore, we sought to capture the interaction between fluorescently tagged Vav proteins and GTPases in the context of this microcluster.

6.5.2 Imaging GEF – GTPase interactions

The first hurdle to overcome with trying to visualize the interaction between a GEF and a GTPase is that this enzymatic interaction is much faster than imaging can capture (see Figure 28 for an overview). In order to overcome this, we took advantage of a well-characterized GTPase mutation. Rho GTPases have a conserved threonine at position 17 (Rac1 numbering) that can be mutated to an asparagine to create a mutant

with low nucleotides affinity (Feig, 1999). These T17N mutants have a higher affinity for the catalytic surface of their activating GEFs than for nucleotides. As these mutants rarely bind GTP, they fail to adopt the conformation that allows dissociation with their GEF. The interaction between T17N GTPase mutants and GEFs is strong enough that one can pull down the other in biochemical assays (Feng et al., 2004; Lin et al., 2006), they can be purified together in complexes (Baird et al., 2005), and the two can be crystallized together (Hanawa-Suetsugu et al., 2012; Harada et al., 2012). We reasoned that we could visualize the interaction between GEFs and GTPases by using fluorescently tagged T17N GTPases and Vav isoforms. These T17N GTPase mutants are commonly called 'dominant negative' (DN) in the literature, even if they do not exactly fit the classic definition, and I have adopted this nomenclature here.

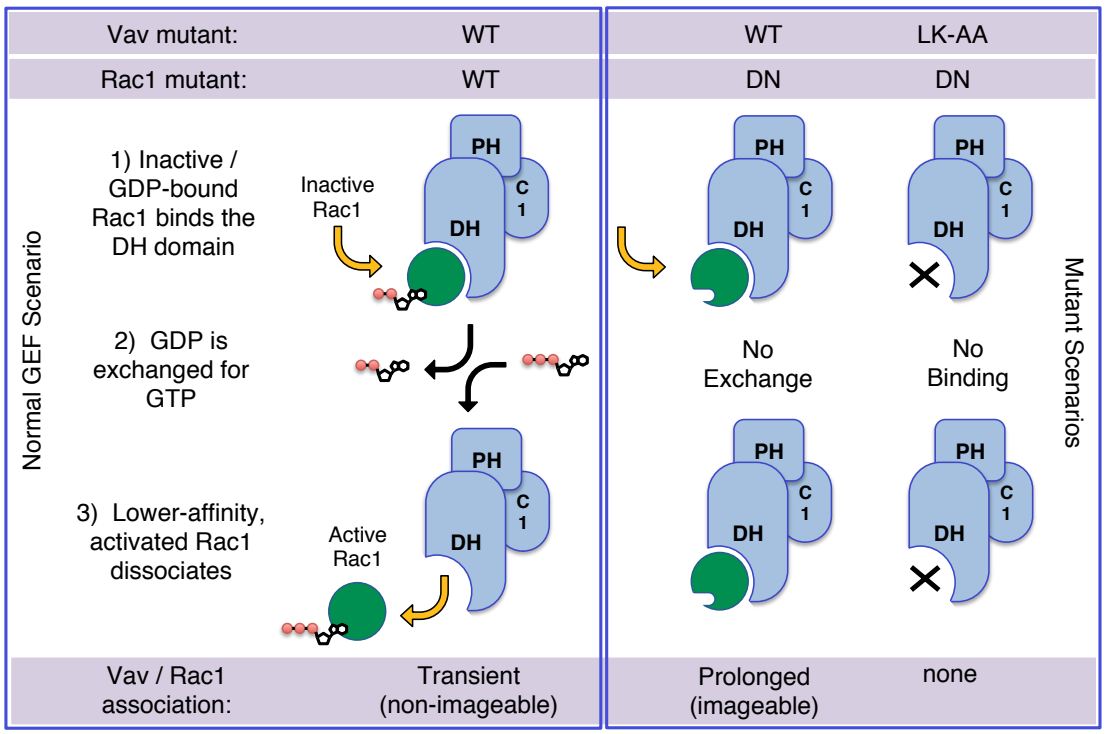

Figure 28: Overview of the 'GEF-trapping' imaging assay

Schematic of the 'GEF Trapping' imaging strategy. The blue shapes represent the DH-PH-C1 domains, or 'GEF cassette' from Vav1, with other domains not depicted for simplicity. Green circles indicate either inactive (GDP-bound), nucleotide-free, or active (GTP-bound) GTPases. From left to right: GEF-GTPase interactions are difficult to image as they are rapidly destabilized upon the acquisition of GTP by the GTPase. However, dominant negative (DN) mutants bind to the catalytic surface of the GEF, and due to their low affinity for nucleotides, remain bound for extended periods of time. Finally, the Vav GEF inactivating LK-AA mutation abrogates GEF binding to GTPases, so no localization between the GEF and GTPases should occur.

6.5.3 'GEF-Trap' Assay shows Rac1 co-localization with catalytically active Vav1 and Vav2

To establish the feasibility of imaging GEF-GTPase interactions by using DN GTPase mutants, I initially imaged different blue (mCerulean3, or mCer3) tagged Vav constructs with red fluorescent (TRT) DN Rac1 mutants. Rac1 was chosen as the consensus target of both Vav1 and Vav2. These imaging assays were performed by transient transfection of Vav and GTPase constructs into Jurkat cells that lack endogenous SLP-76 but have been stably reconstituted with YFP-tagged SLP-76 (J.14.SY). The J.14.SY cells offer a robust system, well-documented system for visualizing SLP-76 microclusters (Bunnell et al., 2006; Nguyen et al., 2008; Ophir et al., 2013; Sylvain et al., 2011). As predicted, both wild type Vav1 and Vav2 captured DN Rac1 in SLP-76 MC (Figure 29, Vav1 WT and Rac1 DN, and Vav2 WT and Rac1 DN). Also as predicted, there was no visible co-localization between wild type Vav1 or Vav2 and WT Rac1 (Figure 29, WT Vav1 and WT Rac1 and results not shown). The co-localization of Vav isoforms with DN Rac1 was not due to the fluorescent tag on the GTPase, as a construct consisting only of TRT did not cluster with Vav and SLP-76 (Figure 29, Vav2 WT and TRT).

To determine if DN Rac1 localizes to SLP-MC due to Vav isoforms rather than an unknown GEF or binding partner for Rac1, I expressed mutants of Vav1 and Vav2 that contained the GEF-inactivating LK-AA mutation (discussed above). When the Vav1 or Vav2 LK-AA mutants were co-expressed with DN Rac1, no clustering of Rac1 was visible (Figure 29, Vav2 LK-AA and Rac1 DN). Therefore, capturing Rac1 in the microcluster is entirely dependent on having a functional catalytic surface on the

Vav GEF. This observation is strong evidence that the GTPase is being trapped in the catalytic pocket of Vav.

One other important aspect of this assay is that DN GTPase trapping relies on the over-expression of the relevant Vav isoform. No clustering of DN Rac1 can be seen with only mCerulean3 co-expression (Figure 29, TRT Rac1 DN and mCer3). I see this reliance on overexpression as both a strength and a weakness of the assay, and explore this issue more in the Discussion. For the sake of the following experiments, this reliance on overexpression is useful, as the results are not complicated by the presence of the endogenous GEFs.

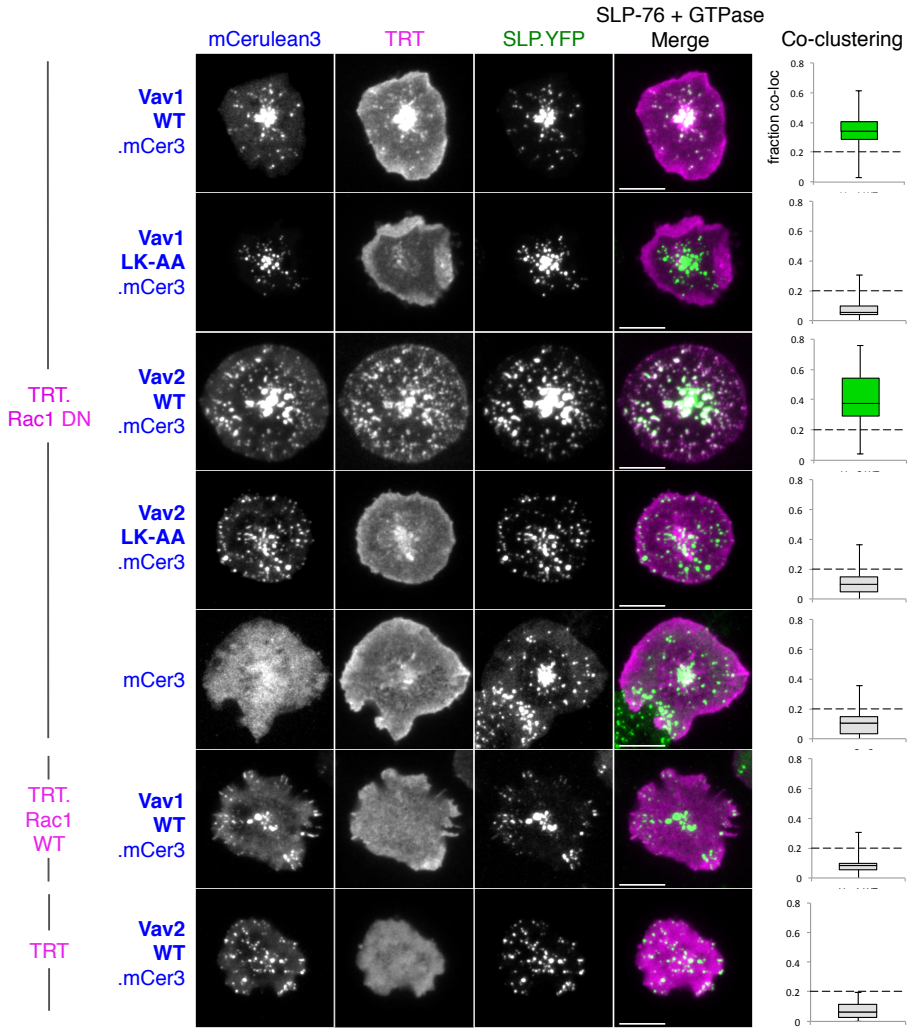

Figure 29: Verifying the 'GEF-Trapping' assay with Vav1, Vav2, and Rac1

Visualization of TRT-tagged Rac1 chimeras (magenta pseudocolor) and mCer3 (mCerulean3) tagged Vav chimeras in cells that stably express a YFP-tagged SLP-76 chimera (J14.SY cells) (green pseudocolor). Cells were plated on OKT3-coated glass surfaces and fixed after 7 minutes. Cells at peak spreading were selected for analysis. Each row of images corresponds to one representative cell. For clarity, the Vav channel is omitted from the merge, as all Vav constructs co-localize with SLP-76. Scale bars represent 10μm. The co-clustering column shows an average of the fraction

of clusters in one channel (green or red) that appear in the other. Boxes enclose the second and third quartiles and whiskers indicate minimum and maximum values. Amounts below the dashed line correspond to no visible co-clustering. Boxes where the media co-localization values were over 0.2 (20%) are highlighted in green. Images are representative of n≥3 experiments for all constructs, quantification from n≥2 experiments, with ≥3 cells per condition per experiment.

6.5.4 Identifying and quantifying co-localization

One difficulty in analyzing GTPase co-clustering with SLP-76 MC is that many cells display a relatively large irregular central pool of the fluorescent SLP-76, Vav, and GTPase that could be co-localizing. However, Rho GTPases are often found basally on the Golgi apparatus (Erickson et al., 1996), which is visible near the center of contact in our imaging assays. Also, SLP-76 MC, including Vav, move radially to the center of contact to form a pool of clusters that only minimally contribute to signaling (Bunnell et al., 2006; Sylvain et al., 2011; Varma et al., 2006). Therefore, I excluded the central 20% of the cell in determining GTPase localization to SLP-76 MC, as actual Vav/GTPase interactions cannot be determined in this area (Figure 30). Clusters in the outer 80% of the cell were identified by software analysis, and co-localization was computed (see Materials and Methods) and is presented here for each set of conditions.

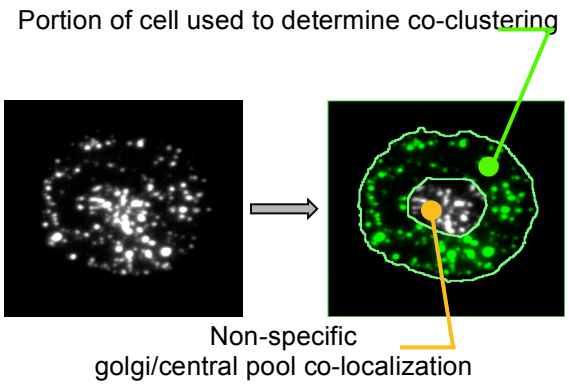

Figure 30: Limiting co-localization assessment to the periphery of the cell

Representation in green of the perimeter 80% of the cell considered in determining co-clustering. At left, an example of the SLP-YFP channel from one cell. The cell contains microclusters, or puncta, across the entire plane of contact. The individual puncta in the periphery are more distinct, and become less defined towards the center of the cell. This central area corresponds to the location of the Golgi apparatus (assessed in other experiments, data not shown). As Rho GTPases often localize to the Golgi, specific co-localization in the central 20% of the cell is too difficult to determine. Therefore, this region was excluded from quantification.

6.6 Cdc42 is trapped in the catalytic core of Vav2, but not Vav1

6.6.1 Vav2 interacts with a wider range of GTPases than Vav1

After confirming that Rac1 co-localizes with both Vav1 and Vav2 in SLP-76 MC downstream of TCR stimulation, I screened the other candidate Rho family GTPases. I predicted that Rac2 would show the same co-localization patterns as Rac1, as the proteins have 92% sequence identity. However, DN Rac2 showed no signs of clustering with WT Vav1 (Figure 31). Vav2 was able to trap DN Rac2 in the SLP-76 MC; but even with Vav2, the fraction of the Rac2 pool that is pulled into clusters is much lower than that of Rac1 with Vav2 (Figure 31 lower, compared with WT Vav2 and DN Rac1 in Figure 29). The reasons for this difference between Rac1 and Rac2 localization with Vav isoforms is unclear; but Rac2 does show different subcellular localization that Rac1, with a much greater fraction of Rac2 in membranes other than the PM (Michaelson et al., 2001). This difference in localization could make Rac2 less accessible to GEFs in the SLP-76 microcluster.

Some studies report that RhoA is robustly activated by Vav1 and Vav2, and one study claims RhoA is the primary target of Vav2 *in vitro* (Schuebel et al., 1998). However, most of the more recent *in vitro* studies show only very weak activation of RhoA, if any, by Vav1 or Vav2 (Abe et al., 2000; Booden et al., 2002; Rapley et al., 2008). The results from my screen support the later reports, as RhoA did not cluster with Vav1, and showed only rare co-clustering with Vav2 (Figure 32).

Although there are relatively few studies of RhoG activation by Vav proteins, there are reports that Vav1 (Vigorito et al., 2003) and Vav2 (Schuebel et al., 1998) can

lead to the activation of RhoG. However, RhoG proved to be more difficult to image than the other GTPases. Cells expressing moderate to high amounts of RhoG failed to adhere to and spread out on surfaces coated with only anti-CD3, rendering imaging unfeasible. To solve this problem, I coated the imaging glass with both anti-CD3 and anti-CD43. Antibodies to the membrane resident glycoprotein CD43 cause Jurkat T cells to land and spread on a coated surface, but do not cause SLP-76 microcluster formation (Bunnell et al., 2002; Nguyen et al., 2008). Adding anti-CD43 coating to the anti-CD3 coated glass surface allowed for imaging of the DN RhoG expressing cells. RhoG was not trapped in clusters by Vav1 (Figure 33). A minimal amount of co-clustering was observed with DN RhoG and or Vav2, but the majority of RhoG was visible outside of the SLP-76 microclusters containing Vav2 (Figure 33).

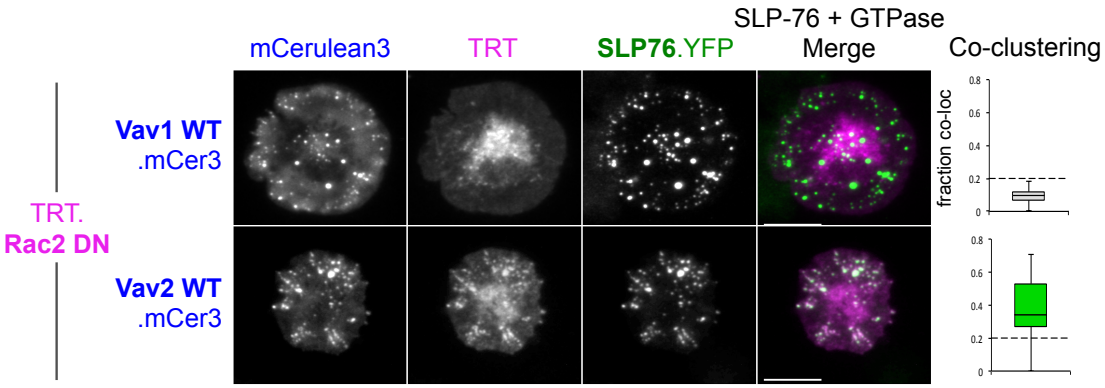

Figure 31: Only Vav2 shows localization with Rac2

J14.SY cells were co-transfected with vectors encoding a TRT-tagged DN chimera of Rac2, and mCer3 tagged chimeras of either wild type Vav1 (top panel) or Vav2 (lower panel). Cells were imaged and co-clustering was quantified as in Figure 29. The left column of each group is a grayscale image of the GEF channel, the second column shows the GTPase channel, the third is of SLP-76, and the fourth column is a pseudocolored image depicts the DN GTPase (magenta) and SLP-76 (green). Scale bars represent 10μm.

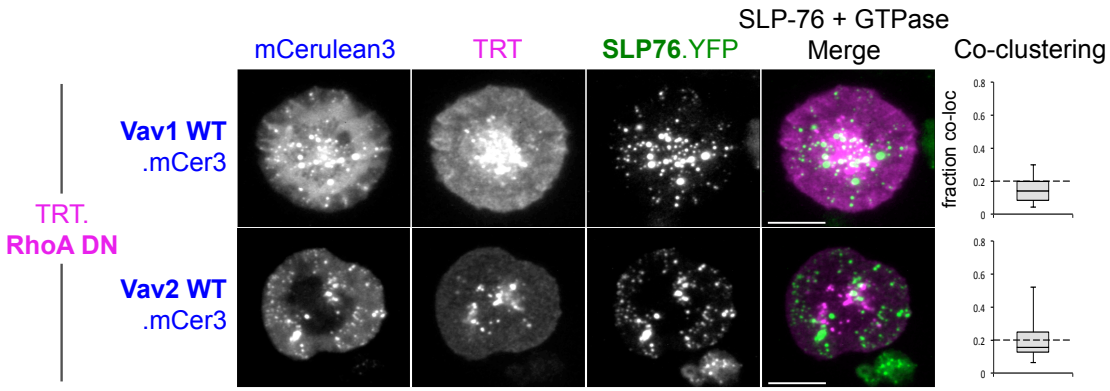

Figure 32: RhoA shows no colocalization with Vav1 and little with Vav2

J14.SY cells were co-transfected with vectors encoding a TRT-tagged DN chimera of RhoA and mCer3 tagged chimeras of either wild-type Vav1 (upper panel) or Vav2 (lower panel). Cells were imaged and co-clustering was quantified as in Figure 29, The left column of each group is a grayscale image of the GEF channel, the second column shows the GTPase channel, the third is of SLP-76, and the fourth column is a pseudocolored image depicts the DN GTPase (magenta) and SLP-76 (green). Scale bars represent 10μm.

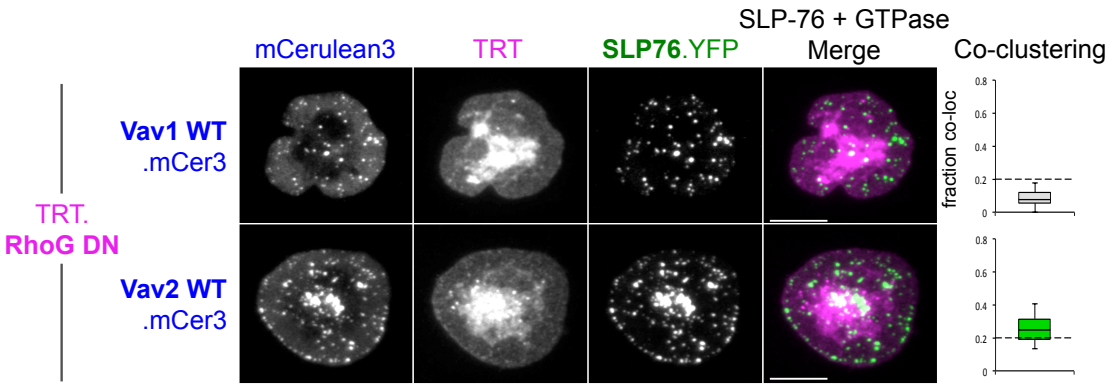

Figure 33: RhoG shows no colocalization with Vav1 and little with Vav2

J14.SY cells were co-transfected with vectors encoding a TRT-tagged DN chimera of RhoG and mCer3 tagged chimeras of either wild-type Vav1 (upper panel) or Vav2 (lower panel). In this instance, cells were plated on glass surfaces coated with anti-CD3 and anti-CD43. Cells were imaged and co-clustering was quantified as in Figure 29, The left column of each group is a grayscale image of the GEF channel, the second column shows the GTPase channel, the third is of SLP-76, and the fourth column is a pseudocolored image depicts the DN GTPase (magenta) and SLP-76 (green). Scale bars represent 10μm.

6.6.2 The Vav2 GEF domains recruit Cdc42 to the SLP-76 MC

As both WT Vav2 and CA Cdc42 show similar inhibition of calcium influx downstream of TCR ligation, I hypothesized that Vav2 can activate Cdc42 in T cells, while Vav1 is unable to activate it. I used the GEF-trapping assay to test this hypothesis, and found that Vav2 and DN Cdc42 show unmistakable co-clustering in activated Jurkat T cells. In contrast, DN Cdc42 shows no signs of clustering with co-expressed Vav1 (Figure 34). To further explore the connection between calcium signaling inhibition and Cdc42 co-localization, I tested another Vav chimera that catalytically inhibited Jurkat T cell calcium influx: the Vav1 construct with the Vav2 catalytic domain (V1.V2 GEF)(see Figure 22). This construct also traps DN Cdc42 in the SLP-76 microcluster (Figure 34). To verify that the capture of Cdc42 by Vav2 requires the catalytic activity of Vav2, I tested the inert, LK-AA Vav2 mutant. As expected, Vav2 LK-AA loses the ability to trap DN Cdc42 in microclusters (Figure 34, Vav2.LK-AA). Overall, the GEF trapping assay showed a perfect correlation with the Vav constructs that can inhibit calcium signaling in T cells and those that can trap DN Cdc42 in clusters.

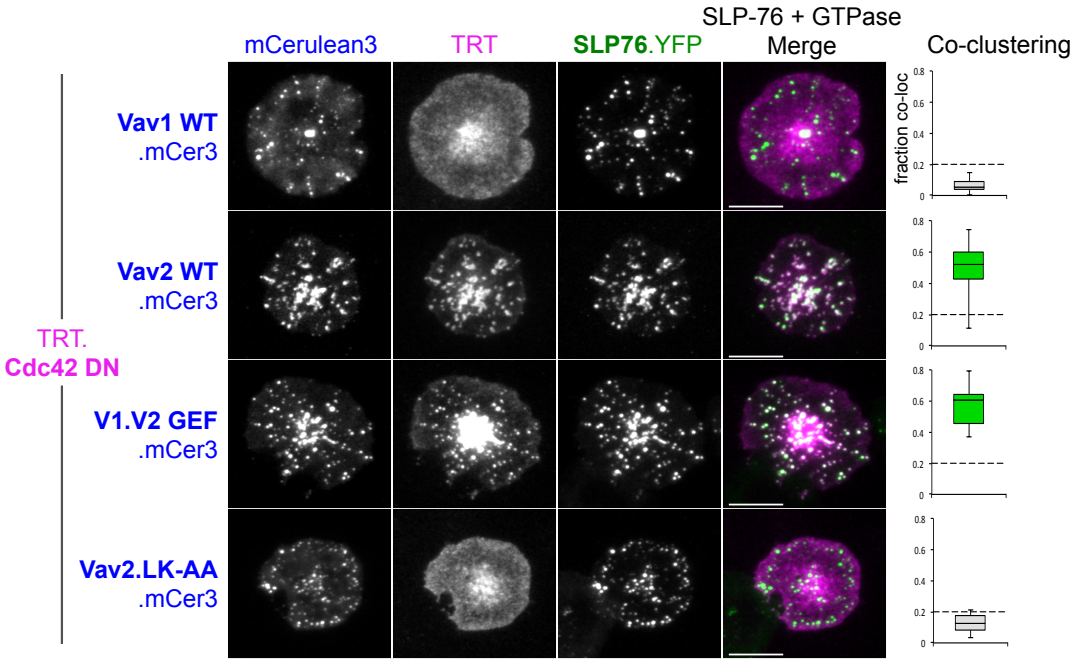

Figure 34: The Vav2 GEF domains recruit Cdc42 to the SLP-76 MC, but the Vav1 GEF does not

J14.SY cells were co-transfected with vectors encoding a TRT-tagged DN Cdc42 chimera and the indicated mCer3 tagged Vav chimeras and mutants. Cells were imaged and co-clustering was quantified as in Figure 29. The left column of each group is a grayscale image of the GEF channel, the second column shows the GTPase channel, the third is of SLP-76, and the fourth column is a pseudocolored image depicts the DN GTPase (magenta) and SLP-76 (green). Images are representative of n≥3 experiments for all constructs, and quantification from n≥2 experiments with ≥5 cells per experiment.

6.7 Narrowing down the portion of Vav1 that excludes Cdc42

6.7.1 GTPase specificity is determined by the DH domain of Vav1

Having discovered a dramatic difference in GTPase specificity between Vav1 and Vav2, I wanted to determine the structural mechanism of this exclusion of Cdc42 by Vav1. Knowledge of this mechanism could pave the way for finding small molecules that could specifically target the GEF activity of Vav1 or Vav2. My initial chimeras used the entire 'GEF core,' or the DH-PH-C1 domains of the proteins for swaps, as these three domains operate as a single functional unit (Chrencik et al., 2008; Rapley et al., 2008). A number of the residues on the PH and C1 domains interact with each other and residues on the DH domain; and breaking these interactions or removing the PH or C1 domain reduces Vav1 catalytic efficiency. Although many of these amino acids are conserved between Vav1 and Vav2, it was not clear if swapping the Vav1 and Vav2 PH and C1 domains would retain the quaternary structure of the GEF core. It was also possible that the influence of the PH and C1 domains accounted for the specificity of the Vav1 and Vav2 GEFs.

To narrow down the mechanism of Vav1 specificity, I began dissecting the GEF core. As Vav2 displays such clear co-localization with both Rac1 and Cdc42, I decided to use Vav2 as the template and swap portions of Vav1 in until the co-localization with Cdc42 was lost. As a control, Rac1 co-localization was also assessed to determine if the resulting Vav chimera was still capable of interacting with this common GTPase target. Thus, three chimeric Vav proteins were created, with the DH, PH, and C1 domains of Vav1 substituted into full-length Vav1 (Figure 35, top panel). Both Vav2 with the Vav1 C1 domain (Vav2.V1 C1) and Vav2 with the Vav1 PH

domains (Vav2.V1 PH) showed strong co-localization with both DN Rac1 and DN Cdc42. However, the transfer of the Vav1 DH domain into Vav2 resulted in a chimera that did not co-localize with DN Cdc42, but retains the ability to interact with Rac1 (Figure 35, lower panels). Thus, it appears that the DH domain is the only portion of the Vav1 protein responsible for its *in vivo* selectivity for Rac1.

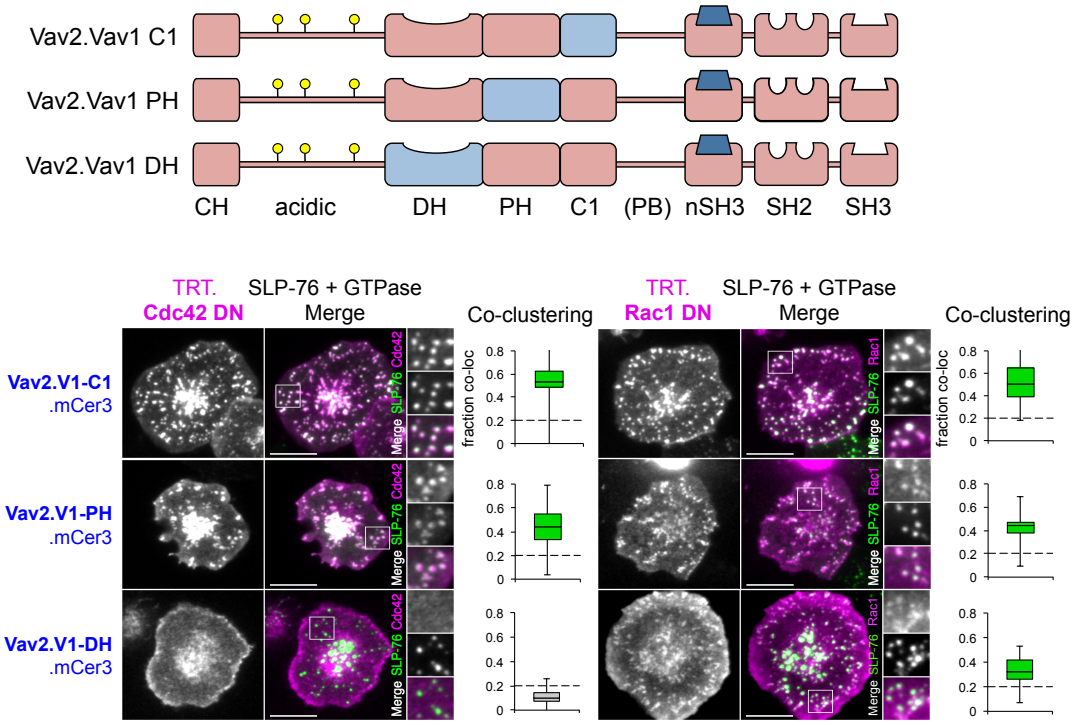

Figure 35: The DH domain of Vav1 conveys GTPase specificity to Vav2

Upper: Schematic of the domain-swapped Vav constructs used in this panel. Individual domains within Vav2 (red) were replaced by the corresponding domains from Vav1 (blue). **Lower panels:** J14.SY cells were co-transfected with vectors encoding a TRT-tagged dominant negative (DN) Rac1 or Cdc42 chimera and the indicated mCer3 tagged Vav chimeras. Cells were imaged and co-clustering was quantified as in Figure 29. Images are representative of n≥3 experiments, quantification from n≥3 experiments with≥4 cells per experiment.

6.7.2 The GTPase proximal amino acids of Vav1 are not sufficient to convey GTPase specificity

I reasoned that the specific amino acids responsible for Vav1 GTPase specificity were likely to be the ones in position to make direct contact with a GTPase. Therefore, I rationally designed a mutant version of Vav2 with amino acids from the Vav1 DH that met the following criteria, they must be: surface exposed; in close proximity to a bound GTPase (given the crystal structure PBD ID 3bji (Chrencik et al., 2008)); and in proximity to a portion of a bound GTPase that is not conserved between Rac1 and Cdc42. With these considerations in mind, I replaced 18 amino acids in the Vav2 DH domain with their Vav1 counterparts (Figure 36, top portion). This construct was made with the assumption that it would clearly fail to co-localize with Cdc42, and would serve as a starting point to use to find the minimal set of amino acids necessary for Cdc42 exclusion. However, when this construct was expressed in J14.SY Jurkat cells, it showed strong co-localization with DN Cdc42 (Figure 36), leaving me somewhat perplexed as to which residues in Vav1 are responsible for the exclusion of Cdc42.

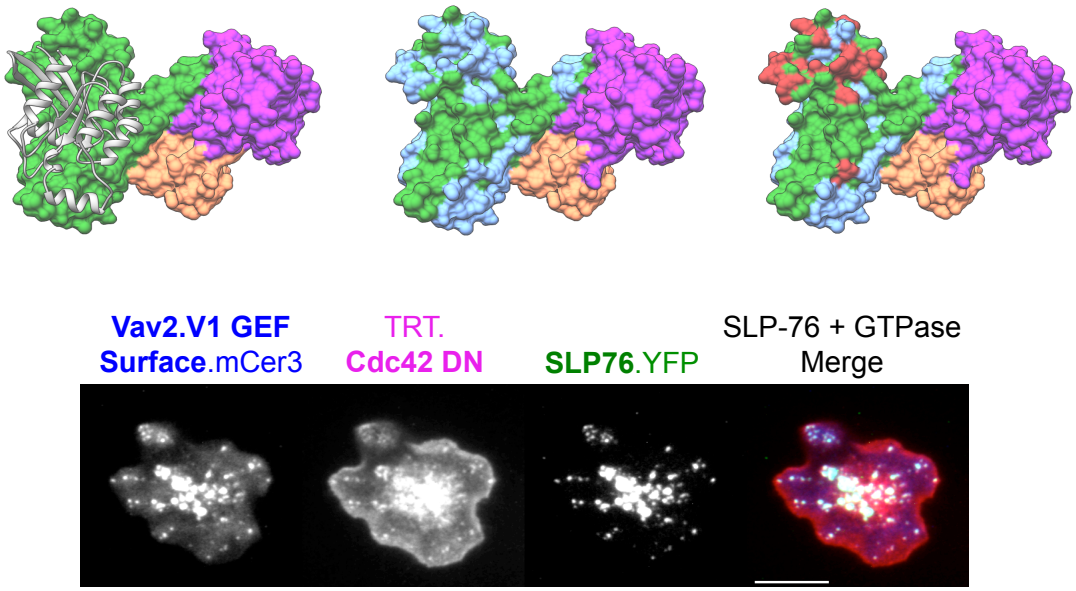

Figure 36: Vav2 with the GEF surface of Vav1 maintains Cdc42 interaction

Upper: Amino acids of Vav2 replaced with Vav1 equivalents. Upper left: the DH (green), PH (purple), and C1 (orange) domains of Vav proteins with a bound Rac1 (gray ribbons) to show orientation. Upper middle: Rac1 removed to show binding surface. Common residues to Vav1 and Vav2 in green, divergent residues in light blue. Upper right: same as the middle, but with red showing the residues of Vav2 replace with the Vav1 equivalent. **Lower:** Representative cell of this construct co-localizing with DN Cdc42.

6.7.3 The first and last helical portion of the Vav1 DH domain do not provide GTPase specificity

After the rational design approach failed to produce a Vav chimera that excluded Cdc42 interaction, we returned to a more systematic mutational strategy. The DH domain of the Vav proteins was logically divided into three pieces, and these portions of Vav1 were swapped into Vav2. The ensuing chimeras were imaged with DN Cdc42 and DN Rac1. The first piece is a single alpha-helix that begins at the N-terminus of the DH domain and makes numerous contacts with Rac1 (in Vav1). But this portion does not convey specificity, as the resulting chimera (V2.V1-1st Helix) co-localizes with both Rac1 and Cdc42 (Figure 37).

The second candidate for DH domain section swaps was a portion that begins after the initial alpha helix and contains five more helixes that form the majority of the DH domain. This portion constitutes most of the core of the folded domain, as well as much of the surface both distal and proximal to the GTPase (Figure 38, left panel). While the substitution of this portion of Vav1 into Vav2 did result in a construct that was no longer able to co-localize with DN Cdc42, the construct also failed to trap DN Rac1 as well (Figure 38, right panel). The most likely explanation for this loss of Rac1 interaction is a loss of the structural integrity of the domain as a whole leading to a non-functioning catalytic surface. More work will need to be done to attempt to transfer the majority of the Vav1 residues in this region while still maintaining the interactions that preserve the structure of the catalytic surface.

The last portion of the Vav1 DH swapped into Vav2 was a long alpha-helix that connects the DH and PH domains, amino acids 348 to 376 (Vav1 numbering) (see

Figure 39, left panel). This portion also appears to have numerous points of contact with a bound GTPase, albeit with a portion of Rac1 and Cdc42 that shares almost complete identity. Accordingly, the construct of Vav2 that contained this portion of Vav1 (V2.V1-LongHelix), is capable of co-localizing with DN Cdc42 in J.14.SY Jurkat cells expressing both constructs (Figure 39). Therefore, only the core of the Vav1 DH domain contains the residues that determine Rac1 specificity; but identification of the minimal subset of necessary amino acids remains unresolved.

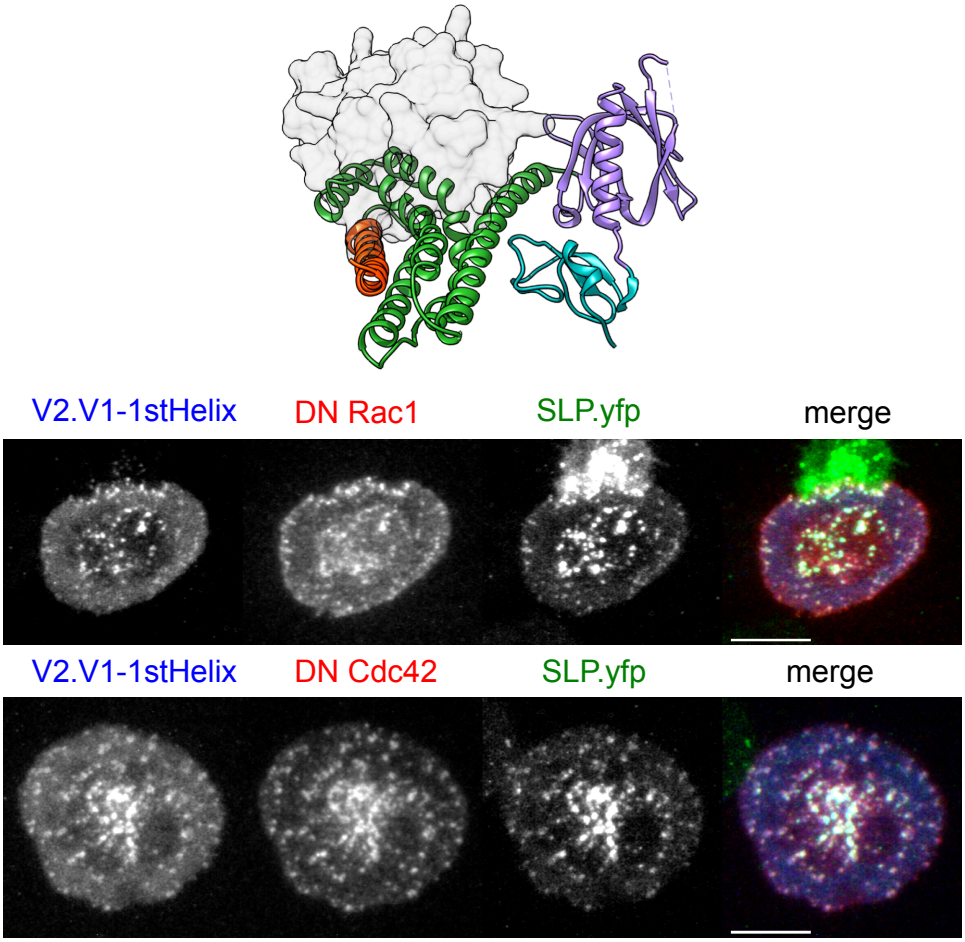

Figure 37: The first helix of the Vav1 DH does not convey Rac1 specificity

Upper: Schematic of the Vav1 initial DH helix transferred into Vav2. The Vav portions are represented as ribbons, with Rac1 as a transparent grey molecular surface. The Vav1 portion of the DH is in orange. The Vav2 DH is in green, the PH in purple, and C1 in cyan. **Lower:** Representative cells, showing both DN Rac1 and DN Cdc42 co-clustering with the Vav chimera (n=1 experiment, n>5 cells per condition).

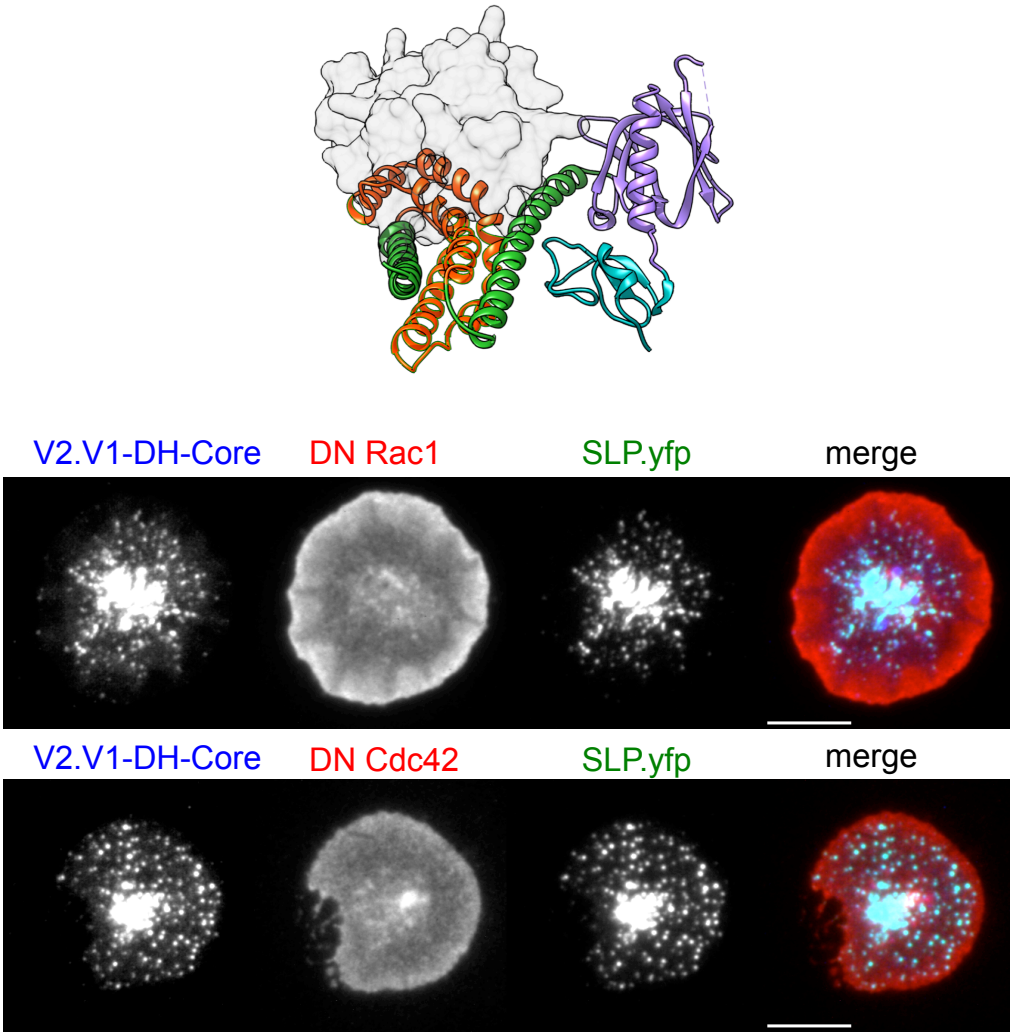

Figure 38: Transfer of the DH core of Vav1 does not support GTPase binding

Upper: Schematic of the Vav1 DH core transferred into Vav2, in orange. Formatted as in Figure 37. **Lower:** Representative cells, showing no DN Rac1 or DN Cdc42 co-clustering with the Vav chimera (n=1 experiment, n>5 cells/condition).

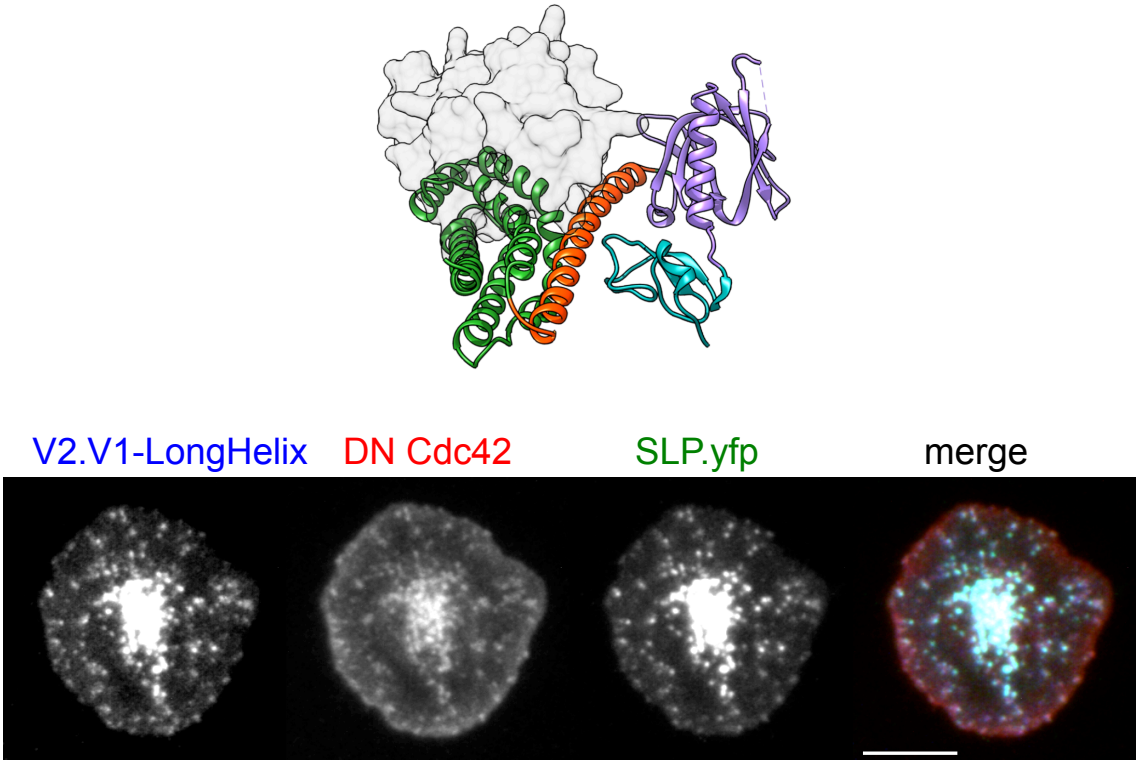

Figure 39: The Vav1 DH long helix does not transfer Rac1 specificity

Upper: Schematic of the Vav1 long helix transferred into Vav2, in orange. Formatted as in Figure 37. **Lower:** Representative cell, showing Cdc42 co-clustering with the Vav chimera. Images of this construct co-clustering with Rac1 as a control were not collected, as the co-clustering with Cdc42 proved that this construct is capable of trapping GTPases (n=1 experiment, >5 cells).

6.8 Vav1 specificity is determined by tryptophan 56 on Rac1

In parallel with my efforts to map the residues of Vav1 that prohibit interaction with Cdc42, I approached the problem from the other direction by mapping the portion of Cdc42 that blocks Vav1 co-localization. To this end, I designed chimeric GTPases by swapping portions between Rac1 and Cdc42. The three chosen breakpoints lie in highly conserved sequences, the first between the β2 and β3 strands, and the next between the α2 helix and the β4 strand, and the third within the terminal alpha-helix (Figure 40). With the help of John Charpentier, an undergraduate student in our lab, a panel of reciprocal section swaps was created, and dominant negative forms of these Rac1/Cdc42 chimeras were screened for co-localization with Vav1 andVav2.

6.8.1 Tryptophan 56 from Rac1 confers interaction with Vav1 to Cdc42

The chimera screen identified that only DN GTPase constructs that contained the first seventy-seven (77) amino acids of Rac1 could co-localize with Vav1 (Figure 41, left panel). All constructs were able to co-localize with Vav2, indicating that the chimeras were expressing as proteins that folded well enough to interact with the catalytic surface of a GEF (Figure 41, right panel). Further investigation determined that amino acids 46-77 of Rac1 allow an otherwise Cdc42 construct to co-localize with Vav1 (Figure 42). Within this stretch of amino acids, only six differ between Rac1 and Cdc42. I mutated those remaining residues in Cdc42 to their Rac1 equivalents either individually or in pairs. I imaged these mutants and found that changing phenyalaine 56 on DN Cdc42 to a tryptophan created a protein that unambiguously co-localized with Vav1 (Figure 43, Cdc42 F56W). Notably, there was no partial localization

phenotype with the other residue swaps, no other amino acids in Cdc42 preclude localization with Vav1.

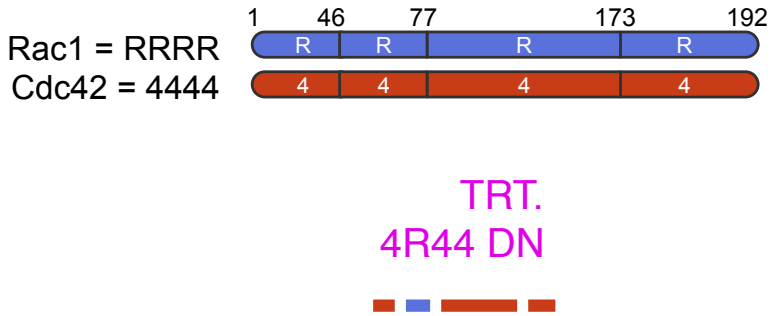

Figure 40: Representation of the Rac1 / Cdc42 divisions used for section swaps

Upper: Schematic of the division points for the section swaps between Rac1 and Cdc42 used in the follow set of imaging experiments. Splice sites were chosen around residues 46, 77, and 173. These are sites of identity between the two sequences, and areas where I predicted splicing would not interfere with folding. Each of the four sections will be represented with either a blue block or a "R" for Rac1, or a red block or a "4" for Cdc42. **Lower:** Example of the nomenclature and graphics used in the following figures. A Cdc42 construct with the second section replaced with that of Rac1 is denoted "4R44," and the four bars below give a visual representation of the same information.

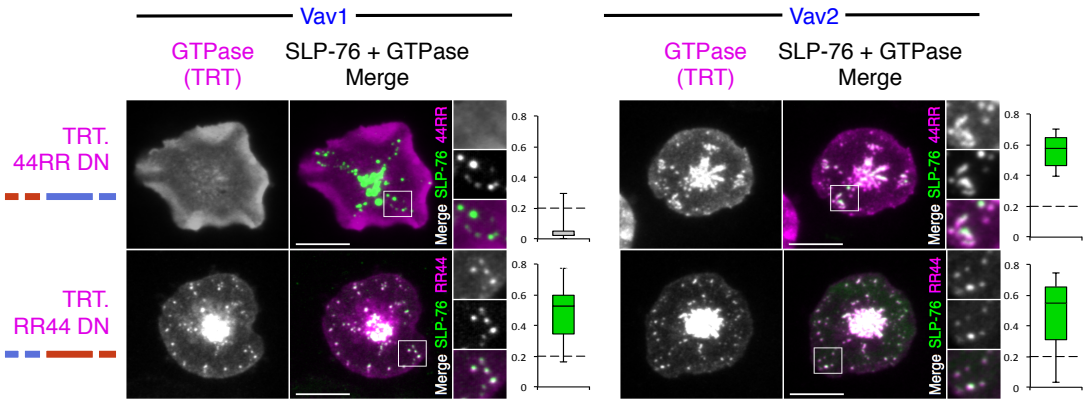

Figure 41: GTPase chimeras with the N-terminus of Rac1 co-localize with Vav1

J14.SY cells were co-transfected with vectors encoding a TRT-tagged DN Rac1/Cdc42 chimera and either mCer3-tagged Vav1 (left) or Vav2 (right). Bars at the far left identify the GTPase of origin for each segment of the chimera (Rac1, blue; Cdc42, red). Images and quantifications were acquired and presented as in Figure 29. Images represent n≥3 experiments for all Vav1 construct pairs, and n≥2 for all Vav2 control construct pairs, with ≥6 cells per experiment.

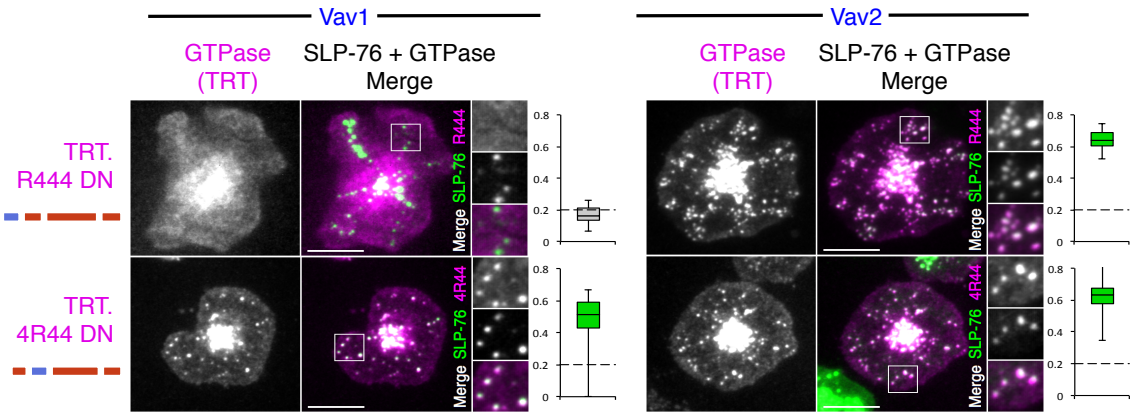

Figure 42: Amino acids 46-77 of Rac1 cause Cdc42 to co-localize with Vav1

J14.SY cells were co-transfected with vectors encoding a TRT-tagged DN Rac1/Cdc42 chimera and either mCer3-tagged Vav1 (left) or Vav2 (right). Bars at the far left identify the GTPase of origin for each segment of the chimera (Rac1, blue; Cdc42, red). Images and quantifications were acquired and presented as in Figure 29. Images represent n≥3 experiments for all Vav1 construct pairs, and n≥2 for all Vav2 control construct pairs, with ≥6 cells per experiment.

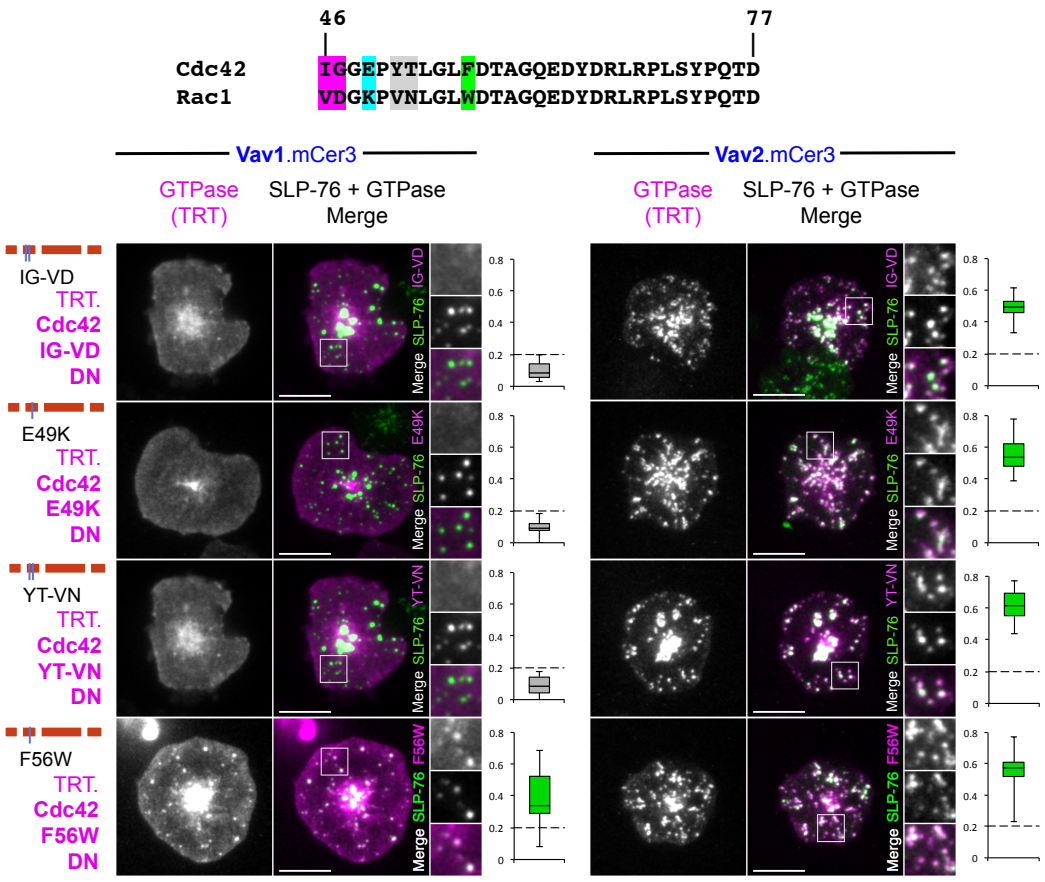

Figure 43: Cdc42 with a F56 to W mutation gains co-localization with Vav1

Upper: The sequence of the GTPase portions between residues 46 and 77 that determines the differential binding of Cdc42 to Vav1 and Vav2. The double and single amino acids of Rac1 that were moved into Cdc42 for colocalization analysis are highlighted. **Lower:** J14.SY cells were co-transfected with vectors encoding a TRT-tagged DN Rac1/Cdc42 chimera and either mCer3-tagged Vav1 (left) or Vav2 (right). Bars at the far left identify the GTPase of origin for each chimera, with the Cdc42 portions indicated as red bars and the amino acid substitutions marked below. Images and quantifications were acquired and presented as in Figure 29. representing n≥3 experiments for all Vav1 construct pairs, and n≥2 for all Vav2 control construct pairs, with ≥6 cells per experiment.

6.8.2 Rac1 tryptophan 56 does not suggest an obvious mechanism of Vav1 specificity

My plan in determining the residues of Rac1 that lead to interaction with Vav1 was to use this piece of data to identify the amino acids of Vav1 or Vav2 that interact with these residues. Unfortunately, the crystal structures of Vav1 in complex with Rac1 do not show any direct interaction of Vav1 with Rac1 W56. In fact, the difference in residue 56 of Rac1 and Cdc42 is a well-known point of selectivity used by other GEFs to distinguish these GTPases (Karnoub et al., 2001). But I had not expected Vav1 to discriminate on the basis of this amino acid, based on the mechanisms used by other GEFs to identify GTPases due to this residue. The tryptophan at position 56 on Rac1 is bulkier than the phenylalanine at this position on Cdc42; and this bulkiness sterically hinders the binding of Rac1 to the Cdc42 specific GEF Intersectin (ITSN) (Snyder et al., 2002). But Vav1 has the opposite specificity, so this mechanism cannot be relevant. On the other hand, the Rac specific GEF T-cell invasion and metastasis (Tiam1) maintains Rac1 specificity by forming a polar bond between a histidine on Tiam1 and the nitrogen in tryptophan 56 of Rac1 (Gao et al., 2001). However, Vav1 forms no bond with Rac1 Trp^{56} (Figure 44) (Chrencik et al., 2008). Nor does switching the residues in Vav2 surrounding Rac1 Trp^{56} to their Vav1 equivalents lead to an exclusion of Rac1, as described above (Figure 36). Also notable is that both Rac2 and RhoG have a tryptophan at position 56, and yet do not co-localize with Vav1 (see Figure 31 for Rac2 and Figure 33 for RhoG). Therefore, the methods by which Vav1 maintains selectivity for Rac1 remain elusive to me. A likely explanation lies in the folding of the DH domain influenced by amino acids that are

not surface exposed. Supporting this hypothesis are findings that show the isolated DH domain of Vav1 is less effective at catalyzing Rac1 activation than the combined DH-PH-C1 catalytic cassette, showing that the catalytic activity of the DH domain is sensitive to changes in structure imposed by the other domains interacting with regions of the DH domain distal to the catalytic pocket (Chrencik et al., 2008).

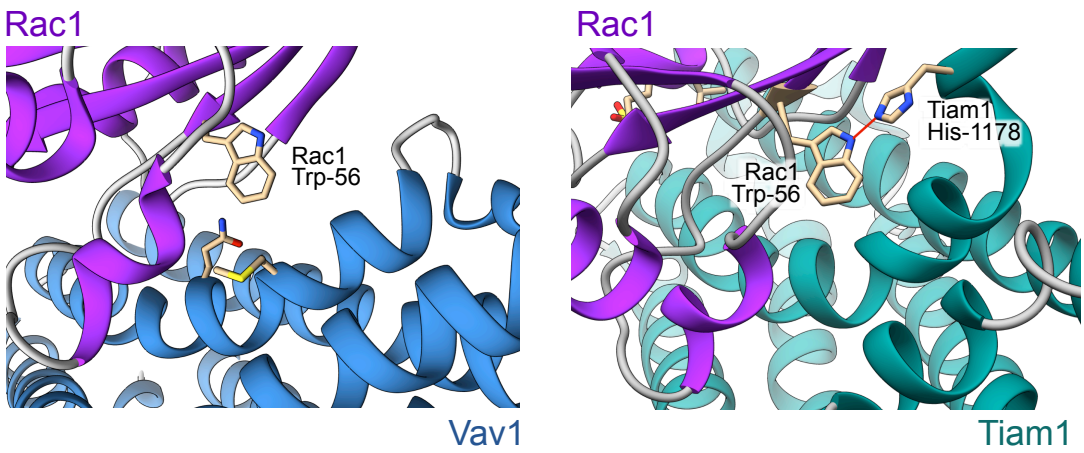

Figure 44: The W56 residue of Rac1 has no obvious interactions with Vav1

The Rac specific GEF Tiam1 uses a hydrogen bond with Trp^{56} of Rac1 to determine specificity, but Vav1 has no such interaction to explain its reliance on this residue of Rac1. **Left:** taken from the crystal structure of Vav1 in complex with Rac1 (pdb id: 3bji). Rac1 is shown in purple as a ribbon diagram, with only Trp^{56} depicted as an individual residue. Vav1 is represented by blue ribbons, and the only amino acid side chains that are close enough to Trp^{56} to make bonds are shown; but no bonds are suggested by this arrangement (Chrencik et al., 2008). **Right:** from the crystal structure of Tiam1 and Rac1 (pdb id: 1foe). Rac1 is shown as on the right. Tiam1 is depicted as a teal ribbon, with His^{1178} that forms a bond with Trp^{56} shown (Snyder et al., 2002).

6.9 Assessing the requirements for Rac1 and Cdc42 on calcium influx downstream of TCR ligation

6.9.1 Vav2 requires Cdc42 to inhibit TCR initiated calcium influx

The data I had collected to this point showed strong correlative evidence that Vav2 inhibits T cell calcium signaling by activating Cdc42. First, a substantial portion of the inhibition by Vav2 is catalytic (Figure 20). Second, an active Cdc42 construct strongly inhibits calcium signaling, while the other Rho GTPase family members tested do not (Figure 25). And third, Vav2 localizes with Cdc42 *in vivo* in our system, while Vav1 does not (Figure 34). However, I still needed to determine if the Jurkat T cell calcium signaling inhibition of Vav2 required the specific activation of Cdc42. I investigated a number of strategies to remove the ability of Vav2 to act on Cdc42 without blocking the ability of Vav2 to act on other GTPases.

I initially attempted knockdowns of Cdc42 with plasmids containing shRNA targeted against Cdc42 and an additional red fluorescent protein. These vectors were then co-expressed with YFP tagged Vav1 or Vav2 constructs by transient transfection into Jurkat cells. Using flow cytometry, I then attempted to perform calcium assays on these cells, gating on levels of expression of both Vav and shRNA. Preliminary results suggested that knocking down Cdc42 eliminated the ability of Vav2 to inhibit calcium in this experiment (results not shown). However, the experiments proved difficult to reliably reproduce. Transient expression of the Cdc42 hairpin requires a few days to show significant knockdown, and the expression of Vav2 drops off in level and effect during this time (personal observations). I next tried to create a stable Cdc42 knockdown Jurkat line to remove one variable from the experiment; but the Cdc42

stable knockdowns proved too inconsistent to use for experiments, as could be expected given the pleiotropic roles of Cdc42 in T cell growth and division (Guo et al., 2010).

I next turned to the use of small molecule inhibitors of Cdc42 and Rac1 to test the effects of acute inhibition. Since Rho GTPases are being investigated as pharmacological targets in cancer therapy (see Introduction), a number of inhibitors have been recently discovered that can selectively block the activation of Rac or Cdc42. For Rac inhibition, I tested the effects of EHT 1864 on calcium influx in Jurkat cells. EHT 1864 binds to Rac1/2/3, but not Cdc42, and prevents Rac from binding downstream effectors (Onesto et al., 2008; Shutes et al., 2007). Knowing the mechanism of action of these inhibitors is crucial, as another frequently used Rac inhibitor, NSC23766, only blocks the activation of Rac by a subset of GEFs, not including Vav1 (Akbar et al., 2006; Gao et al., 2004; Shutes et al., 2007). When I treated Jurkat T cells with EHT 1864 and assessed TCR initiated calcium influx, the cells showed increasing inhibition of calcium influx with increasing concentrations of the inhibitor (Figure 45). These results, combined with my data showing that CA Rac1/2 increase calcium influx, suggests that Rac1 and Rac2 play a necessary and underappreciated role in facilitating calcium signaling in T cells.

To pursue my primary goal of establishing the link between the calcium inhibition of Vav2 and Cdc42, I tested the effects of the Cdc42 inhibitor ML141 (Bologa et al., 2010; Hong et al., 2013). As I expected, this inhibitor did not decrease the calcium influx of untransfected Jurkat T cells even at the highest dose tested (Figure 45). However, the Cdc42 inhibitor ML 141 had an unanticipated property that

confounded my efforts to test its effects on Vav2 suppression: it fluoresces extremely brightly across a wide range of flow cytometry channels. This fact made it unusable in combination with a fluorescent calcium reporter and a fluorescent protein such as Vav2.

Fortunately, another Cdc42 inhibitor had recently been developed that does not interfere with the fluorescence channels required by our lab's calcium assays. The small molecule ZCL278 was identified in a screen of molecules that could directly bind to Cdc42 and prevent its activation by GEFs (Friesland et al., 2013). This inhibitor is reported to be specific for Cdc42, and does not block the activity of Rac or RhoA. I tested the effects of the compound on calcium signaling in Jurkat cells. Acute addition of ZCL278 to Jurkat T cells caused a gradual rise in the basal calcium level of unstimulated cells, but did not affect the peak calcium response. This increase was due to calcium entry, and not autofluorescence of the compound, as adding ZCL278 to cells that had not been loaded with a calcium reporter showed no increase in fluorescence in these channels (results not shown).

When used in my standard calcium assays, inhibition of Cdc42 by ZCL278 had no significant effect on cells expressing YFP only compared to a DMSO control. However, the inhibitor had a strong effect on cells expressing high levels of Vav2. With endogenous Cdc42 acutely inhibited, Vav2 expression only resulted in a mild inhibition of TCR stimulation induced calcium influx (Figure 46).

To determine if this reduction of inhibition was specific to Vav2, I assessed the effects of ZCL278 on the constitutively active Cdc42 mutant. As the mechanism of action of ZCL278 is to interfere with the activation of Cdc42 by GEFs (Friesland et

al., 2013), the inhibitor should not have any effect on the CA Cdc42, as this mutant does not need to be activated by a GEF. As predicted, the strong inhibition of calcium influx by CD Cdc42 was not significantly affected by the presence of ZCL278 (Figure 46). Therefore, the ZCL278 inhibitor reduces the effect of Vav2 upstream of the activation of Cdc42. Unlike the knockdown data, these results were reproducible and consistent, and establish that the catalytic inhibition of TCR induced calcium signaling by Vav2 requires the activation of endogenous Cdc42 in Jurkat T cells.

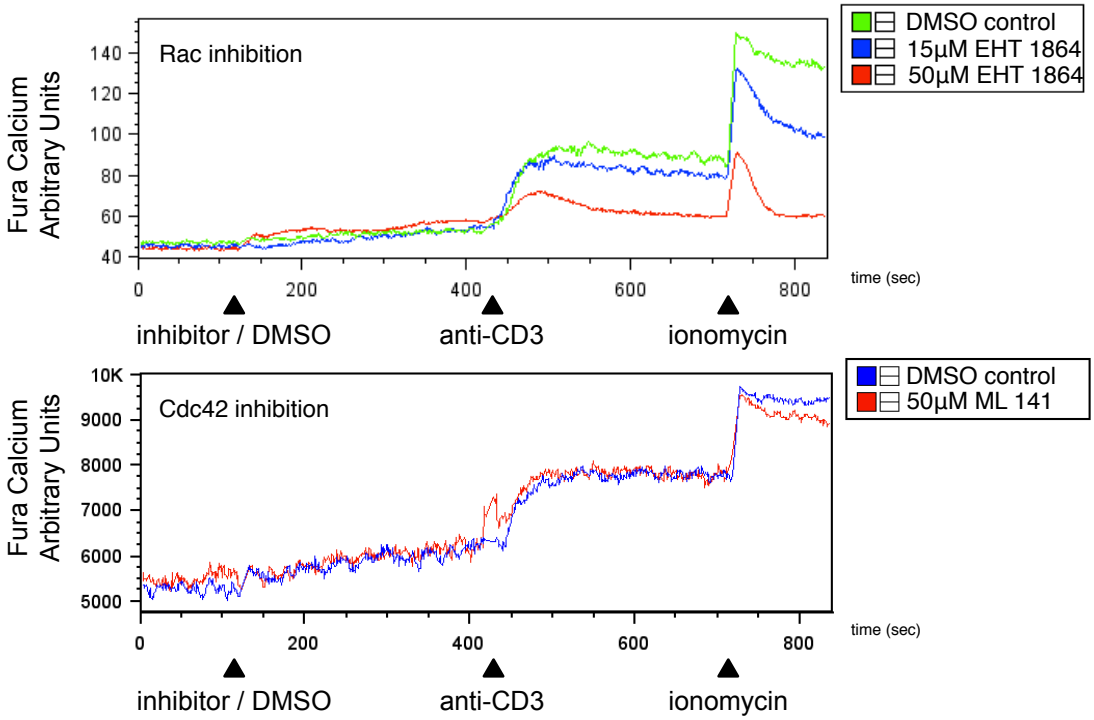

Figure 45: Rac inhibition reduces TCR activation initiated calcium influx, Cdc42 inhibition has no effect.

Preliminary results testing the effects of Rac and Cdc42 inhibitors in Jurkat. Calcium levels over time in E6 Jurkat T cells loaded with the Fura-2 calcium sensitive dye. Jurkat cells were monitored for 2 minutes to establish basal calcium levels. Then either inhibitor or a DMSO control was added. Readings were continued for 5 more minutes, and then anti-CD3 was added to a final concentration of 30ng/ml. After 5 minutes, ionomycin was added and data collected for a final 2 minutes. **Upper:** The effects of either 15µM (blue line) or 50µM (red line) of the Rac inhibitor EHT 1864 compared to control DMSO treated Jurkat (green line). Cells showed a dose-dependent inhibition of calcium influx with the addition of the inhibitor. **Lower:** The effect of the

highest level of the Cdc42 inhibitor ML 141 tested, 50μM. No effect was seen on calcium signaling with this inhibitor. Note only an n=1 for these experiments.

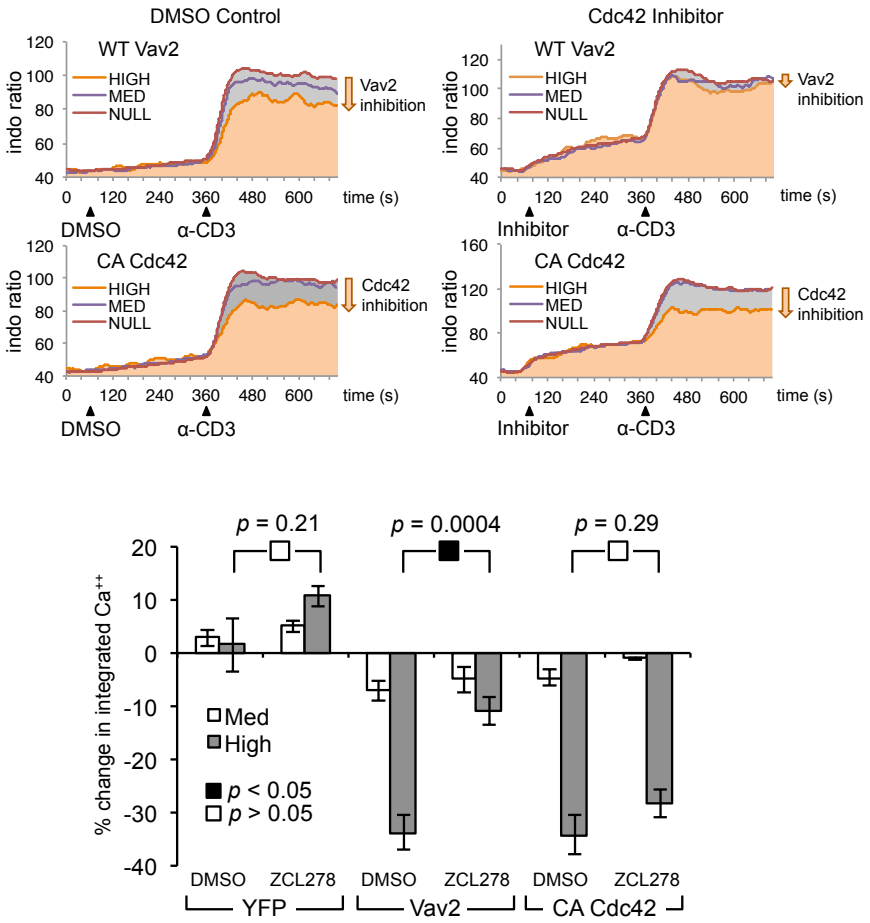

Figure 46: Inhibition of Cdc42 increases the calcium influx of cells expressing Vav2

Upper: Representative calcium response graphs comparing the effects of ZCL278, an inhibitor of Cdc42 activation, on the suppression of calcium influx by Vav2 and constitutively active (CA) Cdc42. Baseline reads were collected for 60 seconds, after which either ZCL278 (100μM final) or an equivalent volume of DMSO was added. After 5 minutes, OKT3 was added and readings were collected for an additional 6 minutes. **Lower:** Calcium responses were quantified as in Figure 16. Graphs depict the mean percentage change in the integrated calcium responses of the moderate and high mYFP expressing cells relative to non-expressing cells within the same sample (n≥3 for all conditions).

6.10 The portions of Vav1 sufficient to positively impact calcium signaling in Jurkat T cells

6.10.1 The GEF region of Vav1 is not sufficient to support strong calcium signaling in T cells

After my investigation of the mechanism by which Vav2 influences calcium signaling in Jurkat T cells, I turned back to explore the impact of the individual Vav1 domains on this pathway. I have shown here that the suppressive calcium phenotype of Vav2 can be transferred into Vav1 through a transfer of the catalytic core of Vav2. This observation led me to test and see if the converse would work. I therefore created a Vav2 construct that contained the DH-PH-C1 core of Vav1 (Vav2.V1 GEF). Unlike full-length Vav2, this construct did not inhibit the baseline calcium influx in TCR stimulated J.Vav1 cells, even in cells expressing high levels of the construct. However, the construct also completely failed to increase calcium influx over that of untransfected cells (Figure 47, Vav2.V1 GEF). As the N-terminal CH domains and the C-terminal SH3-SH2-SH3 portions of Vav1 and Vav2 are equivalent in terms of calcium signaling (see the early results sections), I investigated other portions of Vav proteins.

The two unstructured flanking regions around the catalytic core of Vav proteins are not typically ascribed any signaling properties. However, a previous member of our lab, Nicholas Sylvain, showed that a section of the amino acids, from approximately residue 600 to 620, of Vav1 that link the C1 domain to the N-terminal SH3 domain can influence the roles Vav1 plays in stabilizing SLP-76 MC (Sylvain, 2011). Our lab has named this portion the ‘polybasic’ region of Vav1, as it contains a

number of lysine and arginine residues. The polybasic region of Vav1 is highly conserved in vertebrates. Vav3 only contains a few basic residues in this section, and this region is entirely absent in all species of Vav2 (Figure 48). I turned my attention to this polybasic region of Vav1, and found that it also has roles in calcium signaling. I replaced the polybasic region of Vav1 with the equivalent linker region of Vav2, and this construct had a reduced ability to increase TCR induced calcium signaling compared to wild type Vav1 (Figure 47, Vav1.V2 'PB' vs. Vav1). Furthermore, if the polybasic region of Vav1 is transplanted into Vav2 in addition to the catalytic core of Vav1, it increases the ability of this construct to support calcium influx in our model (Figure 47, Vav2.V1 GEF compared to Vav2.V1 GEF-PB). However, this 'Vav2.V1 GEF-PB' construct still does not boost T cell calcium influx to the extent of wild type Vav1, so I next turned my attention to the N-terminal flanking portion of the GEF region, the acidic linker.

The acidic linker that connects the CH and DH domains is well characterized for its role in maintaining the autoinhibition of Vav in resting cells, and as the location of the three critical tyrosines that are phosphorylated to open up and activate Vav (see Figure 2). These tyrosines are only considered regulatory, and have not been reported to be the targets of binding by other proteins to the best of my knowledge. Nor have any other motifs in this acidic region been identified as ligands for other proteins. Nevertheless, as this was the last portion of Vav1 that I had not investigated, I moved the Vav1 acidic region into the context of Vav2. Starting with the Vav2 chimera that contained the GEF and polybasic region of Vav1, I added in the acidic linker from Vav1. The resulting construct was indistinguishable from Vav1 in its ability to

increase calcium influx downstream of TCR ligation (Figure 47, Vav2.V1 acidic-GEF-PB, compared to Vav1). In summary, the calcium inhibition of Vav2 can be transferred to Vav1 by moving only the GEF region of Vav2 into Vav1. However, creating a Vav2 construct that mimics the calcium phenotype of Vav1 requires moving the acidic, GEF, and polybasic regions of Vav1 into Vav2. These findings suggest that the acidic and polybasic regions of Vav1 may have one or more binding partners that are specific to Vav1 and that support strong T cell calcium signaling. Alternatively, these flanking regions of the GEF core may influence the conformation of this core in a way that supports calcium signaling.

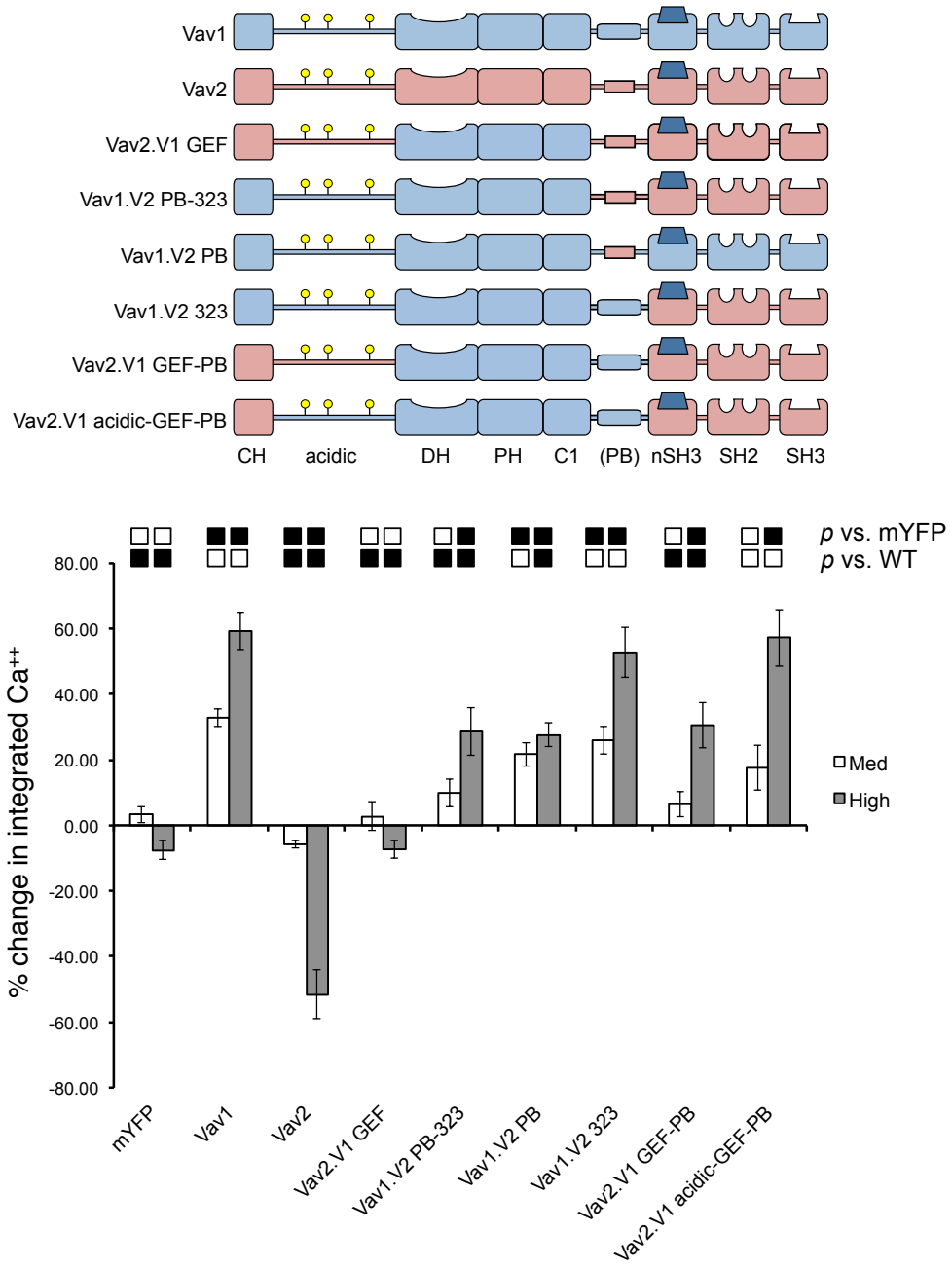

Figure 47: The Minimal Amount of Vav1 that Can Convey Calcium Signaling Enhancement to Vav2

Upper: Vav chimeras used in this figure. Blue represents Vav1 sections, red represents Vav2. In this diagram the portion of Vav2 that corresponds to the polybasic region of Vav1 is depicted with a red box to emphasize the appropriate swaps. **Lower:** Quantification of calcium influx data for the indicated mYFP-tagged Vav chimeras.

The chimeras were expressed in J.Vav1 cells. Experiments were conducted and are presented here as in Figure 16. Graph represents an average of experiments, and error bars show SEM ($n \geq 3$ for all constructs, except n=2 for Vav3). Small boxes depict *p* values for comparisons between chimeras expressed at similar levels. Black boxes represent *p* of < 0.05, white boxes are > 0.05.

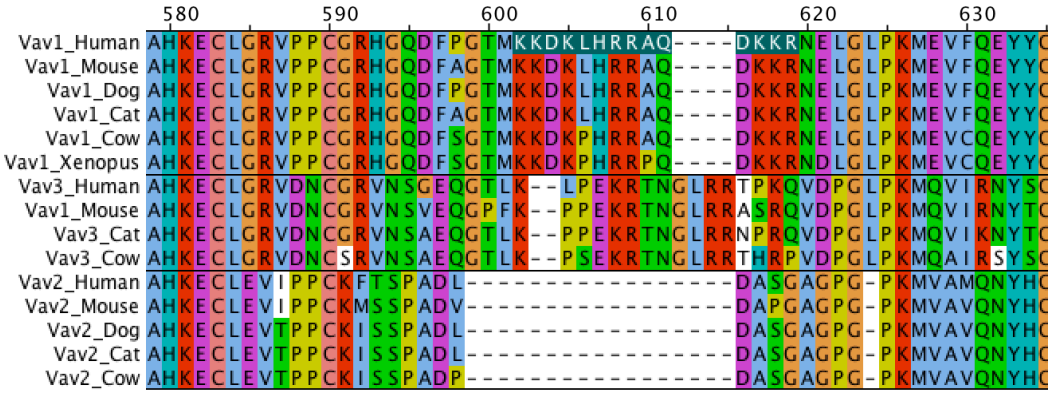

Figure 48: Sequence conservation of the Vav1 polybasic region

A sequence alignment of the amino acid stretch between the C1 and nSH3 portion of Vav proteins in representative vertebrates. The top row is human Vav1, and the dense stretch of basic residues, the 'polybasic' region, is highlighted in dark green. All other residues are colored using the ClustalX scheme, with the basic Arg and Lys residues in red. The sequences are grouped by isoform, and Vav3 shows an intermediate number of basic residues in this region, while Vav2 has virtually no basic residues, and fewer overall amino acids in this region.

7 Discussion

7.1 Summary of major findings

7.1.1 Overview of the differential contributions of Vav1 and Vav2 to calcium signaling in Jurkat T cells

Due to the number of swaps and mutants of Vav proteins presented in this thesis, I have attempted to consolidate the findings in a couple of graphical overviews. One is presented on the next page as Figure 49. I will recap my results with references to this diagram. The next overview is on the following page, in a horizontal orientation. This overview is a summary of all of the major section swaps between Vav1 and Vav2 and the resulting calcium phenotype of Jurkat cells expression high amounts of these constructs.

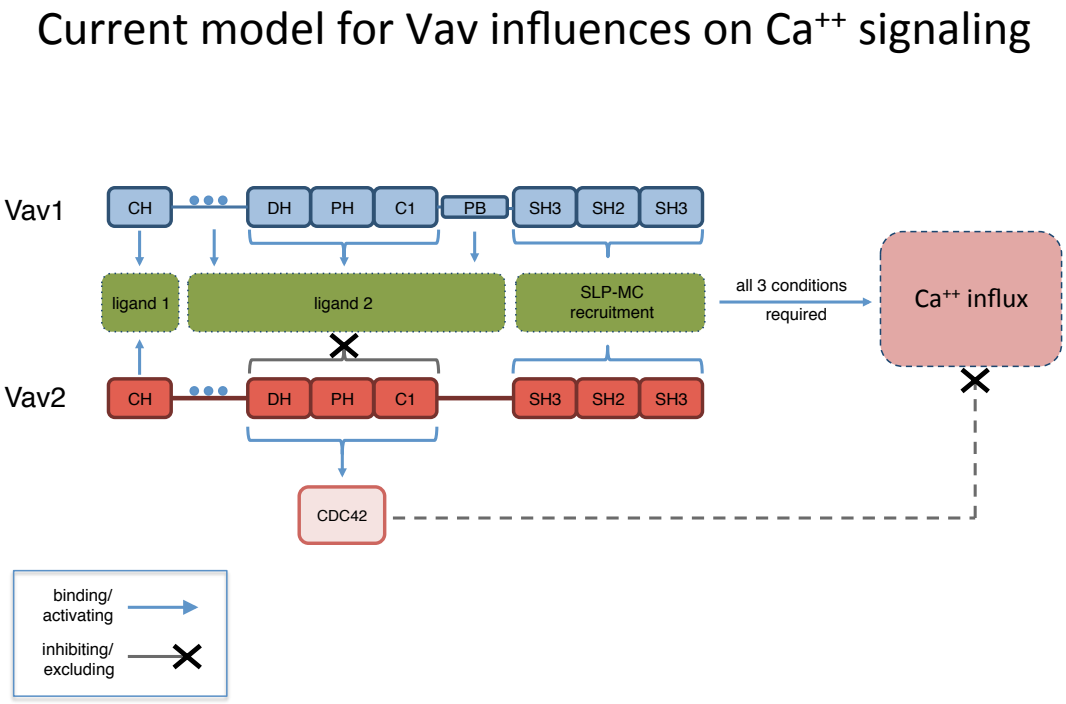

Figure 49: Proposed model of Vav1/2 involvement in T cell calcium signaling

The CH domains of both Vav1 and Vav2 bind an unknown ligand (or ligands) necessary for T cell calcium signaling, shown here as 'ligand 1.' Vav1 has three sections, the acidic, DH-PH-C1, and polybasic regions, that contribute to the binding of another ligand or group of ligands that increases calcium influx into cells after TCR ligation. This is listed here as 'ligand 2.' None of the equivalent regions in Vav2 can support binding to this ligand or group of ligands. Moreover, the catalytic activity of the GEF region of Vav2 activates Cdc42, unlike Vav1. Active Cdc42 suppresses the calcium influx. The C-terminal SH3-SH2-SH3 domains of both Vav1 and Vav2 can support calcium signaling in Jurkat T cells. The full calcium influx that Vav1 supports requires binding to the unknown ligands, recruitment to the SLP-76 microcluster, and a GEF specificity that excludes Cdc42 activation.

Overview of Vav mutants and Calcium:
Domain Deletions and Swaps

An overview of most of the Vav1 and Vav2 mutants, including domain swaps between the two. Vav1 domains are shown in blue, and Vav2 in green. Domain deletions are represented by white space. The effect of high levels of expression of these mutants on calcium signaling is shown in the right columns as numeric values and graphical representations. In the graph, blue bars extending to the right represent positive values, while red bars extending to the left of the center line represent negative values. The upper portion of the graph is an evaluation of domain contributions within Vav1, and the lower portion establishes the necessity of the Vav1 GEF and flanking domains for calcium signaling.

7.1.2 T cell calcium inhibition by Vav2 is independent of its CH domain

I had initially intended on focusing my studies on the role of the Vav1 CH domain in promoting T cell calcium signaling. In order to have a negative control for this study, I planned on using the Vav2 CH domain, which had been reported to not be able to support T cell calcium signaling (Li et al., 2012). Thus, it came as a surprise when my Vav1 chimera with the CH domain of Vav2 was perfectly capable of improving calcium influx in Jurkat T cells. On closer examination, the report by Li *et al.* used a chimera of Vav1 in which only the first 20 amino acids of the CH domain of Vav2 were swapped into Vav1. They found that this chimera could not improve calcium signaling in J.Vav1 Jurkat cells (the same model I use here). As my chimera uses the full 120 amino acids that make up the CH domain, I hypothesize that the partial chimeric CH domains they created were unable to fold correctly and lost the ability to bind to other proteins. No data is presented that their chimeras can support any CH domain related signaling. They also fail to show a gain-of-function in terms of calcium signaling when the 20 amino acids from Vav1 are placed into Vav2. I therefore conclude that the CH domains of Vav1 and Vav2 are equivalent in their ability to a support strong calcium influx in Jurkat T cells when they are expressed as full-length domains. This conclusion is presented in my model as both CH domains able to bind an unknown, but necessary, ligand (Figure 49).

7.1.3 The catalytic activities of Vav1 and Vav2 play different roles in Jurkat T cell signaling

Another mindset that I had when investigating the roles of Vav in T cell calcium signaling was that the GEF activity of the proteins did not influence this

signaling pathway. This assumption was based on the evidence that Vav1 does not need to be catalytically active to support T cell calcium signaling (Kuhne et al., 2000; Miletic et al., 2009; Saveliev et al., 2009). And these findings have been verified in our lab (Sylvain et al., 2011). However, after both the CH and the SH3-SH2-SH3 portions of Vav2 were competent to support calcium signaling in the context of Vav1, I began to investigate the catalytic portion of Vav2. This led to the discovery that the catalytic activity of Vav2 actively inhibits Jurkat T cell calcium signaling (Figure 49). Additionally, the DH-PH-C1 portion of Vav1 appears to play a scaffolding role in T cell calcium signaling. Transferring the DH-PH-C1 domains of Vav2 into Vav1 removes the ability of Vav1 to increase the calcium influx into stimulated J.Vav1 cells, even if those domains have been catalytically inactivated (Figure 22). Thus, I have included in my model an unknown 'ligand 2' that binds to the Vav1 GEF core and is beneficial to calcium signaling (Figure 49). I have indicated a single ligand for the sake of simplicity, but there could certainly be multiple ligands.

7.1.4 Vav1 has multiple regions that are necessary to fully support calcium signaling.

Although the scaffolding role of the Vav1 DH-PH-C1 core is necessary to support Jurkat T cell calcium signaling, it is not sufficient. Adding this section of Vav1 into Vav2 only creates a neutral construct (Figure 47). It is not until the flanking regions of the Vav1 domain have been transferred along with the DH-PH-C1 region into Vav2 that the ensuing construct can increase TCR driven calcium influxes to the same degree as full length Vav1 (Figure 47). The mechanism(s) by which the acidic and polybasic regions of Vav1 contribute to T cell signaling are unclear, but certainly

warrant further investigation. Again, for the sake of simplicity, the model I present has these three regions of Vav1 contributing to the binding of a single ligand ('ligand 2' in Figure 49); but these domains could each contribute individual binding properties that all add to the contribution of Vav1 in facilitating calcium influx.

The C-terminal SH3 and SH2 domains of Vav1 and Vav2 are interchangeable in my calcium assays. The SH2 domains of Vav proteins can all recruit to SLP-76, so the most obvious contribution of this portion is in bringing Vav proteins to the SLP-76 microcluster after TCR activation. The SH3 domains of both Vav1 and Vav2 also have critical signaling binding partners, and earlier findings in our lab suggest that some of these are important for calcium signaling (Sylvain et al., 2011); but these binding partners must not differ between Vav1 and Vav2 (the SH3-SH2-SH3 regions in Figure 49).

To summarize the model, the CH and SH3-SH2-SH3 portions of Vav1 and Vav2 play equivalent roles in Jurkat T cell calcium signaling. No other portions of Vav2 appear to be able to support calcium signaling in these cells. On the other hand, the acidic, catalytic core, and polybasic regions of Vav1 all contribute incrementally to boosting the ability of Jurkat T cells to influx calcium on TCR activation. Contributions from all of these regions are necessary for the effects of Vav1 on this signaling pathway (Figure 49). The final piece of the model involves the inhibitory effects of Cdc42, which I discuss below.

7.1.5 Active Cdc42 dramatically suppresses TCR signaling

One of the most striking discoveries in my research was that active Cdc42 dramatically inhibits calcium signaling in Jurkat T cells. There has been little research

into the role of Cdc42 in proximal TCR signaling. However, recent studies in conditional knockout mice suggest that Cdc42 plays regulatory roles in T cell signaling. These studies used a T-cell specific Cdc42 knockout mouse created by crossing a *Cdc42*$^{flox/flox}$ mouse to an Lck-Cre mouse line (Guo et al., 2010; Guo et al., 2011). When they examined the development of T cells in these mice, they found that T cells in the thymus of these mice show no apparent defects in the double-negative stages of development, indicating that the TCR β chain signals productively. Conversely, earlier work using a knock-in of CA Cdc42 show that the vast majority of DN thymocytes are arrested at the TCR β signaling checkpoint in these mice (Na et al., 1999), suggesting that active Cdc42 signaling disrupts the normal TCR signaling at this point.

Once past the DN stage, Cdc42 knockout T cells do experience a significant block in the transition of thymocytes from double-positive (DP) to single-positive (SP) T cells (Guo et al., 2010). Passing this stage of development is generally thought to require moderate TCR signal strength. Double positive cells 'test' to see if they can achieve a certain threshold of TCR signaling with either CD8 or CD4 co-stimulation. If the TCR reacts too strongly with a ligand, the cell either undergoes apoptosis, anergy, or becomes a regulatory T cell in order to avoid the development of self-reactive T cells. The block that the Cdc42 T cell KO mice experience at this DP to SP transition suggests that their TCR signaling is, on average, either abnormally weak or strong. The authors do not investigate the reasons behind the block from DP to SP T cells. However, my model suggests that Cdc42 serves to partially inhibit TCR signaling, so my prediction would be that the Cdc42 deficient DP T cells are crossing

the upper end of the signaling threshold and therefore failing to move to the SP stage. In support of this theory, the follow up paper by this lab reports that these knockout mice have twice the number of FoxP3+ Treg cells as wild type mice (Guo et al., 2011), suggesting that they are hyper-responsive to self antigen in the thymus.

In further support of Cdc42 playing a modulatory role in T cells, the first study shows that T cells that do become single positive and make it to the periphery display hyperproliferation and increased IL-2 production in response to TCR stimulation (Guo et al., 2010). Notably, the increased proliferation in Cdc42 KO T cells is in direct contrast to dramatic proliferation defects in Rac1/Rac2 knockout T cells (Guo et al., 2008). The two papers that characterize the T cell specific Cdc42 KO mice do not include any calcium or NF-AT assays, so I cannot directly compare my model to the behavior of these T cells. But both my findings in Jurkat T cells and their finding in murine T cells suggest that Cdc42 can inhibit the strength of TCR signals to modulate the activation of T cells.

7.1.6 Vav2 interacts with a number of Rho GTPases, while Vav1 only interacts with Rac1

Vav proteins have been considered to be 'promiscuous' GEFs that can activate multiple GTPases (Chrencik et al., 2008). My findings suggest that Vav1 is actually a very specific Rac1 GEF, while Vav2 has a much broader range of GTPase targets. Considering that Cdc42, Rac1/Rac2, and RhoA show distinct temporal and spatial patterns of activation after TCR ligation and early in the formation of an immune synapse (Singleton et al., 2009), I find the specificity of Vav1 to be more understandable than the promiscuity of Vav2. A model in which Vav1 is recruited to

and activated in SLP-76 microclusters in order to selectively create a local pool of active Rac1, and only Rac1, is simpler than a model in which a less specific GEF is recruited to a microcluster and then subjected to numerous other levels of regulation in order to precisely organize the separate activation of Rac1, Rac2, Cdc42, and RhoA.

Of course, evolution does not always lead to the simplest solutions, and the large number of GEFs and GAPs, combined with the number of ways that these proteins and GDIs can be modified and regulated in mammalian cells, suggest that layers of complexity will confound our attempts to build any simple model system of TCR-driven GTPase activation. Nevertheless, my findings suggest that replacing the specific Vav1 GEF with the non-specific Vav2 GEF in the context of the SLP-76 microcluster has dramatic consequences. As Vav2 is more highly expressed in B cells, and supports productive BCR signaling, it would be very interesting to see if the patterns of GTPase activation differ significantly in B cells and T cells.

7.2 Implications

7.2.1 Other Rho family GEFs in T cells

Vav1 is the major contributor to T cell signaling out of the Vav family, both in terms of expression (Figure 3 and Immgen.com data) and by the severity of the knockout phenotype (Fujikawa et al., 2003). As Vav1 was one of the first GEFs discovered in T cells, and as it clearly plays an important role in T cell signaling, many discussions of GEFs in T cells attribute activation of Rac1/Rac2, RhoA, and Cdc42 to Vav1. However, I show here that Vav1 can only interact with Rac1. Also, the removal of Vav1 from T cells does not result in a complete loss of activation of GTPases. Nor

does the removal of the catalytic activity of Vav1 abolish the activation of even Rac1 (Saveliev et al., 2009). Therefore, there must be other critical Rho GEFs in T cells.

The PIX family of Rho GEFs are likely candidates for important Rho GEFs in T cells. Moreover, these GEFs can function independently of SLP-76 microclusters. Research has found that early TCR signaling activates αPIX and/or βPIX (which could not be differentiated at the time of the study) through a ZAP-70, but not LAT or SLP-76, dependent pathway. The authors of this study linked the activation of the PIX GEFs with the activation of Rac1, but suggested Cdc42 could also be involved (Ku et al., 2001). These data fit with my model, suggesting that Cdc42, and possibly another pool of Rac1, is activated by TCR ligation by a separate pathway from Vav1, in potentially a different subcellular location.

Another, more recent study highlights the importance of the Rho family GEF Dock8 in T cells. Patients that have loss-of-function mutations in Dock8 have immune deficiencies that typically manifest in the inability to clear viral infections in the skin. The authors of this study linked inability of T cells in these patients to clear infections with a lack of Cdc42 activation, due to their non-functioning Dock8 (Zhang et al., 2014). Along with other studies, these reports are part of the accumulating evidence that, while Vav1 is a crucial signaling molecule in T cells, it is likely only one of a number of GEFs that can activate Rho GTPases in these cells.

7.2.2 Differential use of Vav2 in immune cell subsets

The differences in the signaling properties of Vav1 and Vav2 suggest that there are fundamental signaling requirements for the immune cell subsets that rely more on Vav2 than T cells. An examination of the relative expression patterns in different

immune subsets shows that, compared to T cells and NK cells, Vav2 is more highly expressed in dendritic cells, macrophages, and B cells (also Tregs, discussed below). These cells are also considered professional antigen presenting cells. I believe it would be fruitful to investigate signaling properties of Vav2 that could be important for APCs. One interesting connection between APCs and Vav2 is the role of Cdc42 in antigen presentation. A recent study of Cdc42 conditional B cell KO mice found that, although these cells were able to internalize antigen and displayed normal levels of surface MHC II, they exhibited a dramatic reduction in the amount of antigen presented by these MHC II molecules (Burbage et al., 2014). The authors concluded that Cdc42 was critical for the processing of internalized antigen for presentation, but by an unknown mechanism. It would be interesting to determine if APCs upregulated Vav2 in order to activate the Cdc42 pathway that supports antigen processing and loading onto MHC II.

7.2.3 Vav2 upregulation in regulatory T cells

As shown in this thesis and reported in the literature, Vav2 is expressed at low levels in primary T effector, cytotoxic T cells, and Jurkat T cells. However, one subset of T cells shows a substantially higher level of Vav2 expression than others: T regulator cells. Defined as CD3+CD4+CD25^{HIGH},FOXP3+, these Tregs have a three to four fold increase in the ratio of Vav2 to Vav1 compared to T effectors (see Figure 3). In fact, a study that examined the differential expression of genes in Tregs concluded that the *VAV2* gene is one of the direct targets of the FoxP3 transcription factor (Hill et al., 2007). This study was an overview of the regulatory T cell transcriptome, and thus only reported on the upregulation of Vav2, and not the consequences of this

upregulation. In light of the different signaling properties of Vav1 and Vav2 downstream of the TCR, I feel that the role of Vav2 in Tregs bears more study.

The role of calcium signaling in the activity of Tregs is unclear, which is not very surprising considering our incomplete understanding of Tregs in general. However, strong calcium signaling does appear to be necessary for the initial development of Tregs in the thymus. Developing T cells that are strongly activated by self-antigen can become Tregs, so it makes sense that a correspondingly strong calcium influx drives the formation of these Tregs. Numerous studies have shown that mice whose T cells have defects in the ability to initiate a dramatic increase in cytosolic calcium have severe defects in the number and function of FoxP3+ regulatory T cells. Moreover the NF-AT transcription factors at least partially drive FoxP3 expression (see Oh-hora and Rao (2009) for an excellent overview of these observations).

However, the role of calcium signaling in the developed Treg has not been as well studied. One hypothesis I would like to test is that the upregulation of Vav2 in these cells suppresses TCR-induced calcium influx. In support of this theory are reports that Tregs show little to no increases in cytosolic calcium downstream of TCR stimulation (Gavin et al., 2002; Sumpter et al., 2008), and also that NF-AT activity is not necessary for the actual suppressive function of Tregs (Vaeth et al., 2012). If Vav2 plays a role in the altered calcium response of Tregs, then an understanding of the differences in Vav1 and Vav2 signaling could inform the development new types of checkpoint therapies to modulate these cells.

The differences between the signaling properties of Vav1 and Vav2 suggest many new avenues of research. Combining the information presented here on the catalytic specificities of these GEFs with the differential expression of Vav proteins in immune cell subsets should lead to insights on how these different cell subsets use Rac or Cdc42 downstream of receptor ligation. Vav GEFs are critical hubs of signaling within immune cells, and pharmacologically targeting individual Vav isoforms could allow us to hone our control of immune responses. In addition, our growing understanding of the roles that Vav proteins and Rho GTPases play in tumorigenesis will hopefully allow for a better understanding of certain forms of cancer and suggest better ways to target these pathologies in the future.

7.3 A new assay to assess GEF-GTPase interactions

7.3.1 GEF-GTPase interactions can be visualized in live cells

The 'GEF Trapping' assay presented here has the potential to be a beneficial tool across a wide range of cell biology disciplines. The assay was originally conceived by Steve Bunnell and Nicholas Sylvain in their explorations of the structure and function of Vav1 that have served as the foundation for much of my research (Sylvain, 2011). I was able to make substantial use of this GEF trapping assay to determine the specificities of Vav1 and Vav2. The GEF Trapping assay has a number of advantages and disadvantages in comparison to existing assays. In the introduction, I discussed the limitations of *in vitro* systems of assessing the activity of GEFs. In short, the greatest strength of our imaging assay is that occurs in the environment of the cell. Although the GEFs and GTPases we visualize are from exogenous plasmids,

the proteins have been translated in the relevant cell, and exposed to the relevant post-translational modifications. These GTPases and GEFs are also segregated to different subcellular localization, and are exposed to the kinases, GDIs, GAPs, and other proteins that influence the GTPase cycle. My findings with this assay suggest that it can differentiate the interactions of GEFs with GTPases in different subcellular compartments. Namely, the fact that Vav1 shows no co-localization with Rac2, despite its high sequence similarity to Rac1, can be explained by the different membrane pools these two Rac isoforms occupy (Michaelson et al., 2001). I have not explored this aspect of the assay; but it would be very interesting to determine the portions of Rac2 that exclude it from co-localization with Vav1, and see if this portion is also involved with membrane targeting.

7.3.2 Expression levels in the GEF trapping assay

One drawback of the GEF trapping assay is the reliance on the overexpression of fluorescent proteins. Some of the regulatory mechanisms of the cell could be overwhelmed by the amount of protein expressed, as the ratios of GAPs and GDIs to GTPases may be an important aspect of regulation (Falkenberg and Loew, 2013). More information would need to be collected on the amount of endogenous protein normally found in the cell of interest, and the exogenous protein expression may need to be titered accordingly.

However, the fact that the current GEF trapping assay relies on protein overexpression can be quite beneficial for examining specific GEFs. In my assays, even though the J.14.SY Jurkat cells have endogenous expression of all Vav isoforms,

fluorescent GTPase clustering was entirely dependent on the co-expression of exogenous Vav proteins (see Figure 29, mCer3 and Rac1 DN for the negative control). This reliance on Vav over-expression is likely due to the stoichiometry between SLP-76, Vav, and the GTPase. In J14.SY cells, the stable expression YFP tagged SLP-76 is relatively higher than SLP-76 in E6 Jurkat cells (unpublished observations). As Vav recruits directly to phosphorylated SLP-76 on TCR ligation in either a 1:1 or 2:1 ratio (Barda-Saad et al., 2010), the pool of endogenous Vav1 in J14.SY cells is likely diluted to lower than 'wild type' levels in each microcluster. As each GEF molecule only binds a single DN GTPase molecule, the small portion of the exogenous, fluorescent GTPase captured in each microcluster is lower than our imaging can detect. With the addition of exogenous Vav proteins, the ratio of SLP-76 to Vav can again approach 1:1 or 1:2, and each Vav can trap a fluorescent DN GTPase, allowing GTPase clustering to be visualized. If endogenous GEFs caused visible GTPase clustering, then the cells would have to be modified to knock down all relevant endogenous GEFs before a clear baseline could be achieved. The reliance on GEF over-expression also means that the lack of GTPase clustering without Vav overexpression does not rule out other Rho specific GEFs in the SLP-76 MC.

7.3.3 Expanding the reach of the GEF trapping assay

Another use for the GEF Trapping assay that could be explored is as a screen for inhibitors of select GEF-GTPase interactions. Starting with the assay in its current form, we could verify the mechanism of action of inhibitors meant to block the GEF-GTPase interactions. Some of these inhibitors, such as the small molecule EHop-16, are reported to act by interfering with the binding of nucleotide-free GTPases with

their GEFs, and these interactions are exactly the type that the GEF trapping assay visualizes (Montalvo-Ortiz et al., 2012). The addition of inhibitors of this type to our imaging assay should lead to the loss of co-localization of GEF and GTPase if the molecules work as reported. However, different GTPase inhibitors will not lend themselves to screening by our assay. I initially tried to image the effects of the drug Azathioprine. As mentioned in the Introduction, this immunosuppressant is reported to work by forming a GDP analog that binds to Rac1 and cannot be dislodged by a GEF. I had hoped that I could image Azathioprine loaded Rac1 'trapped' by Vav; however, this interaction was not captured in our assay. After more research, I discovered that the affinity for GDP loaded GTPases for the catalytic pocket of a GEF is relatively low, so the interaction between a GEF and a GTPase that can't release GDP is very transient. The high GEF-GTPase affinity interaction is only formed when the GDP is displaced by the GEF and the GTPase is in a nucleotide-free state. It is this state that the T17N, DN GTPases mimic, and explains why these constructs become trapped in the catalytic pocket. Therefore, the GEF trapping assay is ideal for screening compounds that disrupt the interaction of a GEF and a nucleotide-free GTPase, but not ideal for other forms of GTPase inhibition.

Although I have only explored the use of this assay in identifying the targets of Vav1 and Vav2, I believe the assay could be modified to investigate the activities of other GEFs. One limitation with expanding this assay is that imaging the localization of GTPase with GEFs requires the ability to image the precise intracellular localization of the GEFs. However, I feel it likely that a number of GEFs will lend themselves to being imaged in this fashion. For instance, the critical Ras/Rac GEF SOS1 also forms

complexes with LAT in T cells (Houtman et al., 2006), and the GEF trapping assay could potentially be used to determine the dynamics of this GEF in T cell activation. As we learn more about the localization and context of other GEFs in T cells and other cell types, the utility of the GEF Trapping assay will likely continue to grow.

8 References

Abe, K., K.L. Rossman, B. Liu, K.D. Ritola, D. Chiang, S.L. Campbell, K. Burridge, and C.J. Der. 2000. Vav2 is an activator of Cdc42, Rac1, and RhoA. *The Journal of biological chemistry*. 275:10141-10149.

Abraham, R.T., and A. Weiss. 2004. Jurkat T cells and development of the T-cell receptor signalling paradigm. *Nature reviews. Immunology*. 4:301-308.

Acuto, O., and D. Cantrell. 2000. T cell activation and the cytoskeleton. *Annu Rev Immunol*. 18:165-184.

Aghazadeh, B., W.E. Lowry, X.Y. Huang, and M.K. Rosen. 2000. Structural basis for relief of autoinhibition of the Dbl homology domain of proto-oncogene Vav by tyrosine phosphorylation. *Cell*. 102:625-633.

Aguilar, H., A. Urruticoechea, P. Halonen, K. Kiyotani, T. Mushiroda, X. Barril, J. Serra-Musach, A. Islam, L. Caizzi, L. Di Croce, E. Nevedomskaya, W. Zwart, J. Bostner, E. Karlsson, G.P. Tenorio, T. Fornander, D.C. Sgroi, R. Garcia-Mata, M.P. Jansen, N. García, N. Bonifaci, F. Climent, M.T. Soler, A. Rodríguez-Vida, M. Gil, J. Brunet, G. Martrat, L. Gómez-Baldó, A.I. Extremera, A. Figueras, J. Balart, R. Clarke, K.L. Burnstein, K.E. Carlson, J.a. Katzenellenbogen, M. Vizoso, M. Esteller, A. Villanueva, A.B. Rodríguez-Peña, X.R. Bustelo, Y. Nakamura, H. Zembutsu, O. Stål, R.L. Beijersbergen, and M.A. Pujana. 2014. VAV3 mediates resistance to breast cancer endocrine therapy. *Breast cancer research : BCR*. 16:R53-R53.

Akbar, H., J. Cancelas, D.a. Williams, J. Zheng, and Y. Zheng. 2006. Rational design and applications of a Rac GTPase-specific small molecule inhibitor. *Methods in enzymology*. 406:554-565.

Alanio, C., F. Lemaitre, H.K.W. Law, M. Hasan, and M.L. Albert. 2010. Enumeration of human antigen-specific naive CD8+ T cells reveals conserved precursor frequencies. *Blood*. 115:3718-3725.

Arias-Romero, L.E., and J. Chernoff. 2013. Targeting Cdc42 in cancer. *Expert Opin Ther Targets*. 17:1263-1273.

Arrieumerlou, C., C. Randriamampita, G. Bismuth, and A. Trautmann. 2000. Rac is involved in early TCR signaling. *Journal of immunology (Baltimore, Md. : 1950)*. 165:3182-3189.

Babich, A., and J.K. Burkhardt. 2013. Coordinate control of cytoskeletal remodeling and calcium mobilization during T-cell activation. *Immunological reviews*. 256:80-94.

Baird, D., Q. Feng, and R.A. Cerione. 2005. The Cool-2/alpha-Pix protein mediates a Cdc42-Rac signaling cascade. *Current biology : CB*. 15:1-10.

Barda-Saad, M., N. Shirasu, M.H. Pauker, N. Hassan, O. Perl, A. Balbo, H. Yamaguchi, J.C.D. Houtman, E. Appella, P. Schuck, and L.E. Samelson. 2010. Cooperative interactions at the SLP-76 complex are critical for actin polymerization. *The EMBO journal*. 29:2315-2328.

Barreira, M., S. Fabbiano, J.R. Couceiro, E. Torreira, J.L. Martinez-Torrecuadrada, G. Montoya, O. Llorca, and X.R. Bustelo. 2014. The C-terminal SH3 domain contributes to the intramolecular inhibition of Vav family proteins. *Sci Signal*. 7:ra35.

Bartelt, R.R., N. Cruz-Orcutt, M. Collins, and J.C.D. Houtman. 2009. Comparison of T cell receptor-induced proximal signaling and downstream functions in immortalized and primary T cells. *PloS one*. 4:e5430-e5430.

Billadeau, D.D., S.M. Mackie, R.a. Schoon, and P.J. Leibson. 2000. Specific subdomains of Vav differentially affect T cell and NK cell activation. *Journal of immunology (Baltimore, Md. : 1950)*. 164:3971-3981.

Bologa, C., O. Ursu, V. Salas, J.F. Parkinson, G.K. Phillips, E. Romero, A. Wandinger-ness, L.A. Sklar, C. Schroeder, D. Simpson, J. Nöth, J. Wang, and J. Aubé. 2010. A Potent and Selective Inhibitor of Cdc42 GTPase. *Probe Reports from the NIH Molecular Libraries Program [Internet]*:1-27.

Booden, M.A., S.L. Campbell, and C.J. Der. 2002. Critical but distinct roles for the pleckstrin homology and cysteine-rich domains as positive modulators of Vav2 signaling and transformation. *Molecular and cellular biology*. 22:2487-2497.

Braiman, A., M. Barda-Saad, C.L. Sommers, and L.E. Samelson. 2006. Recruitment and activation of PLCgamma1 in T cells: a new insight into old domains. *The EMBO journal*. 25:774-784.

Bunnell, S.C., V.A. Barr, C.L. Fuller, and L.E. Samelson. 2003. High-Resolution Multicolor Imaging of Dynamic Signaling Complexes in T Cells Stimulated by Planar Substrates Costimulation of Spreading in Primary T Cells.1-14.

Bunnell, S.C., M. Diehn, M.B. Yaffe, P.R. Findell, L.C. Cantley, and L.J. Berg. 2000. Biochemical interactions integrating Itk with the T cell receptor-initiated signaling cascade. *The Journal of biological chemistry*. 275:2219-2230.

Bunnell, S.C., D.I. Hong, J.R. Kardon, T. Yamazaki, C.J. McGlade, V.A. Barr, and L.E. Samelson. 2002. T cell receptor ligation induces the formation of dynamically regulated signaling assemblies. *Journal of Cell Biology*. 158:1263-1275.

Bunnell, S.C., A.L. Singer, D.I. Hong, B.H. Jacque, M.S. Jordan, M.-C. Seminario, V.A. Barr, G.A. Koretzky, and L.E. Samelson. 2006. Persistence of cooperatively stabilized signaling clusters drives T-cell activation. *Molecular and cellular biology*. 26:7155-7166.

Bunney, T.D., O. Opaleye, S.M. Roe, P. Vatter, R.W. Baxendale, C. Walliser, K.L. Everett, M.B. Josephs, C. Christow, F. Rodrigues-Lima, P. Gierschik, L.H. Pearl, and M. Katan. 2009. Structural insights into formation of an active signaling complex between Rac and phospholipase C gamma 2. *Molecular cell*. 34:223-233.

Burbage, M., S.J. Keppler, F. Gasparrini, N. Martinez-Martin, M. Gaya, C. Feest, M.C. Domart, C. Brakebusch, L. Collinson, a. Bruckbauer, and F.D. Batista. 2014. Cdc42 is a key regulator of B cell differentiation and is required for antiviral humoral immunity. *Journal of Experimental Medicine*. 212:53-72.

Burkhardt, J.K., E. Carrizosa, and M.H. Shaffer. 2008. The actin cytoskeleton in T cell activation. *Annual review of immunology*. 26:233-259.

Bustelo, X.R. 2012. Vav Family. Vol. 3. 1963-1976.

Cannon, J.L., C.M. Labno, G. Bosco, a. Seth, M.H. McGavin, K.a. Siminovitch, M.K. Rosen, and J.K. Burkhardt. 2001. Wasp recruitment to the T cell:APC contact site occurs independently of Cdc42 activation. *Immunity*. 15:249-259.

Cao, Y., E.M. Janssen, A.W. Duncan, A. Altman, D.D. Billadeau, and R.T. Abraham. 2002. Pleiotropic defects in TCR signaling in a Vav-1-null Jurkat T-cell line. *The EMBO journal*. 21:4809-4819.

Charvet, C., A.J. Canonigo, D.D. Billadeau, and A. Altman. 2005. Membrane localization and function of Vav3 in T cells depend on its association with the adapter SLP-76. *The Journal of biological chemistry*. 280:15289-15299.

Chen, H.-Y., Y.M. Yang, B.M. Stevens, and M. Noble. 2013. Inhibition of redox/Fyn/c-Cbl pathway function by Cdc42 controls tumour initiation capacity and tamoxifen sensitivity in basal-like breast cancer cells. *EMBO molecular medicine*. 5:723-736.

Chrencik, J.E., A. Brooun, H. Zhang, I.I. Mathews, G.L. Hura, S.a. Foster, J.J.P. Perry, M. Streiff, P. Ramage, H. Widmer, G.M. Bokoch, J.a. Tainer, G. Weckbecker, and P. Kuhn. 2008. Structural basis of guanine nucleotide exchange mediated by the T-cell essential Vav1. *Journal of molecular biology*. 380:828-843.

Citterio, C., M. Menacho-Márquez, R. García-Escudero, R.M. Larive, O. Barreiro, F. Sánchez-Madrid, J.M. Paramio, and X.R. Bustelo. 2012. The rho exchange factors vav2 and vav3 control a lung metastasis-specific transcriptional program in breast cancer cells. *Science signaling*. 5:ra71-ra71.

Colomba, A., D. Courilleau, D. Ramel, D.D. Billadeau, E. Espinos, G. Delsol, B. Payrastre, and F. Gaits-Iacovoni. 2008. Activation of Rac1 and the exchange factor Vav3 are involved in NPM-ALK signaling in anaplastic large cell lymphomas. *Oncogene*. 27:2728-2736.

Costello, P.S., S.C. Cleverley, R. Galandrini, S.W. Henning, and D.A. Cantrell. 2000. The GTPase rho controls a p53-dependent survival checkpoint during thymopoiesis. *J Exp Med*. 192:77-85.

Crespo, P., K.E. Schuebel, A.A. Ostrom, J.S. Gutkind, and X.R. Bustelo. 1997. Phosphotyrosine-dependent activation of Rac-1 GDP/GTP exchange by the vav proto-oncogene product. *Nature*. 385:169-172.

Cruz-Orcutt, N., A. Vacaflores, S.F. Connolly, S.C. Bunnell, and J.C.D. Houtman. 2014. Activated PLC-γ1 is catalytically induced at LAT but activated PLC-γ1 is localized at both LAT- and TCR-containing complexes. *Cellular signalling*. 26:797-805.

Davis, M.J., B.H. Ha, E.C. Holman, R. Halaban, J. Schlessinger, and T.J. Boggon. 2013. RAC1P29S is a spontaneously activating cancer-associated GTPase. *Proc Natl Acad Sci U S A*. 110:912-917.

Désiré, L., J. Bourdin, N. Loiseau, H. Peillon, V. Picard, C. De Oliveira, F. Bachelot, B. Leblond, T. Taverne, E. Beausoleil, S. Lacombe, D. Drouin, and F. Schweighoffer. 2005. RAC1 inhibition targets amyloid precursor protein processing by gamma-secretase and decreases Abeta production in vitro and in vivo. *The Journal of biological chemistry*. 280:37516-37525.

Doody, G.M., D.D. Billadeau, E. Clayton, a. Hutchings, R. Berland, S. McAdam, P.J. Leibson, and M. Turner. 2000. Vav-2 controls NFAT-dependent transcription in B- but not T-lymphocytes. *The EMBO journal*. 19:6173-6184.

Du, M.-J., X.-D. Chen, X.-L. Zhou, Y.-J. Wan, B. Lan, C.-Z. Zhang, and Y. Cao. 2014. Estrogen induces vav1 expression in human breast cancer cells. *PloS one*. 9:e99052-e99052.

Edelstein, A., N. Amodaj, K. Hoover, R. Vale, and N. Stuurman. 2010. Computer control of microscopes using μManager. *Current protocols in molecular biology / edited by Frederick M. Ausubel ... [et al.]*. Chapter 14:Unit14.20-Unit14.20.

Elion, G.B. 1989. The purine path to chemotherapy. *Science*. 244:41-47.

Ellenbroek, S.I., and J.G. Collard. 2007. Rho GTPases: functions and association with cancer. *Clin Exp Metastasis*. 24:657-672.

Erickson, J.W., C.J. Zhang, R.a. Kahn, T. Evans, and R.a. Cerione. 1996. Mammalian Cdc42 is a brefeldin A-sensitive component of the Golgi apparatus. *Journal of Biological Chemistry*. 271:26850-26854.

Faccio, R., S.L. Teitelbaum, K. Fujikawa, J. Chappel, A. Zallone, V.L.J. Tybulewicz, F.P. Ross, and W. Swat. 2005. Vav3 regulates osteoclast function and bone mass. *Nature medicine*. 11:284-290.

Falkenberg, C.V., and L.M. Loew. 2013. Computational analysis of Rho GTPase cycling. *PLoS computational biology*. 9:e1002831-e1002831.

Feig, L.a. 1999. Tools of the trade: use of dominant-inhibitory mutants of Ras-family GTPases. *Nature cell biology*. 1:E25-27.

Feng, Q., D. Baird, and R.A. Cerione. 2004. Novel regulatory mechanisms for the Dbl family guanine nucleotide exchange factor Cool-2/alpha-Pix. *EMBO J*. 23:3492-3504.

Feske, S., and M. Prakriya. 2013. Conformational dynamics of STIM1 activation. *Nature structural & molecular biology*. 20:918-919.

Fischer, K.D., A. Zmuldzinas, S. Gardner, M. Barbacid, A. Bernstein, and C. Guidos. 1995. Defective T-cell receptor signalling and positive selection of Vav-deficient CD4+ CD8+ thymocytes. *Nature*. 374:474-477.

Flicek, P., M.R. Amode, D. Barrell, K. Beal, K. Billis, S. Brent, D. Carvalho-Silva, P. Clapham, G. Coates, S. Fitzgerald, L. Gil, C.G. Giron, L. Gordon, T. Hourlier, S. Hunt, N. Johnson, T. Juettemann, A.K. Kahari, S. Keenan, E. Kulesha, F.J. Martin, T. Maurel, W.M. McLaren, D.N. Murphy, R. Nag, B. Overduin, M. Pignatelli, B. Pritchard, E. Pritchard, H.S. Riat, M. Ruffier, D. Sheppard, K. Taylor, A. Thormann, S.J. Trevanion, A. Vullo, S.P. Wilder, M. Wilson, A. Zadissa, B.L. Aken, E. Birney, F. Cunningham, J. Harrow, J. Herrero, T.J. Hubbard, R. Kinsella, M. Muffato, A. Parker, G. Spudich, A. Yates, D.R. Zerbino, and S.M. Searle. 2014. Ensembl 2014. *Nucleic Acids Res*. 42:D749-755.

Friesland, A., Y. Zhao, Y.-H. Chen, L. Wang, H. Zhou, and Q. Lu. 2013. Small molecule targeting Cdc42-intersectin interaction disrupts Golgi organization and suppresses cell motility. *Proceedings of the National Academy of Sciences of the United States of America*. 110:1261-1266.

Fujikawa, K., A.V. Miletic, F.W. Alt, R. Faccio, T. Brown, J. Hoog, J. Fredericks, S. Nishi, S. Mildiner, S.L. Moores, J. Brugge, F.S. Rosen, and W. Swat. 2003. Vav1/2/3-null mice define an essential role for Vav family proteins in lymphocyte development and activation but a differential requirement in MAPK signaling in T and B cells. *The Journal of experimental medicine*. 198:1595-1608.

Gao, Y., J.B. Dickerson, F. Guo, J. Zheng, and Y. Zheng. 2004. Rational design and characterization of a Rac GTPase-specific small molecule inhibitor. *Proceedings of the National Academy of Sciences of the United States of America*. 101:7618-7623.

Gao, Y., J. Xing, M. Streuli, T.L. Leto, and Y. Zheng. 2001. Trp(56) of rac1 specifies interaction with a subset of guanine nucleotide exchange factors. *The Journal of biological chemistry*. 276:47530-47541.

Gavin, M.A., S.R. Clarke, E. Negrou, A. Gallegos, and A. Rudensky. 2002. Homeostasis and anergy of CD4(+)CD25(+) suppressor T cells in vivo. *Nat Immunol*. 3:33-41.

Geczy, T., M.L. Peach, S. El Kazzouli, D.M. Sigano, J.-H. Kang, C.J. Valle, J. Selezneva, W. Woo, N. Kedei, N.E. Lewin, S.H. Garfield, L. Lim, P. Mannan, V.E. Marquez, and P.M. Blumberg. 2012. Molecular basis for the failure of the "atypical" C1 domain of Vav1 to bind diacylglycerol/phorbol ester. *The Journal of biological chemistry*.

Gibson, D.G., L. Young, R.-Y. Chuang, J.C. Venter, C.a. Hutchison, and H.O. Smith. 2009. Enzymatic assembly of DNA molecules up to several hundred kilobases. *Nature methods*. 6:343-345.

Grassilli, S., F. Brugnoli, R. Lattanzio, C. Rossi, L. Perracchio, M. Mottolese, M. Marchisio, M. Palomba, E. Nika, P.G. Natali, M. Piantelli, S. Capitani, and V. Bertagnolo. 2014. High nuclear level of Vav1 is a positive prognostic factor in early invasive breast tumors: a role in modulating genes related to the efficiency of metastatic process. *Oncotarget*. 5:4320-4336.

Guo, F., J.a. Cancelas, D. Hildeman, D.a. Williams, and Y. Zheng. 2008. Rac GTPase isoforms Rac1 and Rac2 play a redundant and crucial role in T-cell development. *Blood*. 112:1767-1775.

Guo, F., D. Hildeman, P. Tripathi, C.S. Velu, H.L. Grimes, and Y. Zheng. 2010. Coordination of IL-7 receptor and T-cell receptor signaling by cell-division cycle 42 in T-cell homeostasis. *Proceedings of the National Academy of Sciences of the United States of America*. 107:18505-18510.

Guo, F., S. Zhang, P. Tripathi, J. Mattner, J. Phelan, A. Sproles, J. Mo, M. Wills-Karp, H.L. Grimes, D. Hildeman, and Y. Zheng. 2011. Distinct roles of Cdc42 in thymopoiesis and effector and memory T cell differentiation. *PLoS ONE*. 6.

Hall, A.B., M.A.M. Gakidis, M. Glogauer, J.L. Wilsbacher, S. Gao, W. Swat, and J.S. Brugge. 2006. Requirements for Vav guanine nucleotide exchange factors and Rho GTPases in FcγR- and complement-mediated phagocytosis. *Immunity*. 24:305-316.

Halstead, J.R., N.E. Savaskan, I. van den Bout, F. Van Horck, A. Hajdo-Milasinovic, M. Snell, W.-J. Keune, J.-P. Ten Klooster, P.L. Hordijk, and N. Divecha. 2010. Rac controls PIP5K localisation and PtdIns(4,5)P_2 synthesis, which modulates vinculin localisation and neurite dynamics. *Journal of cell science*. 123:3535-3546.

Hamann, M.J., C.M. Lubking, D.N. Luchini, and D.D. Billadeau. 2007. Asef2 functions as a Cdc42 exchange factor and is stimulated by the release of an autoinhibitory module from a concealed C-terminal activation element. *Molecular and cellular biology*. 27:1380-1393.

Han, J. 1998. Role of Substrates and Products of PI 3-kinase in Regulating Activation of Rac-Related Guanosine Triphosphatases by Vav. *Science*. 279:558-560.

Han, J., B. Das, and W. Wei. 1997a. Lck regulates Vav activation of members of the Rho family of GTPases. ... *and cellular biology*. 17.

Han, J., B. Das, W. Wei, L. Van Aelst, R.D. Mosteller, R. Khosravi-Far, J.K. Westwick, C.J. Der, and D. Broek. 1997b. Lck regulates Vav activation of members of the Rho family of GTPases. *Mol Cell Biol*. 17:1346-1353.

Hanawa-Suetsugu, K., M. Kukimoto-Niino, C. Mishima-Tsumagari, R. Akasaka, N. Ohsawa, S. Sekine, T. Ito, N. Tochio, S. Koshiba, T. Kigawa, T. Terada, M. Shirouzu, A. Nishikimi, T. Uruno, T. Katakai, T. Kinashi, D. Kohda, Y. Fukui, and S. Yokoyama. 2012. Structural basis for mutual relief of the Rac guanine nucleotide exchange factor DOCK2 and its partner ELMO1 from their autoinhibited forms. *Proc Natl Acad Sci U S A*. 109:3305-3310.

Harada, Y., Y. Tanaka, M. Terasawa, M. Pieczyk, K. Habiro, T. Katakai, K. Hanawa-Suetsugu, M. Kukimoto-Niino, T. Nishizaki, M. Shirouzu, X. Duan, T. Uruno, A. Nishikimi, F. Sanematsu, S. Yokoyama, J.V. Stein, T. Kinashi, and Y. Fukui. 2012. DOCK8 is a Cdc42 activator critical for interstitial dendritic cell migration during immune responses. *Blood*. 119:4451-4461.

Heasman, S.J., and A.J. Ridley. 2008. Mammalian Rho GTPases: new insights into their functions from in vivo studies. *Nature reviews. Molecular cell biology*. 9:690-701.

Heng, T.S.P., and M.W. Painter. 2008. The Immunological Genome Project: networks of gene expression in immune cells. *Nature immunology*. 9:1091-1094.

Herbert, A.D., A.M. Carr, and E. Hoffmann. 2014. FindFoci: A Focus Detection Algorithm with Automated Parameter Training That Closely Matches Human Assignments, Reduces Human Inconsistencies and Increases Speed of Analysis. *PloS one*. 9:e114749-e114749.

Hill, J.a., M. Feuerer, K. Tash, S. Haxhinasto, J. Perez, R. Melamed, D. Mathis, and C. Benoist. 2007. Foxp3 transcription-factor-dependent and -independent regulation of the regulatory T cell transcriptional signature. *Immunity*. 27:786-800.

Hong, L., S.R. Kenney, G.K. Phillips, D. Simpson, C.E. Schroeder, J. Nöth, E. Romero, S. Swanson, A. Waller, J.J. Strouse, M. Carter, A. Chigaev, O. Ursu, T. Oprea, B. Hjelle, J.E. Golden, J. Aubé, L.G. Hudson, T. Buranda, L.a. Sklar, and A. Wandinger-Ness. 2013. Characterization of a Cdc42 protein inhibitor and its use as a molecular probe. *The Journal of biological chemistry*. 288:8531-8543.

Hong-Geller, E., and R.a. Cerione. 2000. Cdc42 and Rac stimulate exocytosis of secretory granules by activating the IP(3)/calcium pathway in RBL-2H3 mast cells. *The Journal of cell biology*. 148:481-494.

Hong-Geller, E., D. Holowka, R.P. Siraganian, B. Baird, and R.a. Cerione. 2001. Activated Cdc42/Rac reconstitutes Fcepsilon RI-mediated Ca2+ mobilization and degranulation in mutant RBL mast cells. *Proceedings of the National Academy of Sciences of the United States of America*. 98:1154-1159.

Hoppe, A.D., and J.A. Swanson. 2004. Cdc42, Rac1, and Rac2 display distinct patterns of activation during phagocytosis. *Molecular biology of the cell*. 15:3509-3519.

Houtman, J.C.D., H. Yamaguchi, M. Barda-Saad, A. Braiman, B. Bowden, E. Appella, P. Schuck, and L.E. Samelson. 2006. Oligomerization of signaling complexes by the multipoint binding of GRB2 to both LAT and SOS1. *Nature structural & molecular biology*. 13:798-805.

Illenberger, D., F. Schwald, D. Pimmer, W. Binder, G. Maier, a. Dietrich, and P. Gierschik. 1998. Stimulation of phospholipase C-beta2 by the Rho GTPases Cdc42Hs and Rac1. *The EMBO journal*. 17:6241-6249.

Imboden, J.B., and J.D. Stobo. 1985. Transmembrane signalling by the T cell antigen receptor. Perturbation of the T3-antigen receptor complex generates inositol phosphates and releases calcium ions from intracellular stores. *J Exp Med*. 161:446-456.

Imboden, J.B., A. Weiss, and J.D. Stobo. 1985. The antigen receptor on a human T cell line initiates activation by increasing cytoplasmic free calcium. *J Immunol*. 134:663-665.

Jaiswal, M., R. Dvorsky, and M.R. Ahmadian. 2013. Deciphering the molecular and functional basis of Dbl family proteins: a novel systematic approach toward classification of selective activation of the Rho family proteins. *The Journal of biological chemistry*. 288:4486-4500.

Kaminuma, O., M. Deckert, C. Elly, Y.C. Liu, and A. Altman. 2001. Vav-Rac1-mediated activation of the c-Jun N-terminal kinase/c-Jun/AP-1 pathway plays a major role in stimulation of the distal NFAT site in the interleukin-2 gene promoter. *Molecular and cellular biology*. 21:3126-3136.

Karnoub, a.E., D.K. Worthylake, K.L. Rossman, W.M. Pruitt, S.L. Campbell, J. Sondek, and C.J. Der. 2001. Molecular basis for Rac1 recognition by guanine nucleotide exchange factors. *Nature structural biology*. 8:1037-1041.

Kataoka, K., Y. Nagata, A. Kitanaka, Y. Shiraishi, T. Shimamura, J.I. Yasunaga, Y. Totoki, K. Chiba, A. Sato-Otsubo, G. Nagae, R. Ishii, S. Muto, S. Kotani, Y. Watatani, J. Takeda, M. Sanada, H. Tanaka, H. Suzuki, Y. Sato, Y. Shiozawa,

T. Yoshizato, K. Yoshida, H. Makishima, M. Iwanaga, G. Ma, K. Nosaka, M. Hishizawa, H. Itonaga, Y. Imaizumi, W. Munakata, H. Ogasawara, T. Sato, K. Sasai, K. Muramoto, M. Penova, T. Kawaguchi, H. Nakamura, N. Hama, K. Shide, Y. Kubuki, T. Hidaka, T. Kameda, T. Nakamaki, K. Ishiyama, S. Miyawaki, S.S. Yoon, K. Tobinai, Y. Miyazaki, A. Takaori-Kondo, F. Matsuda, K. Takeuchi, O. Nureki, H. Aburatani, T. Watanabe, T. Shibata, M. Matsuoka, S. Miyano, K. Shimoda, and S. Ogawa. 2015. Integrated molecular analysis of adult T cell leukemia/lymphoma. *Nat Genet*.

Katzav, S. 2007. Flesh and blood: the story of Vav1, a gene that signals in hematopoietic cells but can be transforming in human malignancies. *Cancer letters*. 255:241-254.

Katzav, S., D. Martin-Zanca, and M. Barbacid. 1989. vav, a novel human oncogene derived from a locus ubiquitously expressed in hematopoietic cells. *The EMBO journal*. 8:2283-2290.

Krawczyk, C., K. Bachmaier, T. Sasaki, R.G. Jones, S.B. Snapper, D. Bouchard, I. Kozieradzki, P.S. Ohashi, F.W. Alt, and J.M. Penninger. 2000. Cbl-b is a negative regulator of receptor clustering and raft aggregation in T cells. *Immunity*. 13:463-473.

Ksionda, O., A. Saveliev, R. Köchl, J. Rapley, M. Faroudi, J.E. Smith-Garvin, C. Wülfing, K. Rittinger, T. Carter, and V.L.J. Tybulewicz. 2012. Mechanism and function of Vav1 localisation in TCR signalling. *Journal of cell science*. 125:5302-5314.

Ku, G.M., D. Yablonski, E. Manser, L. Lim, and A. Weiss. 2001. A PAK1-PIX-PKL complex is activated by the T-cell receptor independent of Nck, Slp-76 and LAT. *The EMBO journal*. 20:457-465.

Kuhne, M.R., G. Ku, and A. Weiss. 2000. A guanine nucleotide exchange factor-independent function of Vav1 in transcriptional activation. *The Journal of biological chemistry*. 275:2185-2190.

Labno, C.M., C.M. Lewis, D. You, D.W. Leung, A. Takesono, N. Kamberos, A. Seth, L.D. Finkelstein, M.K. Rosen, P.L. Schwartzberg, and J.K. Burkhardt. 2003. Itk functions to control actin polymerization at the immune synapse through localized activation of Cdc42 and WASP. *Current biology : CB*. 13:1619-1624.

Lenoir, M., I. Kufareva, R. Abagyan, and M. Overduin. 2015. Membrane and Protein Interactions of the Pleckstrin Homology Domain Superfamily. *Membranes (Basel)*. 5:646-663.

Li, S.-Y., M.-J. Du, Y.-J. Wan, B. Lan, Y.-H. Liu, Y. Yang, C.-Z. Zhang, and Y. Cao. 2012. The N-terminal 20 amino acid region of the guanine nucleotide exchange factor Vav1 plays a distinguished role in T cell receptor mediated calcium signaling. *The Journal of biological chemistry*.

Lin, Q., W. Yang, D. Baird, Q. Feng, and R.A. Cerione. 2006. Identification of a DOCK180-related guanine nucleotide exchange factor that is capable of mediating a positive feedback activation of Cdc42. *J Biol Chem*. 281:35253-35262.

Liu, B.P., and K. Burridge. 2000. Vav2 activates Rac1, Cdc42, and RhoA downstream from growth factor receptors but not beta1 integrins. *Molecular and cellular biology*. 20:7160-7169.

Liu, D., Z.G. Zhao, Z.L. Jiao, and H.J. Li. 2014. Identifying differential expression genes and single nucleotide variations using RNA-seq in metastatic melanoma. *Genetics and molecular research : GMR*. 13:8153-8162.

López-Lago, M., H. Lee, C. Cruz, N. Movilla, and X.R. Bustelo. 2000. Tyrosine phosphorylation mediates both activation and downmodulation of the biological activity of Vav. *Molecular and cellular biology*. 20:1678-1691.

Macian, F. 2005. NFAT proteins: key regulators of T-cell development and function. *Nature reviews. Immunology*. 5:472-484.

Makrogianneli, K., L.M. Carlin, M.D. Keppler, D.R. Matthews, E. Ofo, A. Coolen, S.M. Ameer-Beg, P.R. Barber, B. Vojnovic, and T. Ng. 2009. Integrating receptor signal inputs that influence small Rho GTPase activation dynamics at the immunological synapse. *Molecular and cellular biology*. 29:2997-3006.

Malartre, M., D. Ayaz, F.F. Amador, and M.D. Martin-Bermudo. 2010. The guanine exchange factor vav controls axon growth and guidance during Drosophila development. *J Neurosci*. 30:2257-2267.

Maltzman, J.S., and G.A. Koretzky. 2003. Azathioprine: old drug, new actions. *J Clin Invest*. 111:1122-1124.

Marangoni, F., T.T. Murooka, T. Manzo, E.Y. Kim, E. Carrizosa, N.M. Elpek, and T.R. Mempel. 2013. The Transcription Factor NFAT Exhibits Signal Memory during Serial T Cell Interactions with Antigen-Presenting Cells. *Immunity*:1-13.

Marinkovic, G., J. Kroon, M. Hoogenboezem, K.A. Hoeben, M.S. Ruiter, K. Kurakula, I. Otermin Rubio, M. Vos, C.J. de Vries, J.D. van Buul, and V. de Waard. 2014. Inhibition of GTPase Rac1 in endothelium by 6-mercaptopurine results in immunosuppression in nonimmune cells: new target for an old drug. *J Immunol*. 192:4370-4378.

Markwardt, M.L., G.-J. Kremers, C.a. Kraft, K. Ray, P.J.C. Cranfill, K.a. Wilson, R.N. Day, R.M. Wachter, M.W. Davidson, and M.a. Rizzo. 2011. An improved cerulean fluorescent protein with enhanced brightness and reduced reversible photoswitching. *PloS one*. 6:e17896-e17896.

Martinez Gakidis, M.A., X. Cullere, T. Olson, J.L. Wilsbacher, B. Zhang, S.L. Moores, K. Ley, W. Swat, T. Mayadas, and J.S. Brugge. 2004. Vav GEFs are required for β2 integrin-dependent functions of neutrophils. *Journal of Cell Biology*. 166:273-282.

Michaelson, D., J. Silletti, G. Murphy, P. D'Eustachio, M. Rush, and M.R. Philips. 2001. Differential localization of Rho GTPases in live cells: regulation by hypervariable regions and RhoGDI binding. *The Journal of cell biology*. 152:111-126.

Miletic, A.V., D.B. Graham, K. Sakata-Sogawa, M. Hiroshima, M.J. Hamann, S. Cemerski, T. Kloeppel, D.D. Billadeau, O. Kanagawa, M. Tokunaga, and W. Swat. 2009. Vav links the T cell antigen receptor to the actin cytoskeleton and T cell activation independently of intrinsic Guanine nucleotide exchange activity. *PloS one*. 4:e6599-e6599.

Mohammadi, S., and R.R. Isberg. 2009. Yersinia pseudotuberculosis virulence determinants invasin, YopE, and YopT modulate RhoG activity and localization. *Infection and immunity*. 77:4771-4782.

Montalvo-Ortiz, B.L., L. Castillo-Pichardo, E. Hernández, T. Humphries-Bickley, A. De la Mota-Peynado, L.a. Cubano, C.P. Vlaar, and S. Dharmawardhane. 2012. Characterization of EHop-016, novel small molecule inhibitor of Rac GTPase. *The Journal of biological chemistry*. 287:13228-13238.

Moores, S.L., L.M. Selfors, J. Fredericks, T. Breit, K. Fujikawa, F.W. Alt, J.S. Brugge, and W. Swat. 2000. Vav family proteins couple to diverse cell surface receptors. *Molecular and cellular biology*. 20:6364-6373.

Movilla, N., and X.R. Bustelo. 1999. Biological and regulatory properties of Vav-3, a new member of the Vav family of oncoproteins. *Molecular and cellular biology*. 19:7870-7885.

Müller, M.R., and A. Rao. 2010. NFAT, immunity and cancer: a transcription factor comes of age. *Nature reviews. Immunology*. 10:645-656.

Mulloy, J.C., J.a. Cancelas, M.-D. Filippi, T.a. Kalfa, F. Guo, and Y. Zheng. 2010. Rho GTPases in hematopoiesis and hemopathies. *Blood*. 115:936-947.

Myung, P.S., G.S. Derimanov, M.S. Jordan, J.a. Punt, Q.H. Liu, B.a. Judd, E.E. Meyers, C.D. Sigmund, B.D. Freedman, and G.A. Koretzky. 2001. Differential requirement for SLP-76 domains in T cell development and function. *Immunity*. 15:1011-1026.

Na, S., B. Li, I.S. Grewal, H. Enslen, R.J. Davis, J.H. Hanke, and R.a. Flavell. 1999. Expression of activated CDC42 induces T cell apoptosis in thymus and peripheral lymph organs via different pathways. *Oncogene*. 18:7966-7974.

Negulescu, P.a., T.B. Krasieva, a. Khan, H.H. Kerschbaum, and M.D. Cahalan. 1996. Polarity of T cell shape, motility, and sensitivity to antigen. *Immunity*. 4:421-430.

Nguyen, K., N.R. Sylvain, and S.C. Bunnell. 2008. T cell costimulation via the integrin VLA-4 inhibits the actin-dependent centralization of signaling microclusters containing the adaptor SLP-76. *Immunity*. 28:810-821.

Niedergang, F., and P. Chavrier. 2005. Regulation of phagocytosis by Rho GTPases. *Current topics in microbiology and immunology*. 291:43-60.

Nolz, J.C., T.S. Gomez, P. Zhu, S. Li, R.B. Medeiros, Y. Shimizu, J.K. Burkhardt, B.D. Freedman, and D.D. Billadeau. 2006. The WAVE2 complex regulates actin cytoskeletal reorganization and CRAC-mediated calcium entry during T cell activation. *Current biology : CB*. 16:24-34.

Ogura, K., K. Nagata, M. Horiuchi, E. Ebisui, T. Hasuda, S. Yuzawa, M. Nishida, H. Hatanaka, and F. Inagaki. 2002. Solution structure of N-terminal SH3 domain of Vav and the recognition site for Grb2 C-terminal SH3 domain. *J Biomol NMR*. 22:37-46.

Oh-hora, M., and A. Rao. 2008. Calcium signaling in lymphocytes. *Current opinion in immunology*. 20:250-258.

Oh-hora, M., and A. Rao. 2009. The calcium/NFAT pathway: role in development and function of regulatory T cells. *Microbes and Infection*. 11:612-619.

Olson, M.F., N.G. Pasteris, J.L. Gorski, and a. Hall. 1996. Faciogenital dysplasia protein (FGD1) and Vav, two related proteins required for normal embryonic development, are upstream regulators of Rho GTPases. *Current biology : CB*. 6:1628-1633.

Onesto, C., A. Shutes, V. Picard, F. Schweighoffer, and C.J. Der. 2008. Characterization of EHT 1864, a novel small molecule inhibitor of Rac family small GTPases. *Methods in enzymology*. 439:111-129.

Ophir, M.J., B.C. Liu, and S.C. Bunnell. 2013. The N terminus of SKAP55 enables T cell adhesion to TCR and integrin ligands via distinct mechanisms. *The Journal of cell biology*. 203:1021-1041.

Palomero, T., L. Couronne, H. Khiabanian, M.Y. Kim, A. Ambesi-Impiombato, A. Perez-Garcia, Z. Carpenter, F. Abate, M. Allegretta, J.E. Haydu, X. Jiang, I.S. Lossos, C. Nicolas, M. Balbin, C. Bastard, G. Bhagat, M.A. Piris, E. Campo, O.A. Bernard, R. Rabadan, and A.A. Ferrando. 2014. Recurrent mutations in epigenetic regulators, RHOA and FYN kinase in peripheral T cell lymphomas. *Nat Genet*. 46:166-170.

Patel, J.C., A. Hall, and E. Caron. 2002. Vav regulates activation of Rac but not Cdc42 during FcgammaR-mediated phagocytosis. *Molecular biology of the cell*. 13:1215-1226.

Pernis, A.B. 2009. Rho GTPase-mediated pathways in mature CD4+ T cells. *Autoimmun Rev*. 8:199-203.

Phee, H., R.T. Abraham, and A. Weiss. 2005. Dynamic recruitment of PAK1 to the immunological synapse is mediated by PIX independently of SLP-76 and Vav1. *Nature immunology*. 6:608-617.

Poppe, D., I. Tiede, G. Fritz, C. Becker, B. Bartsch, S. Wirtz, D. Strand, S. Tanaka, P.R. Galle, X.R. Bustelo, and others. 2006. Azathioprine suppresses ezrin-radixin-moesin-dependent T cell-APC conjugation through inhibition of Vav guanosine exchange activity on Rac proteins. *The Journal of Immunology*. 176:640-640.

Rapley, J., V.L.J. Tybulewicz, and K. Rittinger. 2008. Crucial structural role for the PH and C1 domains of the Vav1 exchange factor. *EMBO reports*. 9:655-661.

Razidlo, G.L., C. Magnine, A.C. Sletten, R.M. Hurley, L.L. Almada, M.E. Fernandez-Zapico, B. Ji, and M.A. McNiven. 2015. Targeting Pancreatic Cancer Metastasis by Inhibition of Vav1, a Driver of Tumor Cell Invasion. *Cancer Res*. 75:2907-2915.

Rivas, F.V., J.P. O'Keefe, M.L. Alegre, and T.F. Gajewski. 2004. Actin cytoskeleton regulates calcium dynamics and NFAT nuclear duration. *Mol Cell Biol*. 24:1628-1639.

Rossman, K.L., C.J. Der, and J. Sondek. 2005. GEF means go: turning on RHO GTPases with guanine nucleotide-exchange factors. *Nature reviews. Molecular cell biology*. 6:167-180.

Rougerie, P., and J. Delon. 2012. Rho GTPases: masters of T lymphocyte migration and activation. *Immunology letters*. 142:1-13.

Sakai, A., C. Thieblemont, A. Wellmann, E.S. Jaffe, and M. Raffeld. 1998. PTEN gene alterations in lymphoid neoplasms. *Blood*. 92:3410-3415.

Saveliev, A., L. Vanes, O. Ksionda, J. Rapley, S.J. Smerdon, K. Rittinger, and V.L.J. Tybulewicz. 2009. Function of the nucleotide exchange activity of vav1 in T cell development and activation. *Science signaling*. 2:ra83-ra83.

Schindelin, J., I. Arganda-Carreras, E. Frise, V. Kaynig, M. Longair, T. Pietzsch, S. Preibisch, C. Rueden, S. Saalfeld, B. Schmid, J.-Y. Tinevez, D.J. White, V. Hartenstein, K. Eliceiri, P. Tomancak, and A. Cardona. 2012. Fiji: an open-source platform for biological-image analysis. *Nature methods*. 9:676-682.

Schneider, C.a., W.S. Rasband, and K.W. Eliceiri. 2012. NIH Image to ImageJ: 25 years of image analysis. *Nature Methods*. 9:671-675.

Schuebel, K.E., N. Movilla, J.L. Rosa, and X.R. Bustelo. 1998. Phosphorylation-dependent and constitutive activation of Rho proteins by wild-type and oncogenic Vav-2. *The EMBO journal*. 17:6608-6621.

Sebban, S., M. Farago, D. Gashai, L. Ilan, E. Pikarsky, I. Ben-Porath, and S. Katzav. 2013. Vav1 fine tunes p53 control of apoptosis versus proliferation in breast cancer. *PloS one*. 8:e54321-e54321.

Seminario, M.-c., P. Precht, S.C. Bunnell, S.E. Warren, C.M. Morris, D. Taub, and R.L. Wange. 2004. PTEN permits acute increases in D3-phosphoinositide levels following TCR stimulation but inhibits distal signaling events by reducing the basal activity of Akt. *European journal of immunology*. 34:3165-3175.

Shan, X., M.J. Czar, S.C. Bunnell, P. Liu, Y. Liu, P.L. Schwartzberg, and R.L. Wange. 2000. Deficiency of PTEN in Jurkat T cells causes constitutive localization of

Itk to the plasma membrane and hyperresponsiveness to CD3 stimulation. *Molecular and cellular biology*. 20:6945-6957.

Shaner, N.C., R.E. Campbell, P.a. Steinbach, B.N.G. Giepmans, A.E. Palmer, and R.Y. Tsien. 2004. Improved monomeric red, orange and yellow fluorescent proteins derived from Discosoma sp. red fluorescent protein. *Nature biotechnology*. 22:1567-1572.

Shaner, N.C., M.Z. Lin, M.R. McKeown, P.a. Steinbach, K.L. Hazelwood, M.W. Davidson, and R.Y. Tsien. 2008. Improving the photostability of bright monomeric orange and red fluorescent proteins. *Nature methods*. 5:545-551.

Sherman, E., V. Barr, S. Manley, G. Patterson, L. Balagopalan, I. Akpan, C.K. Regan, R.K. Merrill, C.L. Sommers, J. Lippincott-Schwartz, and L.E. Samelson. 2011. Functional nanoscale organization of signaling molecules downstream of the T cell antigen receptor. *Immunity*. 35:705-720.

Shutes, A., C. Onesto, V. Picard, B. Leblond, F. Schweighoffer, and C.J. Der. 2007. Specificity and mechanism of action of EHT 1864, a novel small molecule inhibitor of Rac family small GTPases. *The Journal of biological chemistry*. 282:35666-35678.

Singer, A.L., S.C. Bunnell, A.E. Obstfeld, M.S. Jordan, J.N. Wu, P.S. Myung, L.E. Samelson, and G.a. Koretzky. 2004. Roles of the proline-rich domain in SLP-76 subcellular localization and T cell function. *The Journal of biological chemistry*. 279:15481-15490.

Singleton, K.L., K.T. Roybal, Y. Sun, G. Fu, N.R. Gascoigne, N.S. van Oers, and C. Wulfing. 2009. Spatiotemporal patterning during T cell activation is highly diverse. *Sci Signal*. 2:ra15.

Skowronek, K.R., F. Guo, Y. Zheng, and N. Nassar. 2004. The C-terminal basic tail of RhoG assists the guanine nucleotide exchange factor trio in binding to phospholipids. *J Biol Chem*. 279:37895-37907.

Snyder, J.T., D.K. Worthylake, K.L. Rossman, L. Betts, W.M. Pruitt, D.P. Siderovski, C.J. Der, and J. Sondek. 2002. Structural basis for the selective activation of Rho GTPases by Dbl exchange factors. *Nature structural biology*. 9:468-475.

Steinbach, W.J., J.L. Reedy, R.A. Cramer, Jr., J.R. Perfect, and J. Heitman. 2007. Harnessing calcineurin as a novel anti-infective agent against invasive fungal infections. *Nat Rev Microbiol*. 5:418-430.

Subauste, M.C., M. Von Herrath, V. Benard, C.E. Chamberlain, T.H. Chuang, K. Chu, G.M. Bokoch, and K.M. Hahn. 2000. Rho family proteins modulate rapid apoptosis induced by cytotoxic T lymphocytes and Fas. *Journal of Biological Chemistry*. 275:9725-9733.

Sumpter, T.L., K.K. Payne, and D.S. Wilkes. 2008. Regulation of the NFAT pathway discriminates CD4+CD25+ regulatory T cells from CD4+CD25- helper T cells. *Journal of leukocyte biology*. 83:708-717.

Swanson, J.A., and A.D. Hoppe. 2004. The coordination of signaling during Fc receptor-mediated phagocytosis. *Journal of leukocyte biology*. 76:1093-1103.

Sylvain, N.R. 2011. Vav1 Controls the Stability and Function of SLP-76 Containing Signaling Microclusters. *In* Immunology. Vol. PhD. Tufts University.

Sylvain, N.R., K. Nguyen, and S.C. Bunnell. 2011. Vav1-mediated scaffolding interactions stabilize SLP-76 microclusters and contribute to antigen-dependent T cell responses. *Science signaling*. 4:ra14-ra14.

Tan, B., Y. Li, Q. Zhao, L. Fan, Y. Liu, D. Wang, and X. Zhao. 2014. Inhibition of Vav3 could reverse the drug resistance of gastric cancer cells by downregulating JNK signaling pathway. *Cancer gene therapy*:1-6.

Tartare-Deckert, S., M.N. Monthouel, C. Charvet, I. Foucault, E. Van Obberghen, a. Bernard, A. Altman, and M. Deckert. 2001. Vav2 activates c-fos serum response element and CD69 expression but negatively regulates nuclear factor of activated T cells and interleukin-2 gene activation in T lymphocyte. *The Journal of biological chemistry*. 276:20849-20857.

Tedford, K., L. Nitschke, I. Girkontaite, a. Charlesworth, G. Chan, V. Sakk, M. Barbacid, and K.D. Fischer. 2001. Compensation between Vav-1 and Vav-2 in B cell development and antigen receptor signaling. *Nature immunology*. 2:548-555.

Tiede, I., G. Fritz, and S. Strand. 2003. CD28-dependent Rac1 activation is the molecular target of azathioprine in primary human CD4+ T lymphocytes. *Journal of Clinical …*. 111:1133-1145.

Turner, M., and D.D. Billadeau. 2002. VAV proteins as signal integrators for multi-subunit immune-recognition receptors. *Nature reviews. Immunology*. 2:476-486.

Tybulewicz, V.L.J., and R.B. Henderson. 2009. Rho family GTPases and their regulators in lymphocytes. *Nature reviews. Immunology*. 9:630-644.

Utomo, A., X. Cullere, M. Glogauer, W. Swat, and T.N. Mayadas. 2006. Vav proteins in neutrophils are required for FcgammaR-mediated signaling to Rac GTPases and nicotinamide adenine dinucleotide phosphate oxidase component p40(phox). *Journal of immunology (Baltimore, Md. : 1950)*. 177:6388-6397.

Vaeth, M., U. Schliesser, G. Muller, S. Reissig, K. Satoh, A. Tuettenberg, H. Jonuleit, A. Waisman, M.R. Muller, E. Serfling, B.S. Sawitzki, and F. Berberich-Siebelt. 2012. Dependence on nuclear factor of activated T-cells (NFAT) levels discriminates conventional T cells from Foxp3+ regulatory T cells. *Proc Natl Acad Sci U S A*. 109:16258-16263.

van Hennik, P.B., J.P. ten Klooster, J.R. Halstead, C. Voermans, E.C. Anthony, N. Divecha, and P.L. Hordijk. 2003. The C-terminal domain of Rac1 contains two motifs that control targeting and signaling specificity. *The Journal of biological chemistry*. 278:39166-39175.

Varma, R., G. Campi, T. Yokosuka, T. Saito, and M.L. Dustin. 2006. T Cell Receptor-Proximal Signals Are Sustained in Peripheral Microclusters and Terminated in the Central Supramolecular Activation Cluster. *Immunity*. 25:117-127.

Vega, F.M., and A.J. Ridley. 2008. Rho GTPases in cancer cell biology. *FEBS Lett*. 582:2093-2101.

Veluthakal, R., R. Tunduguru, D.K. Arora, V. Sidarala, K. Syeda, C.P. Vlaar, D.C. Thurmond, and A. Kowluru. 2015. VAV2, a guanine nucleotide exchange factor for Rac1, regulates glucose-stimulated insulin secretion in pancreatic beta cells. *Diabetologia*.

Vigil, D., J. Cherfils, K.L. Rossman, and C.J. Der. 2010. Ras superfamily GEFs and GAPs: validated and tractable targets for cancer therapy? *Nat Rev Cancer*. 10:842-857.

Vigorito, E., D.D. Billadeau, D. Savoy, S. McAdam, G.M. Doody, P. Fort, and M. Turner. 2003. RhoG regulates gene expression and the actin cytoskeleton in lymphocytes. *Oncogene*. 22:330-342.

Walliser, C., M. Retlich, R. Harris, K.L. Everett, M.B. Josephs, P. Vatter, D. Esposito, P.C. Driscoll, M. Katan, P. Gierschik, and T.D. Bunney. 2008. rac regulates its effector phospholipase Cgamma2 through interaction with a split pleckstrin homology domain. *The Journal of biological chemistry*. 283:30351-30362.

Walmsley, M.J., S.K. Ooi, L.F. Reynolds, S.H. Smith, S. Ruf, A. Mathiot, L. Vanes, D.A. Williams, M.P. Cancro, and V.L. Tybulewicz. 2003. Critical roles for Rac1 and Rac2 GTPases in B cell development and signaling. *Science*. 302:459-462.

Weber, K.S., M.J. Miller, and P.M. Allen. 2008. Th17 cells exhibit a distinct calcium profile from Th1 and Th2 cells and have Th1-like motility and NF-AT nuclear localization. *J Immunol*. 180:1442-1450.

Wilkes, M.M., J.D. Wilson, B. Baird, and D. Holowka. 2014. Activation of Cdc42 is necessary for sustained oscillations of Ca2+ and PIP2 stimulated by antigen in RBL mast cells. *Biology open*:1-11.

Wirth, A., C. Chen-Wacker, Y.-W. Wu, N. Gorinski, M.a. Filippov, G. Pandey, and E. Ponimaskin. 2013. Dual lipidation of the brain-specific Cdc42 isoform regulates its functional properties. *The Biochemical journal*. 322:311-322.

Wu, J., S. Katzav, and A. Weiss. 1995. A functional T-cell receptor signaling pathway is required for p95vav activity. *Molecular and cellular biology*. 15:4337-4346.

Yokosuka, T., and T. Saito. 2009. Dynamic regulation of T-cell costimulation through TCR-CD28 microclusters. *Immunol Rev*. 229:27-40.

Yu, B., I.R.S. Martins, P. Li, G.K. Amarasinghe, J. Umetani, M.E. Fernandez-Zapico, D.D. Billadeau, M. Machius, D.R. Tomchick, and M.K. Rosen. 2010. Structural and energetic mechanisms of cooperative autoinhibition and activation of Vav1. *Cell*. 140:246-256.

Yu, H., D. Leitenberg, B. Li, and R.a. Flavell. 2001. Deficiency of small GTPase Rac2 affects T cell activation. *The Journal of experimental medicine*. 194:915-926.

Zakaria, S., T.S. Gomez, D.N. Savoy, S. McAdam, M. Turner, R.T. Abraham, and D.D. Billadeau. 2004. Differential regulation of TCR-mediated gene transcription by Vav family members. *The Journal of experimental medicine*. 199:429-434.

Zeng, R., J.L. Cannon, R.T. Abraham, M. Way, D.D. Billadeau, J. Bubeck-Wardenberg, and J.K. Burkhardt. 2003. SLP-76 Coordinates Nck-Dependent Wiskott-Aldrich Syndrome Protein Recruitment with Vav-1/Cdc42-Dependent Wiskott-Aldrich Syndrome Protein Activation at the T Cell-APC Contact Site. *The Journal of Immunology*. 171:1360-1368.

Zhang, Q., C.G. Dove, J.L. Hor, H.M. Murdock, D.M. Strauss-Albee, J.a. Garcia, J.N. Mandl, R.a. Grodick, H. Jing, D.B. Chandler-Brown, T.E. Lenardo, G. Crawford, H.F. Matthews, a.F. Freeman, R.J. Cornall, R.N. Germain, S.N. Mueller, and H.C. Su. 2014. DOCK8 regulates lymphocyte shape integrity for skin antiviral immunity. *Journal of Experimental Medicine*. 211:2549-2566.

Zhou, C., S. Licciulli, J.L. Avila, M. Cho, S. Troutman, P. Jiang, A.V. Kossenkov, L.C. Showe, Q. Liu, A. Vachani, S.M. Albelda, and J.L. Kissil. 2013. The Rac1 splice form Rac1b promotes K-ras-induced lung tumorigenesis. *Oncogene*. 32:903-909.

Zhou, Z., J. Yin, Z. Dou, J. Tang, C. Zhang, and Y. Cao. 2007. The calponin homology domain of Vav1 associates with calmodulin and is prerequisite to T cell antigen receptor-induced calcium release in Jurkat T lymphocytes. *The Journal of biological chemistry*. 282:23737-23744.

Zhuge, Y., and J. Xu. 2001. Rac1 mediates type I collagen-dependent MMP-2 activation. role in cell invasion across collagen barrier. *J Biol Chem*. 276:16248-16256.

Zugaza, J., M.a. López-Lago, M.J. Caloca, M. Dosil, N. Movilla, and X.R. Bustelo. 2002. Structural determinants for the biological activity of Vav proteins. *The Journal of biological chemistry*. 277:45377-45392.